



**AUTOMATIC IDENTIFICATION AND MEASUREMENT OF
ANTIBIOGRAM ANALYSIS**

MERVE DUMAN

JULY 2019

AUTOMATIC IDENTIFICATION AND MEASUREMENT OF ANTIBIOGRAM
ANALYSIS

A THESIS SUBMITTED TO
THE GRADUATE SCHOOL OF NATURAL AND APPLIED
SCIENCES OF
ÇANKAYA UNIVERSITY



BY
MERVE DUMAN

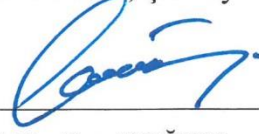
IN PARTIAL FULFILLMENT OF THE REQUIREMENTS FOR THE
DEGREE OF
MASTER OF SCIENCE
IN
COMPUTER ENGINEERING
DEPARTMENT

JULY 2019

Title of the Thesis: **Automatic Identification and Measurement of Antibigram Analysis**

Submitted By **Merve DUMAN**

Approval of the Graduate School of Natural and Applied Sciences, Çankaya University.



Prof. Dr. Can ÇOĞUN

Director

I certify that this thesis satisfies all the requirements as a thesis for the degree of Master of Science.



Prof. Dr. Sıtkı Kemal İDER

Head of Department

This is to certify that we have read this thesis and that in our opinion it is fully adequate, in scope and quality, as a thesis for the degree of Master of Science.



Asst. Prof. Dr. Roya CHOUPANI

Supervisor

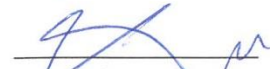
Examination Date: July 26, 2019

Examining Committee Members

Assoc. Prof. Dr. İhsan Tolga MEDENİ
(Ankara Yıldırım Beyazıt Univ.)



Asst. Prof. Dr. Roya CHOUPANI (Çankaya Univ.)



Asst. Prof. Dr. Abdül Kadir GÖRÜR (Çankaya Univ.)



STATEMENT OF NON-PLAGIARISM PAGE

I hereby declare that all information in this document has been obtained and presented in accordance with academic rules and ethical conduct. I also declare that, as required by these rules and conduct, I have fully cited and referenced all material and results that are not original to this work.

Name, Last Name: Merve DUMAN

Signature: 

Date: 07.26.2019

ABSTRACT

AUTOMATIC IDENTIFICATION AND MEASUREMENT OF ANTIBIOGRAM ANALYSIS

DUMAN, Merve
M.Sc., Department of Computer Engineering
Supervisor: Asst. Prof. Dr. Roya CHOUPANI
Co-Supervisor: Dr. Faris Serdar TAŞEL

JULY 2019, 80 pages

In this thesis, an automatic identification method of antibiogram analysis is implemented, existing methods are investigated and results are discussed. In an antibiogram analysis, inhibition zones of drugs read by humans might be measured with some mistakes. These mistakes such as misreading during the analysis process or the conditions like imperfect or partial seeding inhibition zones can be solved with automatic identification methods. Also, there is a need for periodically reading or a tracking system because inhibition zones change with time. To overcome antibiogram analysis problems, some improvements are made on the image. As pre-processing operations, Otsu Thresholding, largest object finding, binary image mask, morphological erosion and closing operations are applied. Circular Hough Transform is used to find drugs and profile lines are drawn to find inhibition zones. The Otsu thresholding is used to determine the zone borders. The results obtained from the algorithm are evaluated and discussed.

Keywords: Antibiogram analysis, Object Identification

ÖZ

ANTİBİYOGRAM ANALİZİNİN OTOMATİK TANIMI VE ÖLÇÜMÜ

DUMAN, Merve
Yüksek Lisans, Bilgisayar Mühendisliği Anabilim Dalı
Danışman: Dr. Öğr. Üyesi ROYA CHOUPANI
Yardımcı Danışman: Dr. Faris Serdar TAŞEL

TEMMUZ 2019, 80 sayfa

Bu tez çalışmasında, otomatik bir antibiyogram analizi tanımlama yöntemi uygulanmış, mevcut yöntemler araştırılmış ve sonuçlar tartışılmıştır. Bir antibiyogram analizinde insanlar tarafından okunan ilaçların inhibisyon bölgeleri ölçümleri sırasında bazı hatalar meydana gelebilir. Analiz işlemi esnasında hatalı okuma, kusurlu veya düzenli olmayan inhibisyon bölgeleri gibi durumlar bu otomatik tanımlama yöntemleri ile çözülebilir. Ayrıca, periyodik olarak okumaya veya bir takip sistemine ihtiyaç vardır, çünkü inhibisyon bölgeleri zamanla değişir. Antibiyogram analizi problemlerinin çözümü için görüntüde bazı iyileştirmeler yapılmıştır. Analiz öncesi, Otsu Eşiklemesi, en büyük nesne bulma, ikili görüntü maskesi, morfolojik erozyon ve kapanma işlemleri uygulanmıştır. İlaçları bulmak için Dairesel Hough Dönüşümü kullanılmış ve inhibisyon bölgelerini bulmak için profil çizgileri çizilmiştir. Otsu eşiklemesi inhibisyon bölge sınırlarını belirlemek için kullanılmıştır. Algoritmadan elde edilen sonuçlar değerlendirilmiş ve tartışılmıştır.

Anahtar Kelimeler : Antibiyogram analizi, Obje Tanıma

ACKNOWLEDGEMENTS

I would like to thank Dr. Faris Serdar TAŞEL and Asst. Prof. Dr. Roya CHOUPANI for their guidance, supervision and suggestions in the development of this thesis and also specialist Osman AYTUZLAR from METU Health and Guidance Center and Düzen laboratory for providing antibiograms.

I would like to express my special thanks to my family for their valuable support and patience.

TABLE OF CONTENTS

STATEMENT OF NON-PLAGIARISM PAGE	iii
ABSTRACT	iv
ÖZ.....	v
ACKNOWLEDGEMENTS.....	vi
TABLE OF CONTENTS.....	vii
LIST OF FIGURES	ix
LIST OF TABLES	xiii
LIST OF ABBREVIATIONS.....	xiv
CHAPTER 1.....	1
INTRODUCTION	1
1.1 Motivation of the Thesis	5
1.2 Organization of the Thesis	5
CHAPTER 2.....	7
LITERATURE SURVEY AND BACKGROUND.....	7
2.1 Reading and Understanding an Antibioqram.....	7
2.1.1 Current Technologies.....	7
2.2 Manual Systems in Clinical Microbiology	8
2.2.1 Broth Dilution Test	8
2.2.2 Agar Dilution Method.....	9
2.2.3 Kirby-Bauer Disk Diffusion Susceptibility Method.....	9
2.3 Image Fundamentals.....	11
2.3.1 Elementary Binary Morphology Method.....	13
2.3.2 Morphological Erosion Operation	13
2.3.3 Morphological Dilation Operation	14
2.3.4 Morphological Opening Process	15
2.3.5 Morphological Closing Process.....	16
2.3.6 Sequential Filtering process	16
2.3.7 Masking Fundamentals Process	17

2.3.8 Distance Transform Process	18
2.3.9 Hough Transform Process	19
2.3.10 Otsu Image Segmentation Algorithm	20
CHAPTER 3.....	22
MATERIAL AND METHODS	22
3.1 Antibigram Plate Images and Software	22
3.2 Manual Readings	23
3.3 Feature Extraction of Antibigram Plate Image	23
CHAPTER 4.....	40
RESULTS AND DISCUSSION	40
4.1 Identification of Inhibition Zones Border Lines	40
4.2 Inhibition Zone Final Reading	72
4.3 Discussion	74
CHAPTER 5.....	77
CONCLUSIONS	77
REFERENCES	78

LIST OF FIGURES

Figure 1. 1 Antibioqram: Zone Inhibitions.....	2
Figure 1. 2 Antibioqram microbiological objects by using image analysis technique	4
Figure 2. 1 Antimicrobial susceptibility testing methods	8
Figure 2. 2 A broth microdilution susceptibility panel containing 96 reagent wells and a disposable tray inoculator [5]	9
Figure 2. 3 Kirby-Bauer Disk Diffusion Method [5].....	10
Figure 2. 4 An original color image	12
Figure 2. 5 A grayscale color image	12
Figure 2. 6 A binary image using thresholding.....	12
Figure 2. 7 Morphological Erosion Process	14
Figure 2. 8 Morphological Dilation Process	15
Figure 2. 9 Morphological Opening Process.....	15
Figure 2. 10 Morphological Closing Process	16
Figure 2. 11 Primarily Closed Image	17
Figure 2. 12 Primarily Opened Image.....	17
Figure 2. 13 Grayscale Image, Grayscale Mask.....	18
Figure 2. 14 Binary Image, Grayscale Mask.....	18
Figure 2. 15 Distance Transform Process	19
Figure 2. 16 a) Coordinate points. b) AND. c) Possible straight line fittings.	20
Figure 2. 17 (A) Original Image (B) Image Using Otsu Thresholding Algorithm [33]	21
Figure 3. 1 An antibioqram plate image.....	22
Figure 3. 2 Image processing parts	23
Figure 3. 3 Raw original image	24
Figure 3. 4 Gray level image	25
Figure 3. 5 Binary image by Otsu thresholding	26
Figure 3. 6 Binary image of largest object.....	26

Figure 3. 7 Binary image (Mask) by filling holes	27
Figure 3. 8 Morphologically eroded Binary image (Mask)	28
Figure 3. 9 Gray level image mask by binary mask	29
Figure 3. 10 Morphologically closed gray level image	29
Figure 3. 11 Circles found by Circular Hough Transform	31
Figure 3. 12 Circles removed to improve border finding	32
Figure 3. 13 Profile lines of detected centers	32
Figure 3. 14 Detected borders shown over closed image	38
Figure 3. 15 Detected borders over antibiogram	39
Figure 4. 1 First antibiogram plate image profiles for detected center no.1	41
Figure 4. 2 First antibiogram plate image profiles for detected center no.2	42
Figure 4. 3 First antibiogram plate image profiles for detected center no.3	42
Figure 4. 4 First antibiogram plate image profiles for detected center no.4	43
Figure 4. 5 First antibiogram plate image profiles for detected center no.5	43
Figure 4. 6 First antibiogram plate image profiles for detected center no.6	44
Figure 4. 7 First antibiogram plate image profiles for detected center no.7	44
Figure 4. 8 First antibiogram plate image profiles for detected center no.8	45
Figure 4. 9 First antibiogram plate image profiles for detected center no.9	45
Figure 4. 10 First antibiogram plate image profiles for detected center no.10	46
Figure 4. 11 First antibiogram plate image profiles for detected center no.11.....	46
Figure 4. 12 Second antibiogram plate image profiles for detected center no.1	47
Figure 4. 13 Second antibiogram plate image profiles for detected center no.2	48
Figure 4. 14 Second antibiogram plate image profiles for detected center no.3	48
Figure 4. 15 Second antibiogram plate image profiles for detected center no.4	49
Figure 4. 16 Second antibiogram plate image profiles for detected center no.5	49
Figure 4. 17 Second antibiogram plate image profiles for detected center no.6	50
Figure 4. 18 Second antibiogram plate image profiles for detected center no.7	50
Figure 4. 19 Second antibiogram plate image profiles for detected center no.8	51
Figure 4. 20 Second antibiogram plate image profiles for detected center no.9	51
Figure 4. 21 Second antibiogram plate image profiles for detected center no.10	52

Figure 4. 22	Second antibiogram plate image profiles for detected center no.1152
Figure 4. 23	Third antibiogram plate image profiles for detected center no.153
Figure 4. 24	Third antibiogram plate image profiles for detected center no.254
Figure 4. 25	Third antibiogram plate image profiles for detected center no.354
Figure 4. 26	Third antibiogram plate image profiles for detected center no.455
Figure 4. 27	Third antibiogram plate image profiles for detected center no.555
Figure 4. 28	Third antibiogram plate image profiles for detected center no.656
Figure 4. 29	Third antibiogram plate image profiles for detected center no.756
Figure 4. 30	Third antibiogram plate image profiles for detected center no.857
Figure 4. 31	Third antibiogram plate image profiles for detected center no.957
Figure 4. 32	Third antibiogram plate image profiles for detected center no.1058
Figure 4. 33	Third antibiogram plate image profiles for detected center no.1158
Figure 4. 34	Third antibiogram plate image profiles for detected center no.1259
Figure 4. 35	Fourth antibiogram plate image profiles for detected center no.160
Figure 4. 36	Fourth antibiogram plate image profiles for detected center no.260
Figure 4. 37	Fourth antibiogram plate image profiles for detected center no.361
Figure 4. 38	Fourth antibiogram plate image profiles for detected center no.461
Figure 4. 39	Fourth antibiogram plate image profiles for detected center no.562
Figure 4. 40	Fourth antibiogram plate image profiles for detected center no.662
Figure 4. 41	Fourth antibiogram plate image profiles for detected center no.763
Figure 4. 42	Fourth antibiogram plate image profiles for detected center no.863
Figure 4. 43	Fourth antibiogram plate image profiles for detected center no.964
Figure 4. 44	Fourth antibiogram plate image profiles for detected center no.1064
Figure 4. 45	Fourth antibiogram plate image profiles for detected center no.1165
Figure 4. 46	Fourth antibiogram plate image profiles for detected center no.1265
Figure 4. 47	Fifth antibiogram plate image profiles for detected center no.166
Figure 4. 48	Fifth antibiogram plate image profiles for detected center no.267
Figure 4. 49	Fifth antibiogram plate image profiles for detected center no.367
Figure 4. 50	Fifth antibiogram plate image profiles for detected center no.468
Figure 4. 51	Fifth antibiogram plate image profiles for detected center no.568

Figure 4. 52 Fifth antibiogram plate image profiles for detected center no.6.....	69
Figure 4. 53 Fifth antibiogram plate image profiles for detected center no.7.....	69
Figure 4. 54 Fifth antibiogram plate image profiles for detected center no.8.....	70
Figure 4. 55 Fifth antibiogram plate image profiles for detected center no.9.....	70
Figure 4. 56 Fifth antibiogram plate image profiles for detected center no.10.....	71
Figure 4. 57 Fifth antibiogram plate image profiles for detected center no.11	71
Figure 4. 58 Fifth antibiogram plate image profiles for detected center no.12	72
Figure 4. 59 First antibiogram plate images inhibition zones calculation	73
Figure 4. 60 Second antibiogram plate images inhibition zones calculation.....	73
Figure 4. 61 Third antibiogram plate images inhibition zones calculation.....	73
Figure 4. 62 Forth antibiogram plate images inhibition zones calculations	74
Figure 4. 63 Fifth antibiogram plate images inhibition zones calculations	74

LIST OF TABLES

Table 3. 1 Centers of the circles found.....	30
Table 3. 2 Radii of the circles found	31
Table 3. 3 Some values of profiles matrix.....	34
Table 3. 4 Some values of nonzeroprof matrix.....	35
Table 3. 5 Sum of the second axis of nonzeroprof matrix.....	35
Table 3. 6 Some values of nonnanprof matrix.....	36
Table 3. 7 Sum of the second axis of nonnanprof matrix	36

LIST OF ABBREVIATIONS

1D	One-Dimensional
2D	Two-Dimensional
3D	Three-Dimensional
AST	Antibiotic Susceptibility Testing
CLSI	Clinical Laboratory Standards Institute
DICOM	Digital Imaging and Communications in Medicine
GIF	Graphics Interchange Format
IEEE	Institute of Electrical and Electronics Engineering
ISMM	International Symposium on Mathematical Morphology
JPEG	Joint Photography Experts Group
MATLAB	Matrix Laboratory
MIC	Minimum Inhibitory Concentration
MM	Mathematical Morphology
MRI	Magnetic Resonance Imaging
NaN	Not a Number
RGB	Red Green Blue
SE	Structuring Element
TIF	Tagged Image File

CHAPTER 1

INTRODUCTION

Antibiogram is a disk diffusion test applied to determine the antimicrobial susceptibility of microorganisms in microbiology [1]. The best use of the medical antibiogram data supports specialist with empirical treatment for suspected infection [2]. Although the antibiogram is used for many purposes, the most common is to contribute to the clinical trials of experimental treatments for suspected infection in the clinical setting [3]. Some researchers have suggested that the consistency of the antibiogram to be used for this purpose varies because of the differences of the conditions [4, 5]. However, more accurate test reports are required to obtain a better treatment result for the clinical patient. Although many investigations have been carried out in the medical microbiology laboratory, the best method for investigating and presenting these data has not been established.

Antibiogram is used by clinician on a regular basis to evaluate local susceptibility rate as assistance in selecting empirical antibiotic treatment and monitoring resistance conventions over time within an organization. Many researchers have previously suggested that antibiotic diversity is appropriate for various critical infections in humans. The meaning of antibiotic is an antimicrobial chemicals produced by microorganisms against other microorganisms. Scientists use these antimicrobials properly in the fight against epidemic diseases [2, 5]. The antimicrobial susceptibility of the microorganism has significant importance in medical microbiology especially for monitoring the therapeutic results in the infection, also examining the growth and epidemiology of resistances [6]. These are very important factors for medical preventions. Antimicrobial susceptibility experiments are used to observe the in vitro activity of various antimicrobial agents opposed to a particular microbial. Until now, there are many special applications have been applied for the antimicrobial susceptibility tests, as well as agar dilution,

broth microdilution and disk diffusion. Most of the methods are applied under a certain standard condition such as temperature, culture medium and maturation time to get measurable, interpretable and equivalent clinical results [7, 8].

The Kirby-Bauer method, known as the disk diffusion technique, is commonly used in antibiotic susceptibility testing to determine which antibiotic option should be applied to treat infection. Disk diffusion or the Kirby-Bauer method is also called the antibiogram test, a qualitative clinical process widely applied in all regular microbiological experiments, especially in bacteriological isolates due to its accessibility, consistency and low price [7, 8]. In disk diffusion or Kirby-Bauer process, the cellulose disc is filled with a dilution of various antimicrobial agents present on a surface of the agar plate prior to being immunized with a standard suspension of microorganisms [9]. Agar plate is incubated according to the condition of microorganisms. After that, the diameter (in millimeters) of each growth inhibition area surrounded by the antimicrobial disc is measured (Figure 1.1). The diameter of the inhibition areas is dependent on the isolate susceptibility and the antimicrobial diffusion rates completed the agar medium [10]. This process allows the classification of bacterial isolates as intermediary and resistant for each antimicrobial drug test according to the International Clinical and Laboratory Standard Institutes (CLSI). According to the principal, the organism can be classified as Resistant (R), Intermediate (I) or Susceptible (S).



Figure 1. 1 Antibiogram: Zone Inhibitions

In the antibiogram, zone inhibition diameters are measured by a Kirby-Bauer or disk diffusion test which is commonly done manually by experts using a ruler. At the same time, experts check the antibiogram in the standard breakpoint; also classify bacteriological isolates as susceptibility and drug resistant for each drug test. In addition, the zone inhibition diameters depend on the quality of the expert in the measurement process, but also a time-consuming procedure. Therefore computerized inhibition zone reader and quick program analysis system can be reduced the operative variable in reading plate also reduced the possibility of presenting error in the result. Therefore, the computerized inhibition zone reader and the rapid program analysis system can reduce the operative variable in the reading plate and consequently reduce the probability of the resulting error. However, computerized automated inhibition zone readers are costly because of the expensive software tools and major changes in test design [2, 5].

Image processing analysis enhances the quality, efficiency and characterization of optical images of clinical microbiology research. In this way, conducting research analysis of various visuals are increasingly more objective, more productive and time consuming. In addition, digital image processing can provide more adopted visual unreachable information about the relationships in other visual parameters and different relevant features of biological principles. Furthermore, the main focus of image processing analysis is to open the forward paths of using the Disk Diffusion based method for the broth microdilution test on the antibiogram. So far, in this field, using image processing analysis especially in antibiogram microbiological object by using image analysis technique is present (Figure 1. 2).

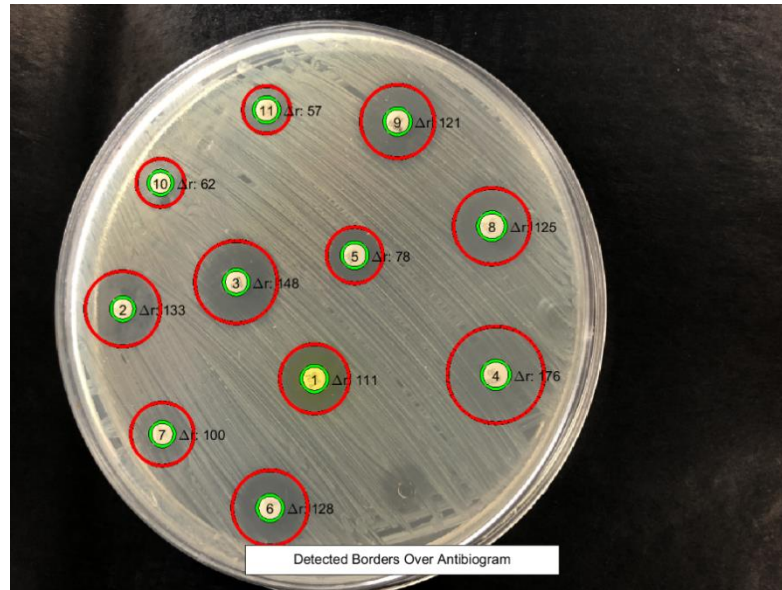


Figure 1. 2 Antibiogram microbiological objects by using image analysis technique

As far as is known, many researches are done for the antimicrobial test, but these processes depend on some certain standard conditions. Image processing methods provide efficiency to determine the antibiogram plate classification. Image processing method can be performed for antibiogram plate classification to get clearer and more accurate information which can be very beneficial for microbiology laboratories and doctor analyses. Furthermore, digital image processing methods can give clear clinical features of antibiogram plate image. These features can be used in another antibiogram research for statistical analysis. Many studies have been conducted to read and interpret the antibiogram analysis frequently performed by scientific research medical laboratories. As is known, the antibiogram is a clinical test of the susceptibility of the microorganism to antibiotics. Reading the interpretation of the antibiogram test results is usually performed manually that can lead to human errors and longtime process. Until now, many researches have been done for an automated device which can read and interpret antibiograms, but most of the time these medical devices are expensive and costly to operate in different places. Therefore, the automated computerized image processing method shows an algorithm for detection and interpretation of reading antibiograms. In this study, an original and new image processing method is described for automatic reading of antibiogram. Some new solutions are proposed to overcome these problems mentioned with the identification of antibiogram inhibition zones. The software

executing the method automatically measures the inhibition zones. The results are given in minimum inhibitory concentration and as a significant intermediate of resistant susceptibility. The process is quite fast and accurate according to laboratory measurements. Automated measurements create real clinical trials possible and awareness. In the future, the accuracy of these measurements allows the prediction of the resistance of the bacteria to different antibiotics. Finally, it can be said that this software tool implemented for antibiogram analysis can be applied in any antibiogram as an open source and free tool without any investment in new equipment or making any changes in the laboratory.

1.1 Motivation of the Thesis

The aim of the thesis is to evaluate the Antibiogram, getting an accurate image processing algorithm for identifying, calculating and classifying growing regions of inhibition from plate images captured by a digital device. Antibiogram is an accessible platform with self-determining open source and tools. Although there are many studies on manual physicians based examinations of an antibiogram analysis has been found, but automated antibiogram image processing has not reached the desired point and routine clinical use has not been reached. Therefore, further research is needed in the development of computerized image processing methods in order to provide a close cooperation between manual reading antibiogram analysis and computerized image processing antibiogram analysis.

1.2 Organization of the Thesis

The chapters of this thesis are organized as follows:

Chapter 1 is an introduction to the thesis, general information about the Antibiogram is given.

Chapter 2 In this chapter, the purpose of this thesis is discussed and the background about the antibiogram analysis is explained, also analysis of the organisms' susceptibility and resistance to antibiotics, determining genetic relatedness and the literature review of Kirby-Bauer Method, image acquisition and the literature review of computerized image processing algorithm parts are included.

Chapter 3 This chapter discusses the Material and Methods of Automatic Computerized Image Processing Algorithm, Manual Readings, Image Classification and Accuracy.

Chapter 4 overall study is discussed and evaluated the results of this study.

Chapter 5 summarizes the thesis work, discusses the result in conclusion part and presents some suggestions for future research and finally the references, the publications used in this research are listed.



CHAPTER 2

LITERATURE SURVEY AND BACKGROUND

2.1 Reading and Understanding an Antibigram

Nowadays, there is major increase in antimicrobial resistance with the multiple and often combined enzymatic mechanisms that affect an increasing number of microorganisms. In order to understand the resistance of the mechanism behind the phenotype resistances in the past, an interpretive analysis of an antibiogram was used, but the automatic or program readings could effectively classify the resistance mechanism [3, 11]. A microorganism may have several synchronized mechanism of resistance; this resistance may be caused by unique phenomenon mutation in objective genes or by the acquisition of other genes. Furthermore, when resistance to an antibiotic develops from a high frequency, there is a major risk that resistance may be chosen during treatment with mono-therapy [1, 12]. Many methods have been used to describe the resistance mechanism. Unfortunately, these methods have not been used everywhere, because they are quite expensive and also have many limitations.

2.1.1 Current Technologies

Furthermost new knowledge in the field of Antibiotic Susceptibility Testing (AST) Systems is usually used for bacterial development or metabolism to determine the consequence of antibiotics. Antibiotic susceptibility testing systems are categorized into three groups according to the principle applied. The most common tests are shown in Figure 2.1.

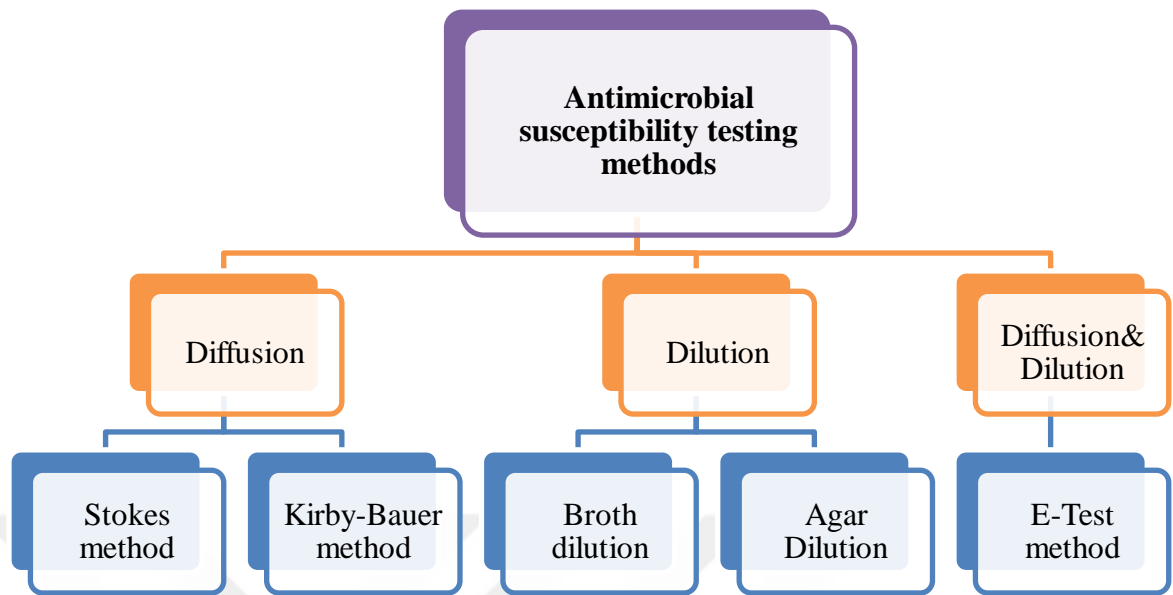


Figure 2. 1 Antimicrobial susceptibility testing methods

2.2 Manual Systems in Clinical Microbiology

2.2.1 Broth Dilution Test

The broth dilution method was the most primitive clinical microbial manual technique [13]. In this method, multiple tubes are used, each containing a two-fold concentration of the tested antibiotic organism. Each tube volume is 1 ml or greater, so it is called a macro broth dilution test. Because of the large amount of exercise for dilutions of antibiotics, the accuracy of this test was measured with a 2-fold concentration plus or minus 1 [14]. The main advantage in this method was the group of measurable results. The disadvantages of this technique were the tedious manual system in which the antibiotic solution was prepared for each test. Therefore, it is necessary to prepare a large amount of component and space for each test. Small, disposable and plastic practical and common trays are used for this test. It is a standard tray with 96-well plates each having a volume of 0.1 mL and contains about 12 antibiotics for each tray in the 8 two-fold dilution range (Figure 2. 2).

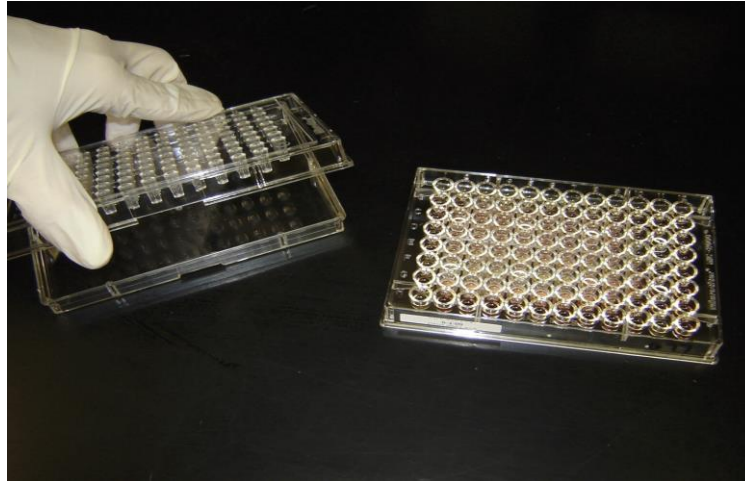


Figure 2. 2 A broth microdilution susceptibility panel containing 96 reagent wells and a disposable tray inoculator [5]

2.2.2 Agar Dilution Method

The agar dilution method is a well-known method of combining antibiotic testing directly into agar medium compared to a particular bacterium. The bacteria are then inoculated into internal agar plates with diameters of 5 to 8 mm. These plates are allowed to maintain and enlarge them within 16 to 18 hours. The lowest absorption of antibiotic plates is used without bacterial growth is measured, even though only one antibiotic absorption could be tried for each plate. However, in this method, more than one organism can be examined in a plate using the inoculum replicator, which can be allocated 32-36 mm in each plate [12]. In contrast, this manual test determines the Minimum Inhibitory Concentration or MIC value, and can sometimes be misunderstood when the inhibition regions are not visible.

2.2.3 Kirby-Bauer Disk Diffusion Susceptibility Method

In 1928, Alexander Fleming discovered antimicrobial compounds, a turning point in history. It has been discovered that infectious diseases can be eliminated by using antimicrobials [14]. Unfortunately, after several years these antimicrobials were gradually decreased because all patients were called for test to determine the susceptibility or resistance of the drug by physicians in the microbiology laboratory. A new method for susceptibility to antimicrobials based on the broth dilution approaches was then established [5, 14]. In this method, a disk diffusion process was used (Figure 2. 3).

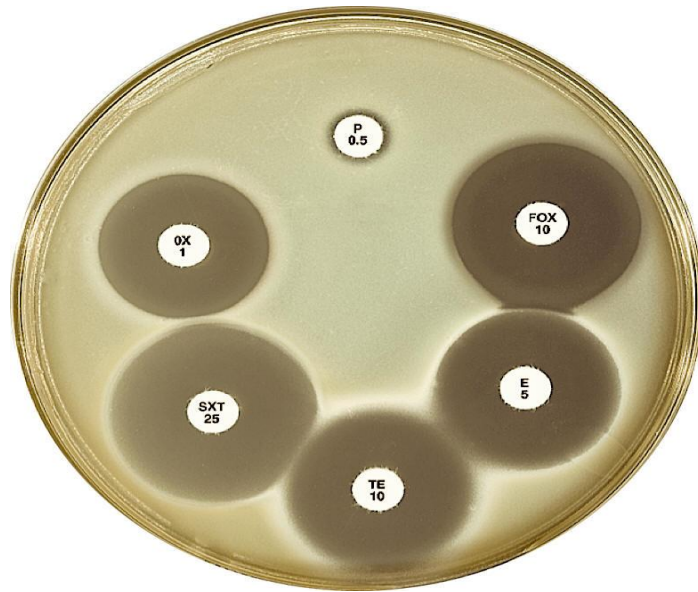


Figure 2. 3 Kirby-Bauer Disk Diffusion Method [5]

In the 1950s, all medical microbiology laboratories, especially in the United States, used disk diffusion technique for susceptibility to antimicrobials. Each laboratory had its own system to meet the individual needs. Many studies have published different results and processes in order to achieve better results that create more confusion. Therefore, in 1956, W. M. M. Kirby and his associates at the University of Washington and the king county clinic proposed a single disc technique for antimicrobial susceptibility testing [7, 8]. In 1960, they updated the literature and standardized the Kirby-Bauer disk diffusion method. The Kirby-Bauer disk diffusion method has been changed globally by the Clinical Laboratory Standards Institute (CLSI).

The Kirby-Bauer disk diffusion test is a simple, more practical and standard technique. In this process, large diameter Mueller Hinton agar plates are used. The diameter of the region is related to the susceptibility of the isolate and the rate of diffusion through the agar medium of the drug [9]. The diameters of the regions depend on the liability of the diffusion rates of the preparation on the agar standard. In this test, bacterial samples are isolated from the patients, spread on a new agar plate with the swab used. Several predetermined antibiotic saturated filter disc concentrations are placed in the plate at 37 degrees for 16 to 23 hours. In this test, a

large number of drug concentrations can be tested in a single agar plate, but the results were unable to identify the MIC value, which is the perfect medical result for the treatment of real patients [9, 10].

2.3 Image Fundamentals

Image processing is a technique that makes some operations on the image to get more useful and clear information from the image. Image processing is a similar type of signal processing method that the input is an image and the output can be image features. At the present time, image processing applications are rapidly increasing technology. Its main research areas are Computer Engineering and Clinical Microbiology Laboratory.

Image processing has three fundamental steps:

- Importing the images through image acquisition tool
- Image analyzing and classification
- Making an image altered outcomes that are obtained in the image analysis.

Moreover, two types of methods are used for image processing, where the first one analog image processing and second one is digital image processing. Analog image processing can be used in hard copies, such as printouts or photographs, and in many different graphics applications. Digital image processing methods are computer based. Digital images are expressed in n-dimensional matrix. Each element is basically in a two-dimensional matrix called pixels. Multi-dimensional images are able to be used in biomedical and medical science. Also, all images can be seen by mixing the three main colors visible spectrum in the human eye. As a result, all pixels of a color image can be characterized by 3 different channels. They are called RGB (red, green and blue) colors represent the true natural life colors.

It is also characterized by a 3-dimensional matrix of width, height and color proportions for the three-dimensional planar image. However, a total of 4-dimensional matrix is needed for volumetric image. Also, if the image changes in time in this case, a dimension is added. The output of the clinical image process may be monochrome, even if the actual color is present. For example, Magnetic

Resonance Images can be characterized by a 2-dimensional matrix in which the element represents the density value. These images consist of 1 value pixels called grayscale. A true color image can be changed with a grayscale image by selecting only 1 color channel [15, 16].



Figure 2. 4 An original color image



Figure 2. 5 A grayscale color image



Figure 2. 6 A binary image using thresholding

Other common image types used in image processing are called binary images. Binary images consist of two numbers 1 and 0. Since binary images have been adopted in binary image processing, they are used for different operations, in object calculating or features extraction. Scientific Morphology is primarily proposed for binary image after using more general grayscale images. Therefore, grayscale images are converted to binary images using thresholding or region magnification algorithms. In general, clinical or medical images are grayscale, so they are often converted to binary images. In Figure 2.4, general color images are shown. In Figure 2.5, it is converted to grayscale using the summation of the channel. In Figure 2.6, binary images were obtained using the threshold method [15, 16].

2.3.1 Elementary Binary Morphology Method

The systematic morphology method is first applied to the binary image after it is generalized for grayscale and true color image. The simple processes of the binary morphology are often complemented by a probe called Structure Element or shortly SE. The structural elements may be considered as another binary image that is the same as the original images. Disc, ellipse, square, diagonal can also be applied as a Structuring Element in any arbitrary shapes. In Structuring Elements, most significant applications are size and shape. The SE can also change the original image detail smaller than the Structuring Element. In addition, Structuring Elements can change the original image details smaller than the SE, but they cannot change the original structures that are larger than the Structuring Element.

2.3.2 Morphological Erosion Operation

In the morphological erosion process, it focuses on the origin of the Structuring Element in which it scans the shapes of the main image without overcoming the boundary. In another way, it can be said that in the erosion operation, it is scanned by the origin image of structuring element, the outcome of AND operations within all pixels in Structuring Element and similar pixel in the original image is true. In Figure 2.7, the original image is blue on the left side and the green image on the right side is eroded from where the red color border traces the main image. In this process, the

disk shape Structuring Element is used which can be seen in Figure 2.7. In fact, morphological erosion affects the lines around the shapes, hence it is called erosion.

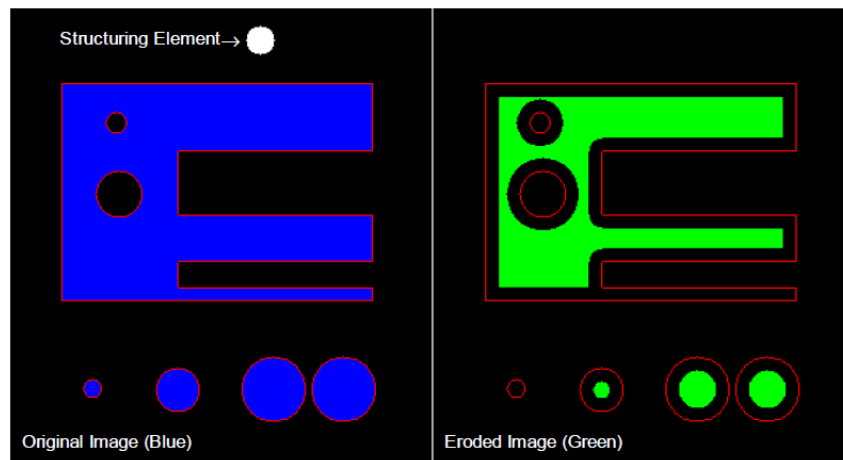


Figure 2. 7 Morphological Erosion Process

2.3.3 Morphological Dilation Operation

In the morphological dilation operation, SE element extends around the boundary, so it is called dilation. In the morphological dilatation process, it scans the original image without exceeding its original boundary. In another way, it can be said that in dilation operations, it is scanned by the Structuring Element while the output of AND operations within image of the structuring element and the corresponding pixel in the original image is true. In Figure 2.8, the left side blue color original image and the right side green image is dilated shape, and the red color border traces the original image. In this process, a disk shape Structuring Element is used which can be seen in Figure 2.8.

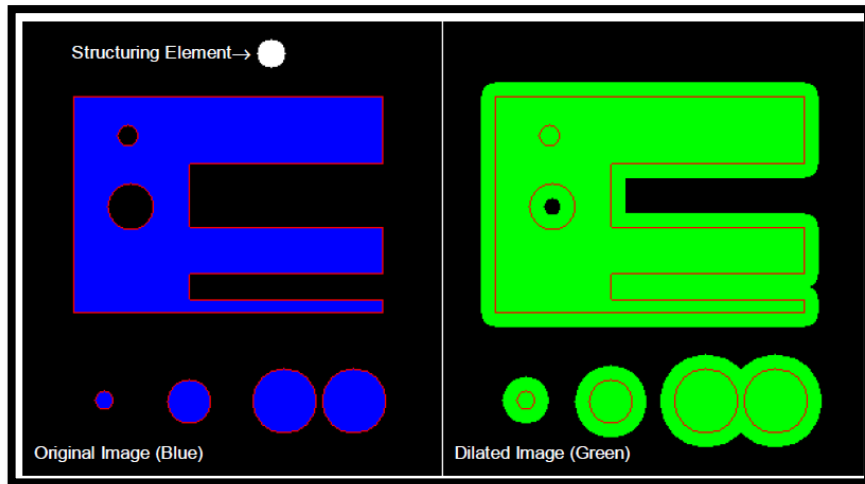


Figure 2. 8 Morphological Dilation Process

2.3.4 Morphological Opening Process

In the morphological opening process, it is applied in the dilation after erosion. In Figure 2.9, the blue on the left side is the original image after using the opening process, it can be seen the right side green image is opened form after that red plot is traced for the original image. In the morphological opening process, the image is scanned with the Structuring Element from inside without exceeding the original image boundary. In this process sharp corner, peninsula and objects smaller than the Structuring Element are eliminated.

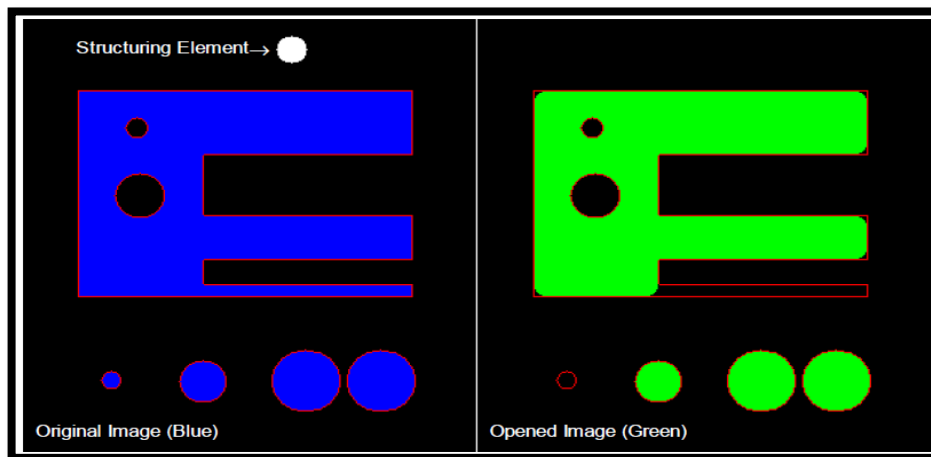


Figure 2. 9 Morphological Opening Process

2.3.5 Morphological Closing Process

In the process of morphological closing, an erosion process is applied to an image after dilation. Where 'I' stands for original images and 'S' stands for Structuring Element, finishing can be specified as follows: In Figure 2.10, the original image (I) in left side is represented with blue color, and in the right side green image is its closed form, also red color traces the original image. In this process, a disc-shaped Structuring Element (S) which can be shown in Figure 2.10 is used. In addition, images are scanned by Structuring Element from the outside without exceeding the boundaries of the original image. Also, in this process smaller cover and hole are filled from the Structuring Element.

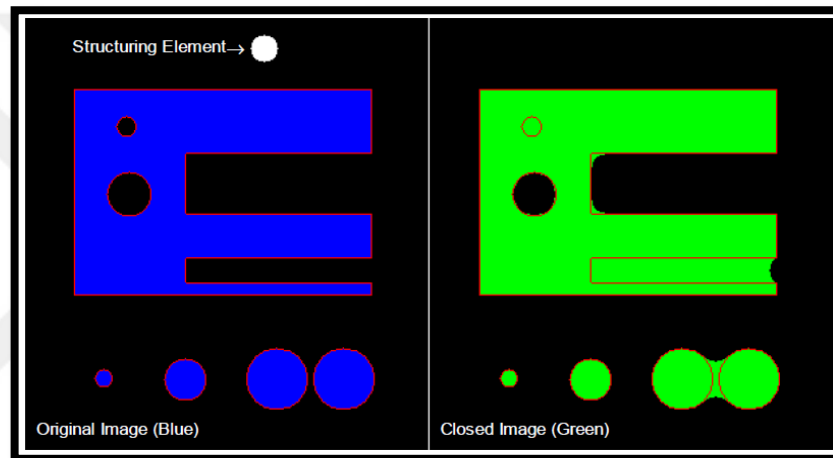


Figure 2. 10 Morphological Closing Process

2.3.6 Sequential Filtering process

In sequential filtering process, first the opening operation is performed after the closing operation or the closing operation is performed after the opening operation. In this process, an object and peninsula smaller than the Structuring Element are removed, such as cover and holes smaller than the Structuring Element. Using sequential filtering, the boundaries of shapes are smoothen. If peninsula by cove is there, both peninsula and cove remain, even though the other that allows opening and closing process disappears. If closing operation is performed first, cover is filled; also if opening operation is performed first, peninsula is eliminated. Moreover, smoothing is achieved. Both of these conditions are shown in Figure 2.11 and Figure 2.12.

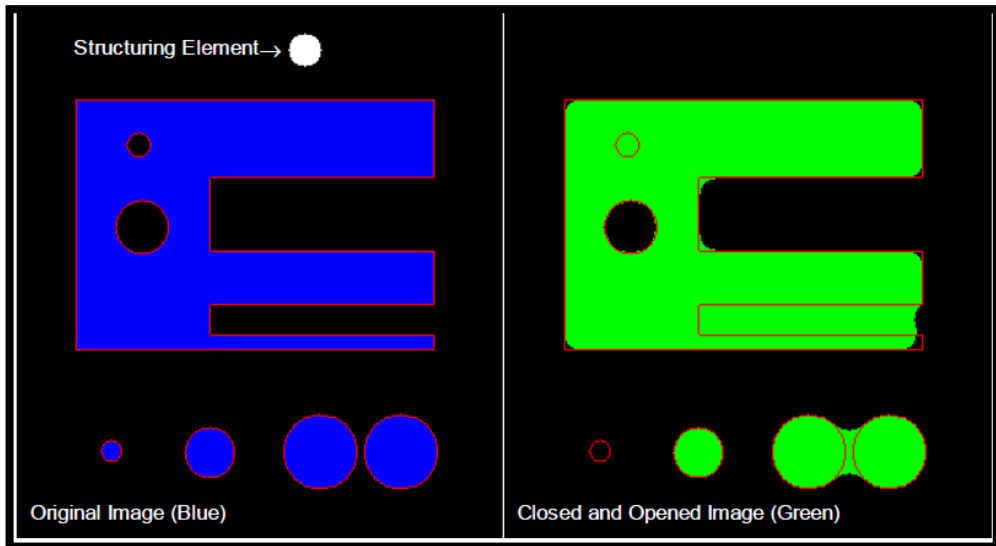


Figure 2. 11 Primarily Closed Image

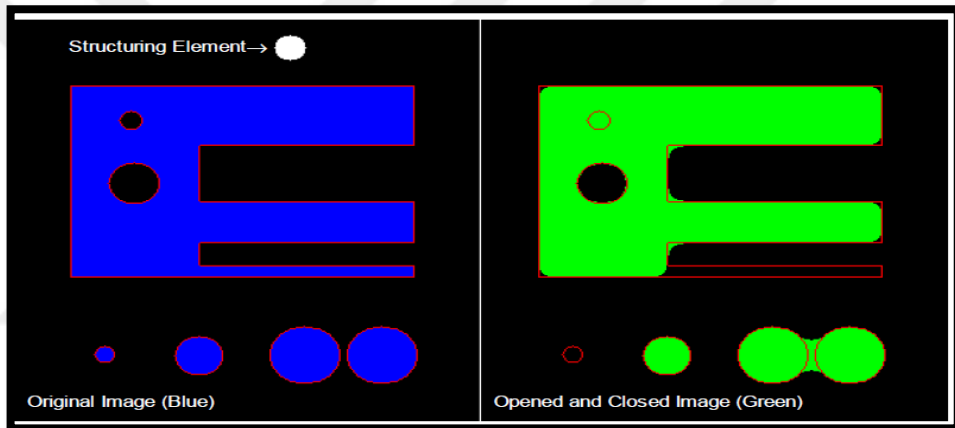


Figure 2. 12 Primarily Opened Image

2.3.7 Masking Fundamentals Process

The limitation of the image by using a similar size of another image is called masking. The limitation of the image is called a mask. Therefore, the mask image or original image can be binary or grayscale. These two cases are shown in Figure 2.13 and Figure 2.14. In these figures, the green plot is a one-dimensional original image, the red plot is a one-dimensional mask image and the black plot is the result of the masking process [17].

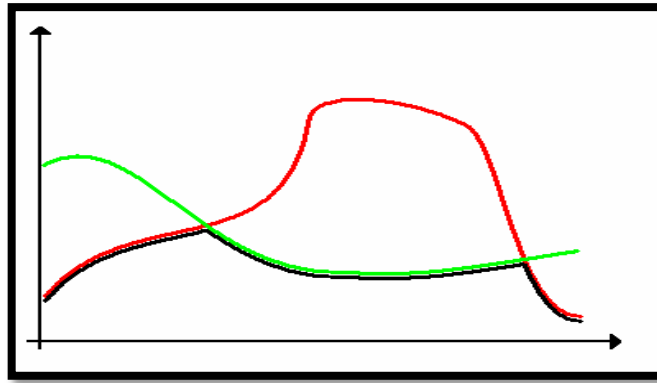


Figure 2. 13 Grayscale Image, Grayscale Mask

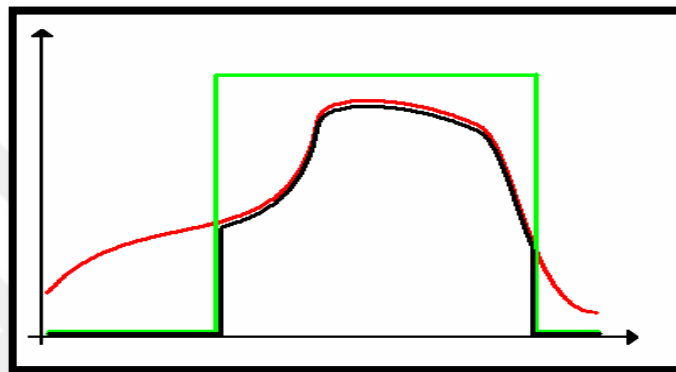


Figure 2. 14 Binary Image, Grayscale Mask

2.3.8 Distance Transform Process

In distance transform process, each zero value pixel in a binary image is converted to the distance values from the nearby nonzero value pixel. There are many different distance approaches where the shortest path between the two points is a straight line called Euclidean distances. Euclidean distances can be calculated using the Pythagorean Formula. In Figure 2.15, red stars showing the “1” valued pixels in image, where the rest is distance transform that affects the binary images. The brighter the pixels, the better the minimum distances.

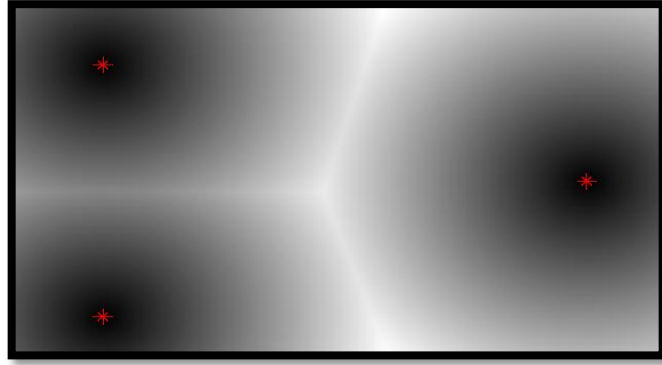


Figure 2. 15 Distance Transform Process

2.3.9 Hough Transform Process

The Hough transform method uses the isolation feature of a particular shape in images, since it is necessary to specify the desired feature in some parametric forms. The most common Hough transformation is the classic Hough transformation technique mostly used to detect regular curves such as straight lines, circles, ellipses and so on. A general Hough transformation can be performed in a particular application where an image is transformed into a parameter field that logically defines the selected shape. Due to the computational complication of generalized Hough transformation, the main application of this discussion is limited to classical Hough transformation. Also, with domain restriction, the classical Hough transformation, especially in the manufacturing part, maintains a variety of applications, it contains feature borders that can be defined by fixed curve. The biggest advantage of the Hough transform technique is that the gap in the border recognition is tolerated without being affected by image noise.

The Hough transform method is mainly useful for calculating a global definition of features and is less noisy for local measurement. The common fitting problem to set up a line segment to a set of separate image points and the possible solution to this problem are shown in the Figure 2.16 [17, 18].

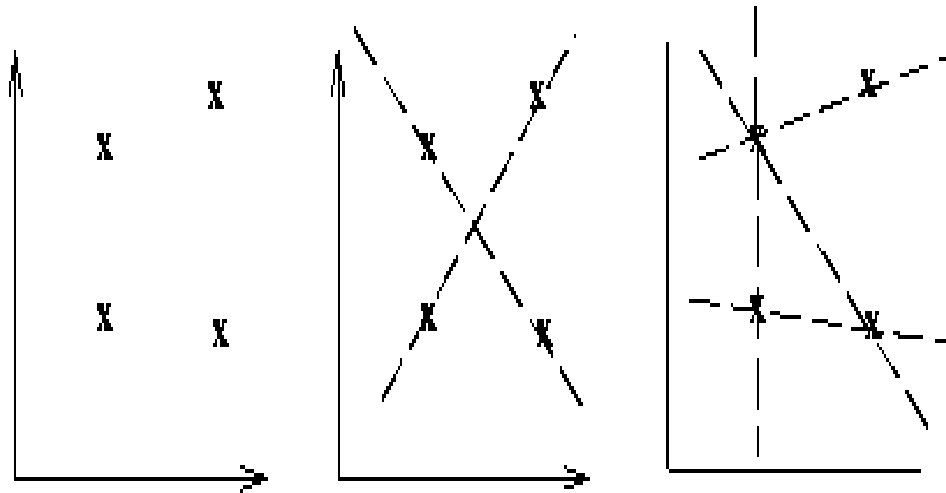


Figure 2. 16 a) Coordinate points. b) AND. c) Possible straight line fittings.

2.3.10 Otsu Image Segmentation Algorithm

There are many different algorithms and techniques for image segmentation. Until now, there is no common explanation of the image segmentation dilemma. Converting the image into a meaningful structure, image segmentation is the important step in image processing analysis. Image Segmentation is a methodology of separating digital images into various segments. Many image segmentation techniques are used in image processing where Otsu technique is one of the most effective methods for image thresholding. There are various image segmentation techniques, in all of them, Otsu method, one of the most successful methods due to the basic calculations. The Otsu thresholding is an automatic selection region based on the image segmentation algorithm.

In 1979, Nobuyuki Otsu first developed the class variance or Otsu's thresholding method for ease of calculation, consistency and also effectiveness. Otsu's thresholding method is very effective procedures used in thresholding selections, which are popular in rare time consumptions [19]. The Otsu threshold technique includes iterations with a total possible threshold value and regular layout evaluations for the total pixel level, including both sides of the threshold [20]. The predominant objectives are computed at the position where the threshold values, front and back ground addition are likely to spread. In the Otsu thresholding method,

the grayscale histogram is the main requirement but does not give a satisfactory segmentation result for the one-dimensional plane [21]. Therefore, the two-dimensional Otsu algorithm was proposed to overcome this problem. The two-dimensional Otsu algorithm also performs spatial correlation information on the grayscale threshold for each pixel. Therefore, the two-dimensional Otsu algorithm can achieve satisfactory segmentation result in noisy conditions. In addition, the Otsu thresholding method is one of the best threshold selection techniques for real time images in terms of uniform and shape measurements. Also, the total number of classes in the image increased the time limit of the multi-level thresholding options [19, 20].

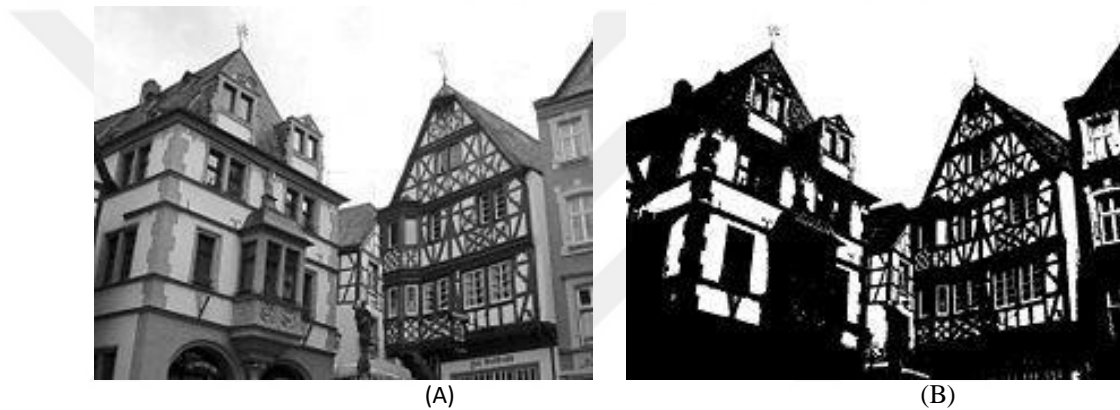


Figure 2. 17 (A) Original Image (B) Image Using Otsu Thresholding Algorithm [33]

CHAPTER 3

MATERIAL AND METHODS

In this chapter, each step defining Bacterial Isolates and Antibiotics, Manual Readings, Image Acquisition, Image Classification, Inhibition Zone Algorithm are explained. Identification of Inhibition Zones and Accuracy of the Measurements are examined.

3.1 Antibiogram Plate Images and Software

In this study, 16 different antibiogram Petri dishes with different bacterial habitats for each and a set of total 122 antibiotics are analyzed for susceptibility test. The size of 90x15 mm Petri dishes are used for the test. Image acquisition is performed using a device camera. Images are captured using a phone camera on the black background in jpeg format. The system is configured to obtain images with a size of 3024 x 4032 and 256-level colored with RGB channels.



Figure 3. 1 An antibiogram plate image

3.2 Manual Readings

In manual reading, each plate is analyzed by 2 independent human readers. A ruler is used to measure the diameter of each inhibition region. Normally, most of the specialists compare inhibition zone lengths by sense of proportion. So, the margin of human reading error is greater with this approach.

3.3 Feature Extraction of Antibioqram Plate Image

Computerized image processing gives clear information to extract features of Antibioqram Petri dish images. The image processing method supports common standard image formats such as tiff format, jpeg format, png format and bmp format. Therefore, for plate analysis, images in these formats can be used according to the available antibioqram search. In this study, the plate image analysis program is organized in 6 parts: input data, image preprocessing, feature extraction, reading and annotations of inhibition zones and extraction, analysis and determination of the original numerical properties (Figure 3.2). The algorithm that is implemented in MATLAB and includes all image processing parts is explained step by step below.

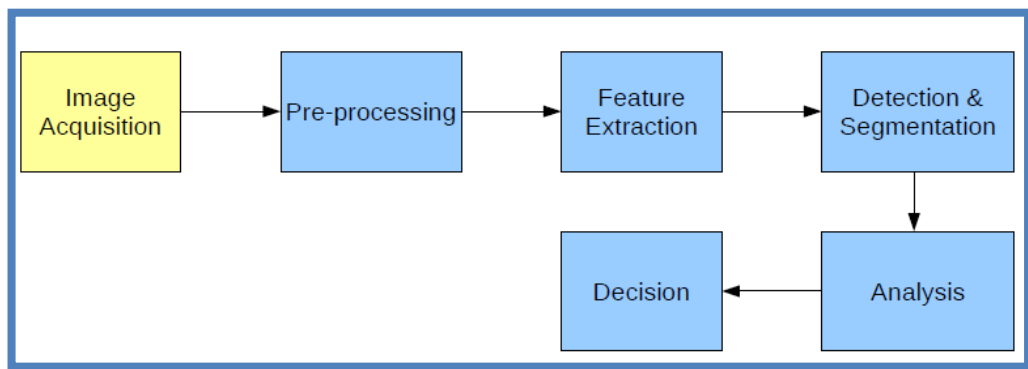


Figure 3. 2 Image processing parts

First step: All original antibioqram plate images accessed are saved in JPEG format. Besides, these JPEG format images are in non-standard directories. Therefore, first of all, all Petri dishes are checked and placed automatically on the antibioqram image files. These antibioqram image files are selected by user from a file selection

window. Multiple selections can be done and got file names “filename” and their path names “pathname”. The “filename” is checked for conditions that do not have a cell array or make no selection. If a file is selected and is not a cell, it is converted char array to a cell array. Variable “imgname” is obtained from first cell of “filename” cell array. Finally, image is read with the parameter resulting from concatenation of “pathname” and “imgname” and named as “img”. Images are checked that the image dimensions are 3024 x 4032 x 3, because the dimensions of the discs and the plate are predefined, and the change of size affects the algorithm.

Second step: These raw images are in RGB format that is 3-dimensional matrix. A color-related feature does not need to be used for antibiogram images. So, all raw original antibiogram images (Figure 3.3) are converted into grayscale images (Figure 3.4). After this operation, 1-dimensional matrix named as “imggray” is obtained. Grayscale image pixels are gray in color, typically ranging from 0 (black) to 255 (white), which means that each pixel can be represented by only eight bits or only one byte.

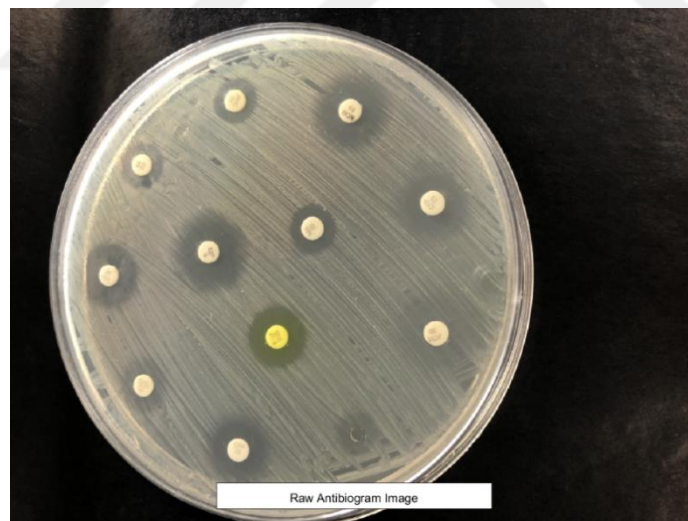


Figure 3. 3 Raw original image

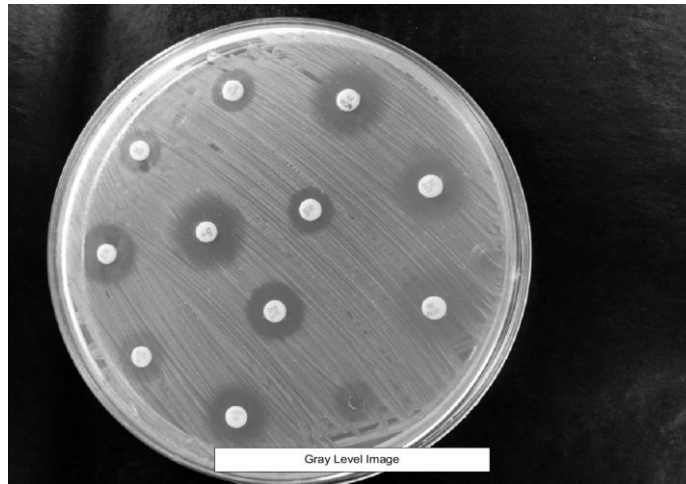


Figure 3. 4 Gray level image

All types of internal and external artifacts must be eliminated to extract the numerical features related to antibiogram images other than Petri dishes, therefore Petri dish images are the main interest. The grayscale image is converted to the binary image using Otsu thresholding (Figure 3.5). This operation is performed in 2 steps that are finding a gray level threshold and using it for binary image transformation. A gray level threshold (global image threshold) is obtained by Otsu thresholding from the image "imggray" and named as "graylevel". Otsu thresholding provides separating 2 groups that the variation within the group is at least so that the variation between the groups is at most. After this operation, "graylevel" is obtained in normalized form in the range from 0 to 1. In binary image, pixels are considered within two possible values as 0 (image background pixels) and 1 (image foreground pixels). In addition, pixels are represented by only two colors black and white. To convert the gray level image to binary image, a replacement operation is performed. In this operation, according to the luminance, all pixels having greater luminance than obtained gray level threshold value "graylevel" are replaced with 1 (white) and all other pixels are replaced with 0 (black) in "imggray" image. Using "imggray" and "graylevel" with the result of this operation, the output image is obtained and named as "imgbwmask". The unrelated parts of the image will be discarded using this mask later. After that, the aim is to discard the artifacts such as glares out of the plate which can be seen in Figure 3.5. For this operation, objects are extracted from the image "imgbwmask" by size. The first largest object is obtained when objects are filtered by size and the result is overridden on the "imgbwmask". The first largest

object is the plate. As a result, the maximum objects in terms of zones are measured; binary image is converted to the binary image of the largest object (Figure 3.6).

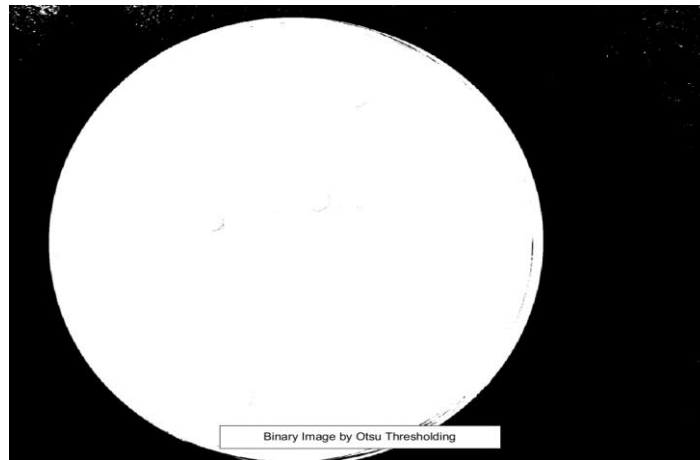


Figure 3. 5 Binary image by Otsu thresholding

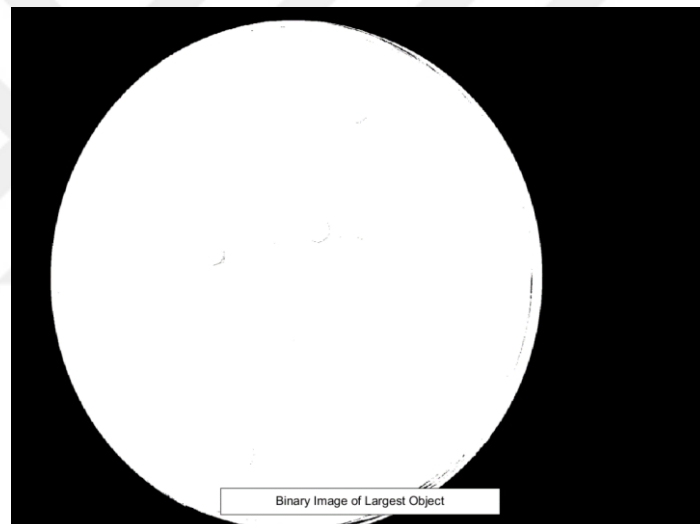


Figure 3. 6 Binary image of largest object

Third Step: In the third step, as shown in the binary image of the largest object, some extra objects are surrounded by the Petri Dish (Figure 3.6). The smallest rounded polygon that enclosed total white object in the image is used to select all the small parts between them. All objects touching this polygon are selected and morphological erosion is applied. The minimum curved polygon itself is selected after morphological erosion method is applied. To smooth the sharp edge of selected boundary, closing morphological operation is performed by using disk shaped operations. Moreover, the gaps inside the area of mask are filled, and finally the total

boundary is determined using Binary image (Mask) by the filling holes method (Figure 3.7 and 3.8). For these operations, firstly, filling operation and then erosion operation is applied. Holes of the binary image “imgbwmask” are filled and the result is overridden on the “imgbwmask”. In filling holes operation, a hole is a set of background pixels, but it is not from the edge of the image. These holes are filled as in the example of these matrices A (before filling holes) and B (after filling holes):

$$A = [1\ 0\ 0\ 0; 1\ 1\ 1\ 0; 1\ 0\ 1\ 0; 1\ 1\ 0\ 0]$$

$$B = [1\ 0\ 0\ 0; 1\ 1\ 1\ 0; 1\ 1\ 1\ 0; 1\ 1\ 0\ 0]$$

After filling the holes of the image, operation gets rid of gaps that could affect the algorithm in the image in Figure 3.7. The gaps of the plate can be seen in Figure 3.6. After that, the aim is to get rid of the edges of the plate, because there are some artifacts that caused by glares that can affect the algorithm. So, morphological erosion is applied to the image. The erosion operation uses the “imgbwmask” image and a structuring element and the result is overridden on the “imgbwmask”. Morphological structuring element is created as a disc shaped and radius of 200 pixels. The structuring element is chosen as a disc which is suitable for the plate and 200 pixels which is radius of the disc to erode the edge of the plate. The eroded image can be seen in Figure 3.8.

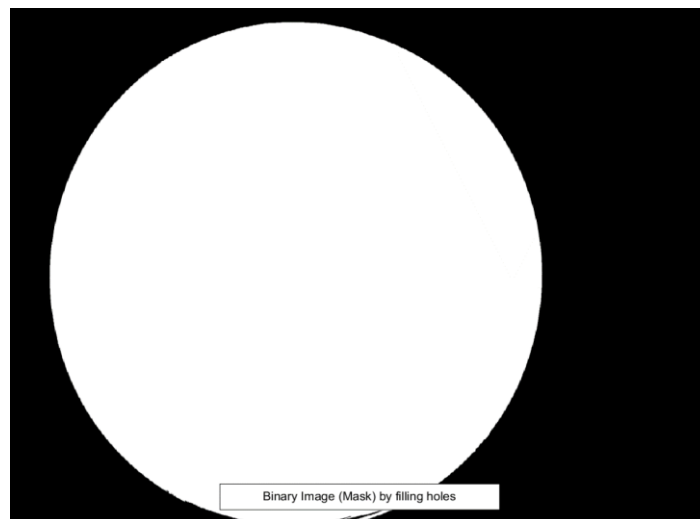


Figure 3. 7 Binary image (Mask) by filling holes

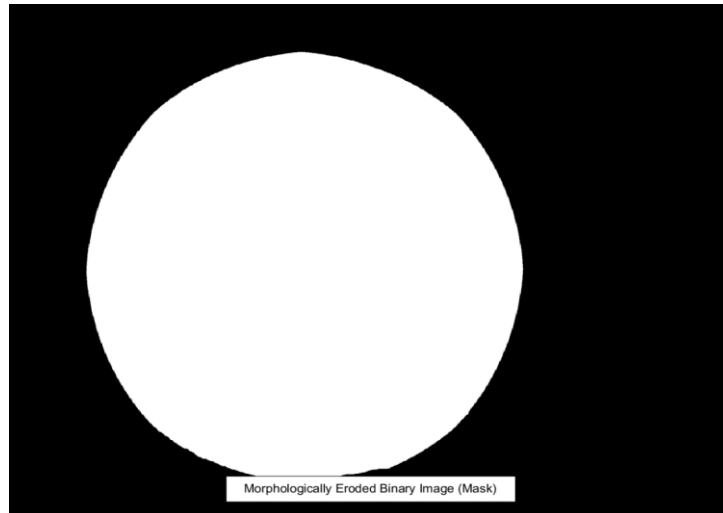


Figure 3. 8 Morphologically eroded Binary image (Mask)

Fourth step: Since the antibiogram does not have any limitations or conditions for the device that captures the image of the Petri Dishes, thus that creates a massive inconsistency on these images. Therefore, the quality of the Petri Dish image is tried to be adjusted using the morphologically closed gray level image function. Using these functions, the brightness and contrast of the plate images can be adjusted more carefully. So in this step, first the Petri dish images are converted by getting the gray level image mask by the binary mask. The morphologically eroded image and gray level image are used to obtain masked image. In mask operation 2 parts exist that one part is white area which is kept and other one is the black area which is disposed of. So, pixel to pixel product of “imggray” and uint8 (8 bit gray level image having values from 0 to 255) of “imgbwmask” matrices is used with element wise multiplication. 1’s are kept and 0’s are discarded in “imgbwmask” matrix. After this product operation, “imggray” are masked with “imgbwmask” and named as “imgmasked”. The result can be seen in Figure 3.9.

Then, morphologically closing operation is applied to gray level image (Figure 3.10). In the morphologically closing function, the plate having the same original structure elements retained the image background region and eliminated all other regions of the background pixel. In the image, the bacterial culture is irregularly applied and there are drugs’ identical numbers on them which can be seen in Figure 3.9. Morphological closing provides smoother area of bacterial culture and getting rid of the drugs’ numbers. Also, the borders of the inhibition zones are smoothen and

become easier to detect. For this operation, “imgmasked” image and a structuring element are used and the result is named as “imgclosed”. The morphological closing operation is dilation and then an erosion operation applied using the same structuring element. Morphological structuring element is created as a disc shaped and radius of 10 pixels. The structuring element is chosen as a disc which is suitable for the plate and 10 pixels which is radius of the disc for closing. The closed image can be seen in Figure 3.10.

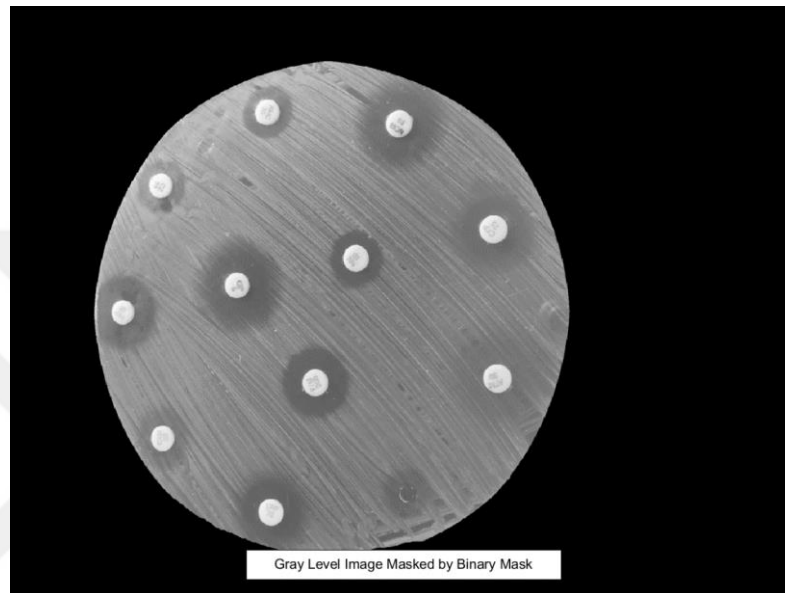


Figure 3. 9 Gray level image mask by binary mask

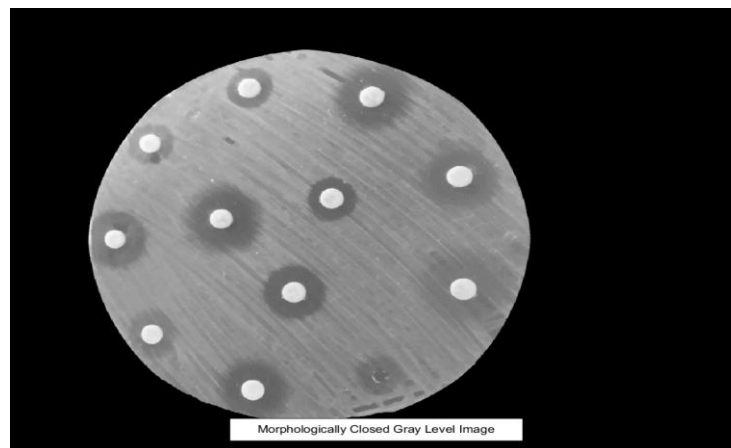


Figure 3. 10 Morphologically closed gray level image

Fifth step: After that, Circular Hough Transform method is applied to find circles. The Circular Hough Transform is used to find out instances image of the object within a positive class of circular shapes centers. The method is applied to image

“imgclosed” specifying the range of radii of circles to be found. The range is determined as 50 to 80. If the range is increased, the probability of finding incorrect results increases. “ObjectPolarity” feature is set as “bright”. The “bright” is chosen to indicate finding bright circles that are brighter than the background. “Sensitivity” feature is chosen as 0.95 and “EdgeThreshold” feature is chosen as 0.05. These parameters are given as different values for different circles to find. These parameters are determined for the antibiogram image as a result of trials. After Circular Hough Transform operation, 3 outputs are obtained as centers matrix of circles with x and y coordinates named as “centers”, radii matrix of the circles and metric that indicates the information of how close it is to the circle. Then found circles which can be seen in Figure 3.11 are drawn on the image using the parameters “centers”, “radii” and “EdgeColor” as ‘g’ which ‘g’ stands for green. The “centers” and “radii” matrices results are shown in Table 3.1 and Table 3.2 for first antibiogram image as an example. Also, the circle numbers are added to the image (Figure 3.11) using “centers” matrix.

Table 3. 1 Centers of the circles found

Circles/ Coordinates	X	Y
1	2481,12759504471	1840,66289546505
2	1229,85629362719	1389,98446425862
3	1793,77571624851	1251,91985219815
4	2463,89174790328	1098,59806797669
5	1597,36352707095	1860,38330691262
6	1381,69558757350	2496,26246684907
7	697,105870801017	1522,11434264547
8	875,483017925440	2130,05418125351
9	2004,36128133489	588,807310850691
10	1375,71525673289	548,668903108606
11	875,045260475246	914,070504026698

Table 3. 2 Radii of the circles found

Circles/ Radii	1
1	70,7549824364222
2	60,1940632528359
3	63,3666859522703
4	69,3791086659913
5	64,5599123278149
6	62,5271575888343
7	56,7239745056716
8	57,6961346706111
9	64,4236220010461
10	61,5967102097206
11	56,9907093859490

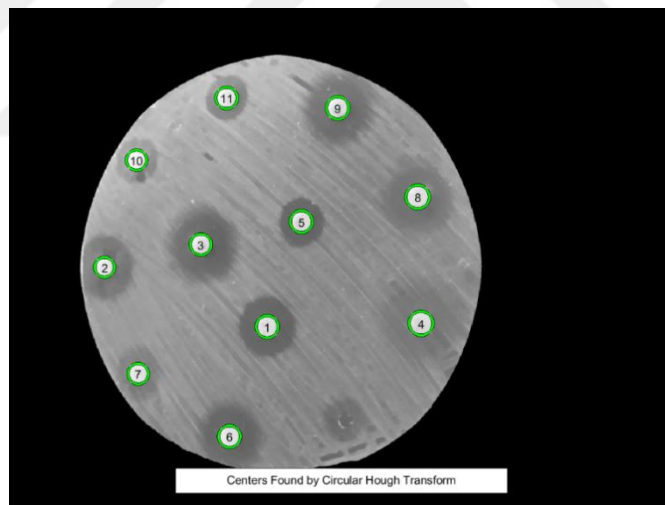


Figure 3. 11 Circles found by Circular Hough Transform

Then, found circles are removed to improve the inhibition zone border finding (Figure 3.12). First, the values corresponding to circles of the image must be set to NAN to remove these areas. For all circles, subtraction from the x coordinate by a radius, insertion from the x coordinate by a radius, subtraction from the y coordinate by a radius and insertion from the y coordinate by a radius are equalized to NAN. So, the “imclosed” matrix is modified with this block:

```

For i = 1 to size of first axis of “centers” matrix do
    imgclosed(y coordinate of center(i) - radii(i) converted to 16-bit unsigned
integer to
        y coordinate of center(i) + radii(i) converted to 16-bit unsigned integer,
        x coordinate of center(i) - radii(i) converted to 16-bit unsigned integer to
        x coordinate of center(i) + radii(i) converted to 16-bit unsigned
integer)=NaN;
Endfor

```

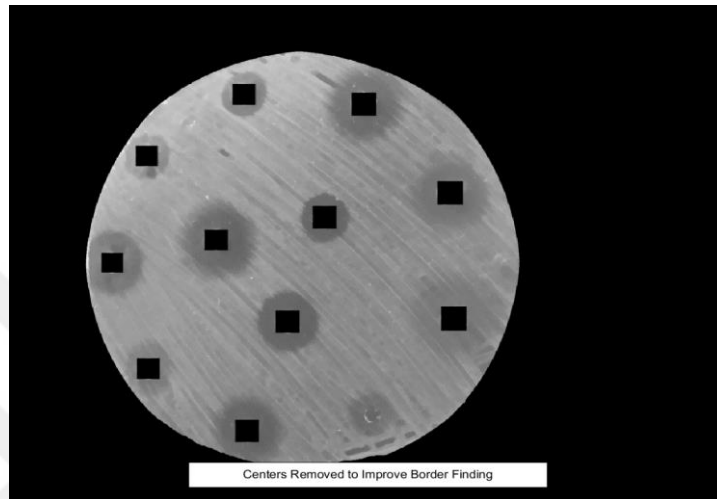


Figure 3.12 Circles removed to improve border finding

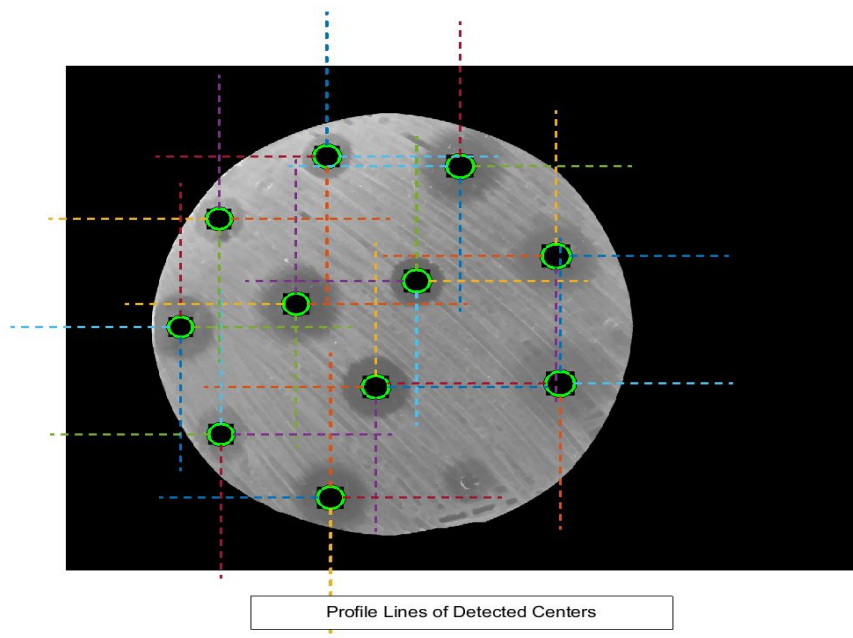


Figure 3.13 Profile lines of detected centers

After that, for each selected image zones, circles with specified centers and radii are drawn on the present axes separately (Figure 3.13). Subsequently, profiling operation is applied to get the intensity value of pixel along the multiline paths of the plate zones images in the present axes and shows a plot of the intensity values. Border detection of inhibition zones is performed at this stage and these operations are applied for all centers. For profiling, first, 2 matrices are created and the profile unit is chosen as 800 pixels for the antibiogram images. For all centers, xi and yi matrices are created to be used for profiling process which are shown below:

```
xi=[centers(i,1)+radii(i)
    centers(i,1)+radii(i)+800
    centers(i,1)-radii(i)
    centers(i,1)-radii(i)-800
    centers(i,1)
    centers(i,1)
    centers(i,1)
    centers(i,1)];
yi=[centers(i,2)
    centers(i,2)
    centers(i,2)
    centers(i,2)
    centers(i,2)-radii(i)
    centers(i,2)-radii(i)-800
    centers(i,2)+radii(i)
    centers(i,2)+radii(i)+800];
```

Then, an algorithm is performed to create “profiles” matrix using xi and yi matrices. The “profiles” matrix is filled with 4 profiles. In each loop, two elements of the xi and yi matrices are added to profile matrix. So, y coordinate is constant where x coordinate from center plus radii to 801 is drawn, y coordinate is constant where x coordinate from center minus radii to 801 is drawn, x coordinate is constant where y coordinate from center plus radii to 801 is drawn and x coordinate is constant where y coordinate from center minus radii to 801 is drawn with below block:

```
For p = 1 to 4 do
    profiles(first axis, p) = profiling on “imgclosed” with xi(2*p-1 to 2*p),
    yi(2*p-1 to 2*p) and 801 that the number of points to include.
Endfor
```


The result of first circle of the “profiles” matrix is an 801x4 matrix. So, some of the results are shown in Table 3.3 as an example. After that, finding the nonzero values of this “profiles” matrix is aimed. So, “nonzeroprof” matrix is created from the “profiles” matrix with the condition not equal to 0 values. In “nonzeroprof” matrix, nonzero values are represented with 1, and zero values are represented with 0. Table 3.4 shows the result of first circle of the “nonzeroprof” matrix which is an 801x4 matrix. Then, the second axis values of the “nonzeroprof” matrix are summated and the result is overridden to “nonzeroprof” matrix. The result is shown in Table 3.5. After that, the variable ‘k’ is found where the summation of profiles decreases from 3 to 2 in “nonzeroprof” matrix. For this operation, occurrences of this pattern are searched. The output ‘k’ indicates the initial index of each occurrence. If ‘k’ is not empty, values from the first element of k to the end, first axes of the “profiles” matrix are deleted. ‘k’ is found as 510 for first circle in the example and “profiles” matrix size decreases from 801x4 to 509x4.

Table 3. 3 Some values of profiles matrix

Pixels/Profiles	1	2	3	4
1	0	0	0	0
2	154	140	130	159
3	134	140	130	123
400	0	149	141	149
401	0	145	141	150
601	0	145	112	0
602	0	145	114	0
603	0	145	0	0
604	0	145	0	0
800	0	0	118	0
801	0	0	118	0

Table 3. 4 Some values of nonzeroprof matrix

Pixels/Profiles	1	2	3	4
1	0	0	0	0
2	1	1	1	1
3	1	1	1	1
400	0	1	1	1
401	0	1	1	1
601	0	1	1	0
602	0	1	1	0
603	0	1	0	0
604	0	1	0	0
800	0	0	1	0
801	0	0	1	0

Table 3. 5 Sum of the second axis of nonzeroprof matrix

Pixels/Sum	1
1	0
2	4
3	4
400	3
401	3
601	2
602	2
603	1
604	1
800	1
801	1

Some values can be NaN because the profile lines may have gone out of the plate. Getting rid of any NaN value is needed, so that, the same process applied for nonzero values is applied for nonnan values. So, “nonnanprof” matrix is created from the “profiles” matrix with the condition of being NaN. In “nonnanprof” matrix, nonnan

values are represented with 1, and NaN values are represented with 0. Table 3.6 shows the result of first circle of the “nonnanprof” matrix which is a 509x4 matrix as an example. Then, the second axis values of the “nonnanprof” matrix are summated and the result is overridden to “nonnanprof” matrix. The result is shown in Table 3.7. After that, the variable ‘k’ is found where the summation of profiles decreases from 4 to 3 in “nonnanprof” matrix. For this operation, occurrences of this pattern are searched. The output ‘k’ indicates the initial index of each occurrence. If ‘k’ is not empty, values from the first element of k to the end, first axes of the “profiles” matrix are deleted. In the example, ‘k’ is not found for first circle, so there are no NaN values in the “nonnanprof” matrix.

Table 3. 6 Some values of nonnanprof matrix

Pixels/Profiles	1	2	3	4
1	1	1	1	1
2	1	1	1	1
...	1	1	1	1
508	1	1	1	1
509	1	1	1	1

Table 3. 7 Sum of the second axis of nonnanprof matrix

Pixels/Sum	1
1	4
2	4
...	4
508	4
509	4

Sixth step: In this step, the undetected inhibition zones are eliminated. The original inhibition zones boundaries are determined and minimum distance to these boundaries for all pixels inside the inhibition zones are calculated and indicated by four different profile lines as Profile 1, Profile 2, Profile 3 and Profile 4. The distance

profile lines are shown in Figure 3.13. Furthermore, median values array of detected inhibition zones is calculated. Then, the smooth median values are obtained representing the inhibition zones, or the smoothing with the median values. After that, detected inhibition zones are shown in Figure 3.14 on closed image and in Figure 3.15 on antibiogram image.

After adjustments in “profiles” matrix, “medianprofile” matrix is obtained from “profiles” matrix by taking the median of the second axis. In sorted order, the median value is the mean of the middle two numbers. The median is taken to find out the most reasonable value and eliminate outliers. Then, getting smoother bacterial culture and inhibition zone borders is aimed to obtain explicit image before the inhibition zone finding operation for the same purpose of closing operation. So, smoothing operation is performed using “lowess” smoothing method on “medianprofile” and the output is named as “smoothedmedianprofile”. “lowess” uses linear 1st degree polynomial model to use in the regression. The first ten element of the “smoothedmedianprofile” matrix equalized to NaN, because finding the zone border for this range is not expected. In this range, some errors can be occurred because of the smoothing operations.

Again, Otsu thresholding method is used to differentiate the pixels that are in the zone and out of the zone on the profile lines and where the distinction is provided is detected. So, a global image threshold is obtained by Otsu thresholding for this operation from the nonnan values of “smoothedmedianprofile” matrix in type of uint8 (8 bit gray level image having values from 0 to 255) and the result is named as “valleylevel”. This “valleylevel” variable is found in normalized form in the range from 0 to 1, so this is multiplied with 255 and got the value in the range from 0 to 255. This “valleylevel” is used as the distinction value, so that, values greater than “valleylevel” are out of the zone and values under the “valleylevel” are in the zone. For finding the transition, a zero matrix is created with size of “smoothedmedianprofile” matrix and named as “isplateau”. Then, the values of “isplateau” matrix greater than the “valleylevel” are set to 1 and again, the first ten elements of the “smoothedmedianprofile” matrix equalized to NaN, because finding the zone border for this range is not expected and to avoid the errors. After that, to

find distinction value with the transition condition [0 0 0 1 1 1], occurrences of this pattern are searched and the result indicating the initial index of each occurrence named as “border”. 3 zeros and 3 ones is used, because there may be some noise for the transition from zero to one. If “border” is not empty which means borders are found, first border is chosen, because multiple borders can be found due to noise. This border found is added to the “borderlist” variable and it is drawn on image using parameters centers(i, 1 to 2) and border+radii(i). The center coordinates and radius of the drug plus found border length are given. If “border” is empty, “Border is not found” is printed and the next element of the “borderlist” is set to NaN. The result border and the radius in pixels are shown in the Figure 3.14 and Figure 3.15. Also, borders are kept in the “borderlist” and displayed. All antibiogram image processing calculations and statistical analyses are performed using MATLAB environment.

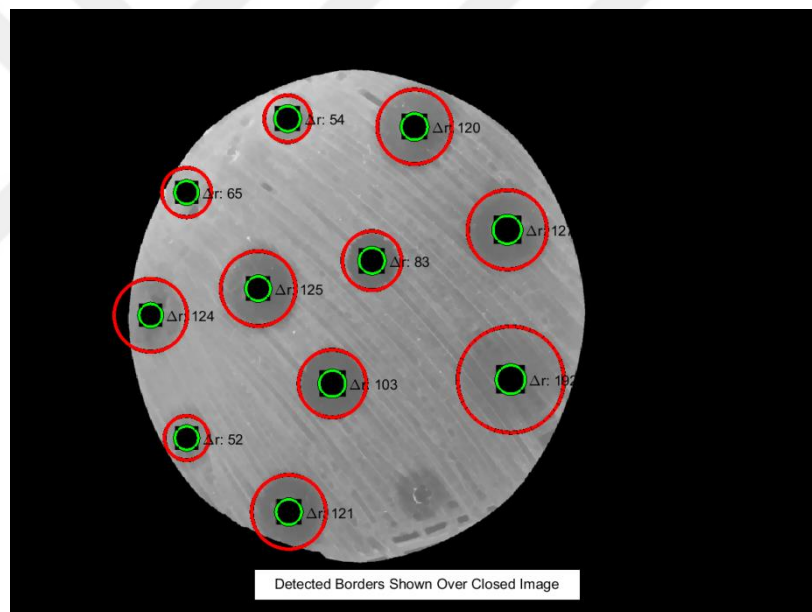


Figure 3. 14 Detected borders shown over closed image

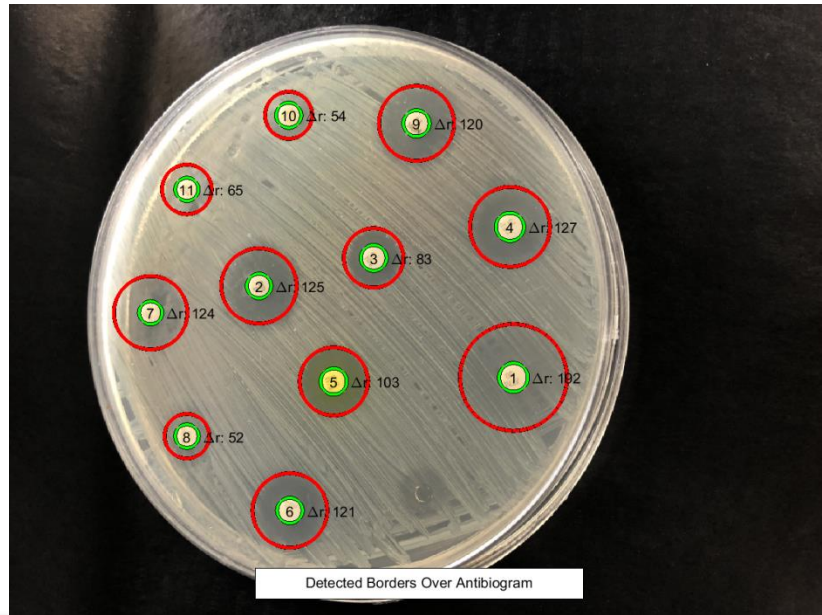


Figure 3. 15 Detected borders over antibiogram

CHAPTER 4

RESULTS AND DISCUSSION

4.1 Identification of Inhibition Zones Border Lines

Two main steps are performed in this study, the first step is identification of the inhibition zones borders and the second step is to measure the diameter of the inhibition zones. In the previous chapter, automatic antibiogram image processing border line identification algorithm is mentioned. In this chapter, overall study is discussed and the measurement of the diameter results of the inhibition zones is evaluated.

The identification of inhibition zones is limited to diameters of 50 to 200 pixels, which is sufficient for the antibiotics tested. In the antibiogram images, each region of interest, including the disc circle and each side, is drawn in four lines: two vertical, two horizontal. These four lines cross the circle of the disc and name them Profile 1, Profile 2, Profile 3 and Profile 4. The average of each profile is calculated and a median value is obtained. After that, a new average smoothed median value is calculated to make the inhibition zone more evident. In some cases it is really difficult to obtain the desired accurate original border zones, but in some cases it is easier to obtain the exact border zones, as shown in the Figure 4.1. Finally, the diameter of the inhibition zone of each antibiogram is identified. This strategy allows overcoming the problem of overlapping. All antibiogram disc image processing calculations and analyses are performed using MATLAB software.

On the first antibiogram plate, circles are found showing a total of 11 inhibition zones detected. In each case to achieve good features between the four graphs, it performs averages plots for each group. In the graphs shown in Figure 4.2, Figure 4.4, Figure 4.6, Figure 4.7, Figure 4.11 and Figure 4.12, to get the better images

profiles center is really difficult. In some profiles, a remarkable decrease in some certain point values and also in some points sharp higher values can be seen. Graphics that “profiles”, “medianprofile” and “smoothedmedianprofile” are plotted. Estimated border level is indicated and drawn. Legend and title are also added to the graphs. In the first antibiogram plate for each detected inhibition zones, the estimated border level centers are given below:

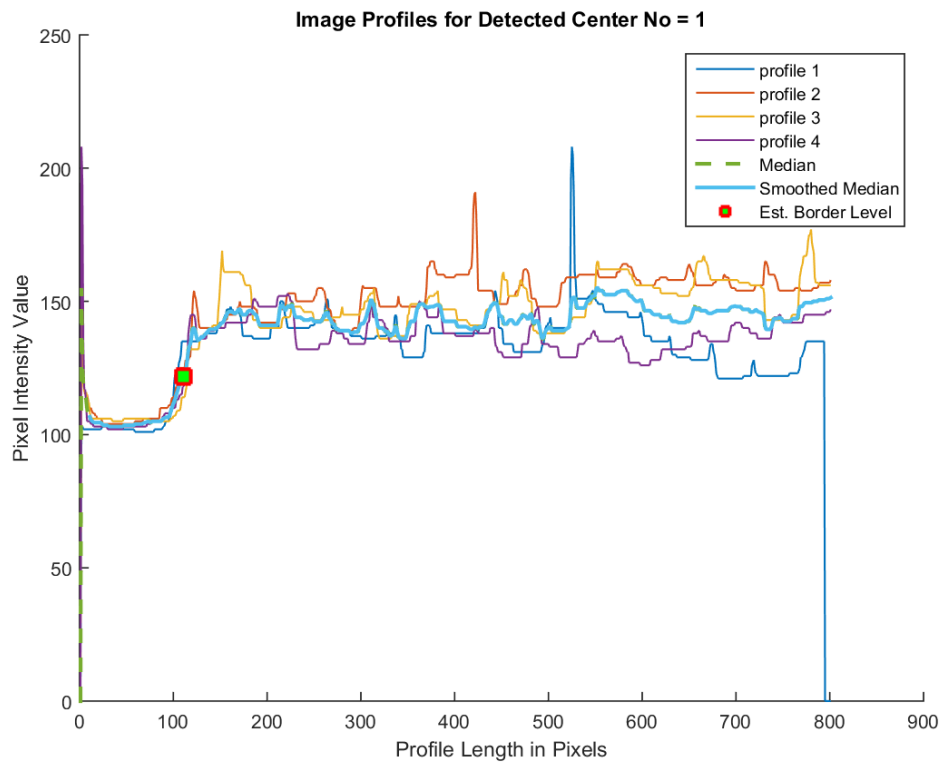


Figure 4. 1 First antibiogram plate image profiles for detected center no.1

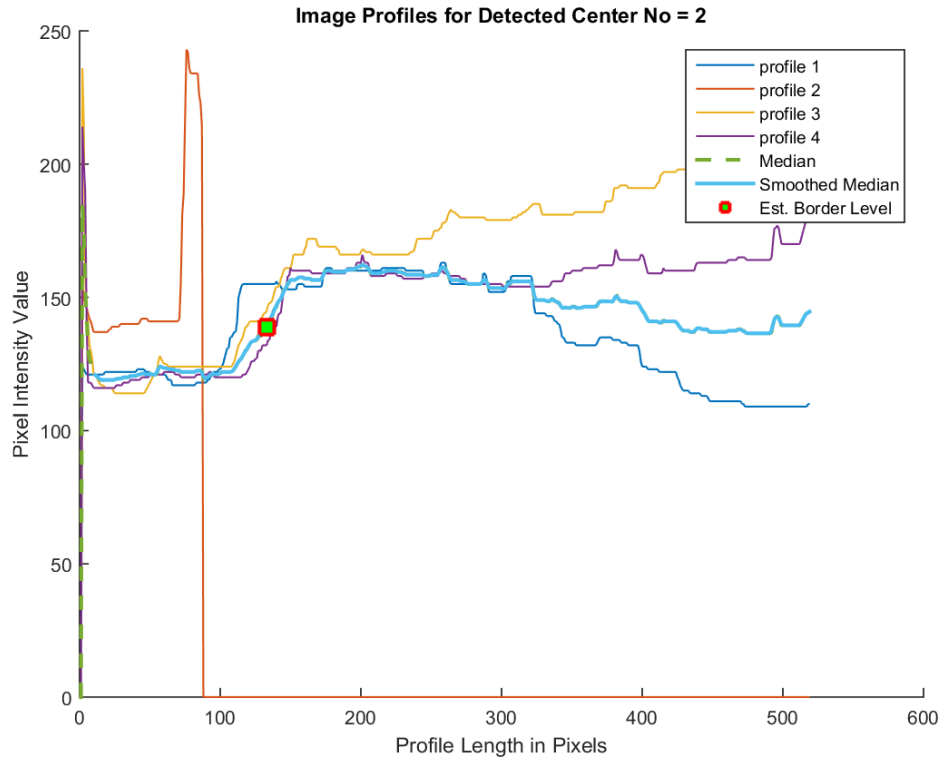


Figure 4. 2 First antibiogram plate image profiles for detected center no.2

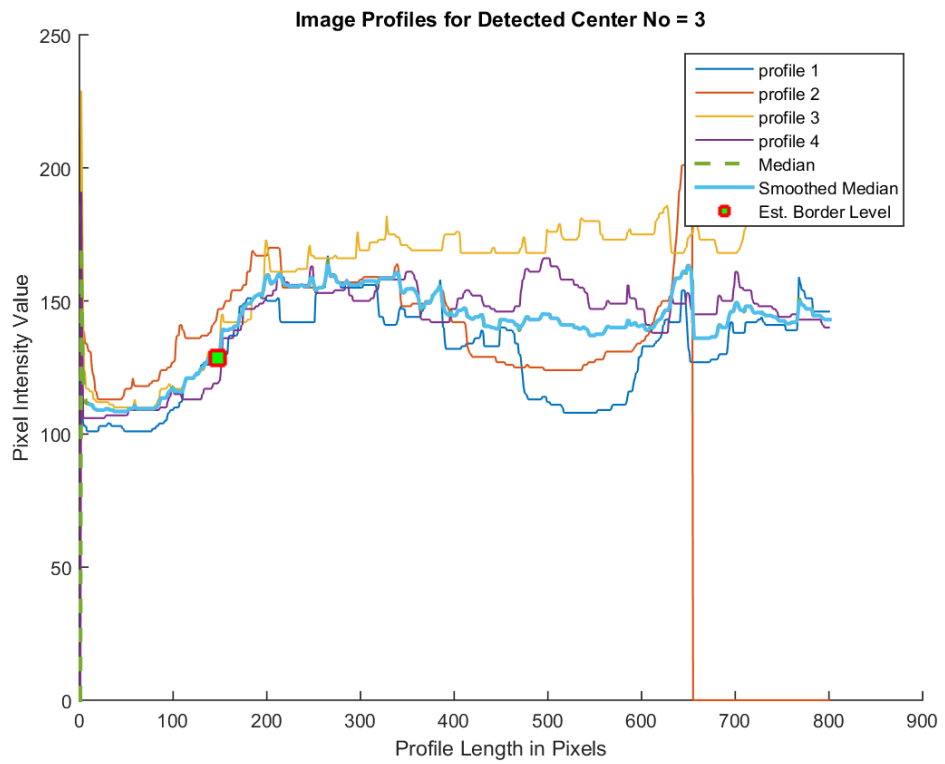


Figure 4. 3 First antibiogram plate image profiles for detected center no.3

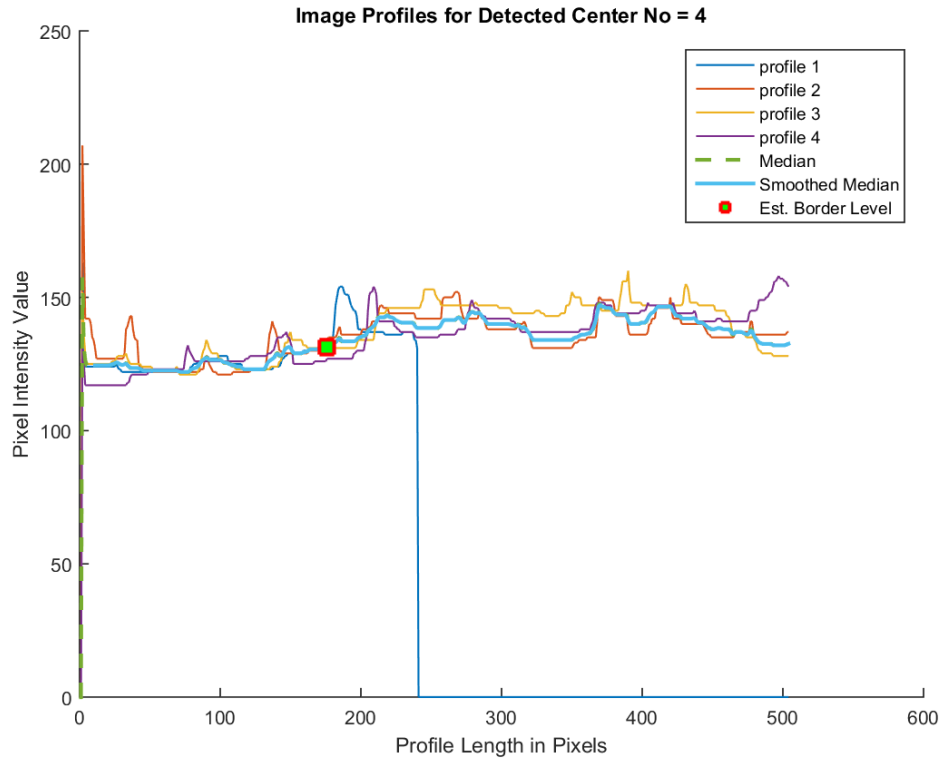


Figure 4. 4 First antibiogram plate image profiles for detected center no.4

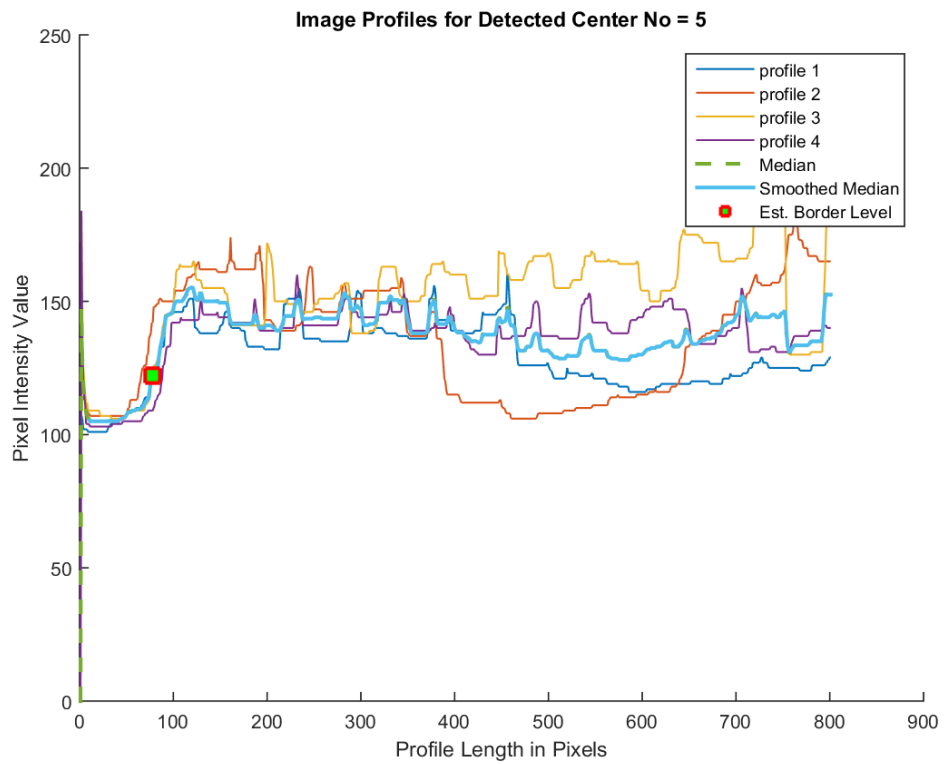


Figure 4. 5 First antibiogram plate image profiles for detected center no.5

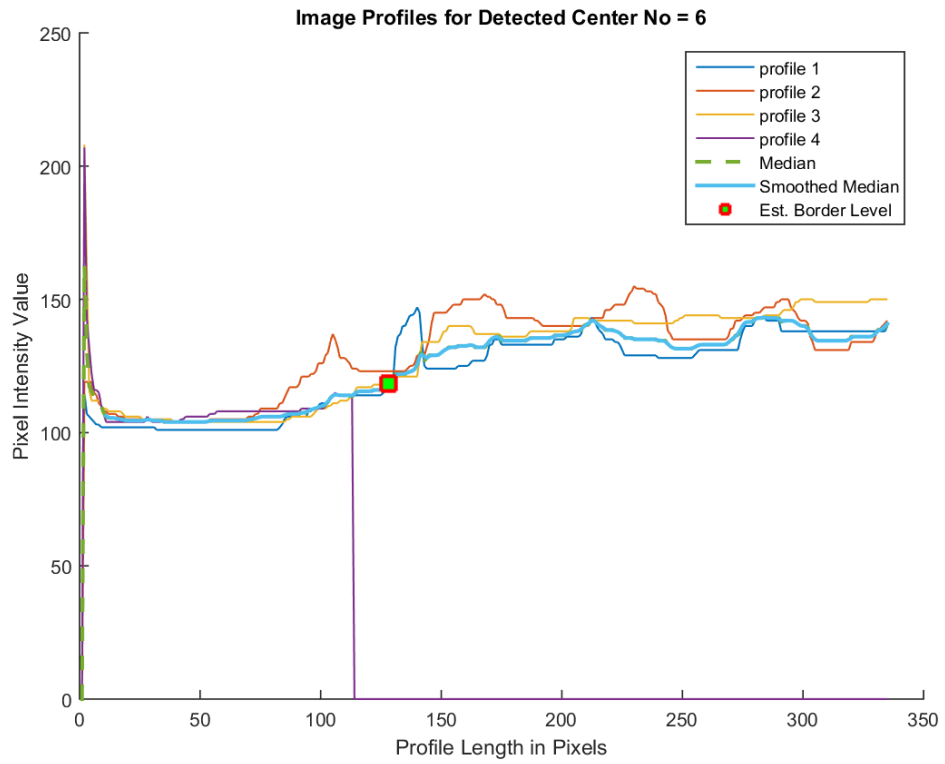


Figure 4. 6 First antibiogram plate image profiles for detected center no.6

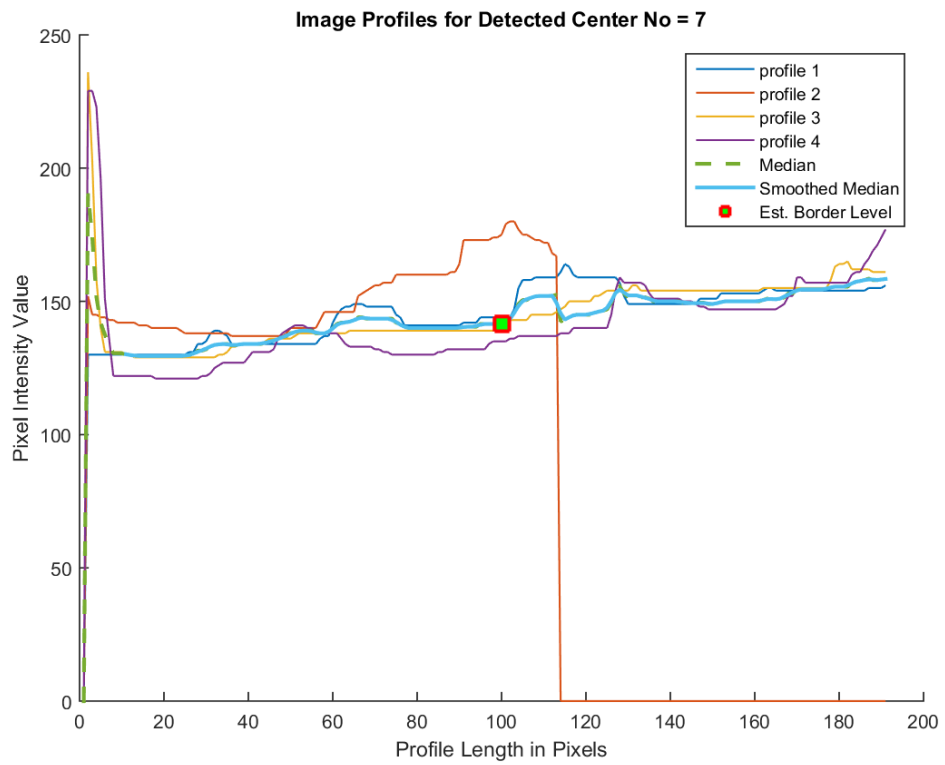


Figure 4. 7 First antibiogram plate image profiles for detected center no.7

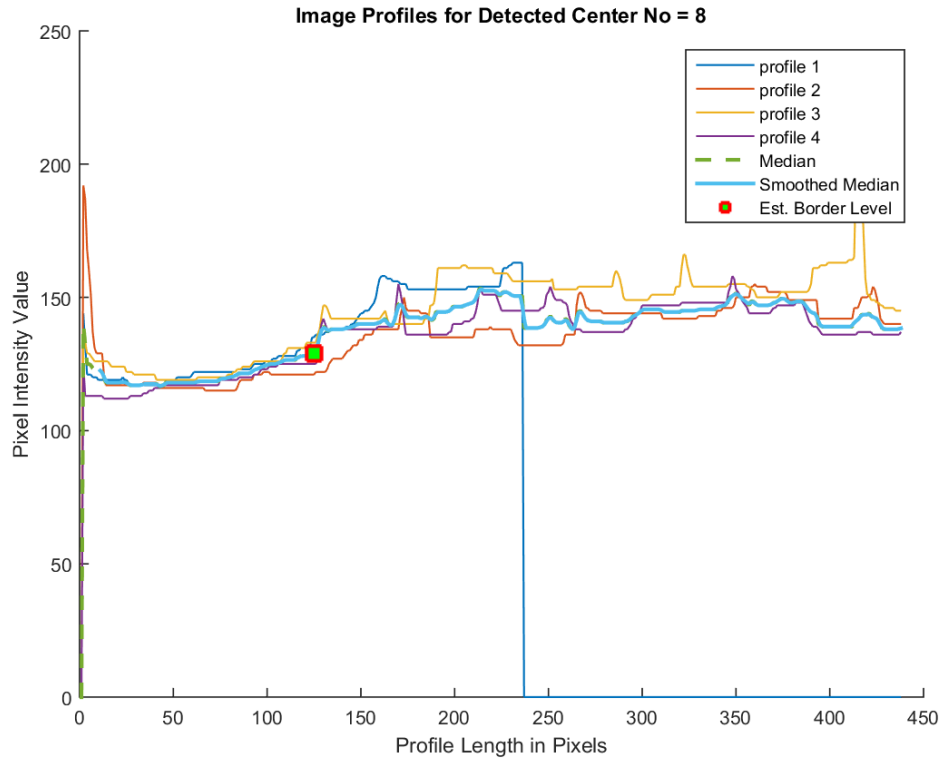


Figure 4. 8 First antibiogram plate image profiles for detected center no.8

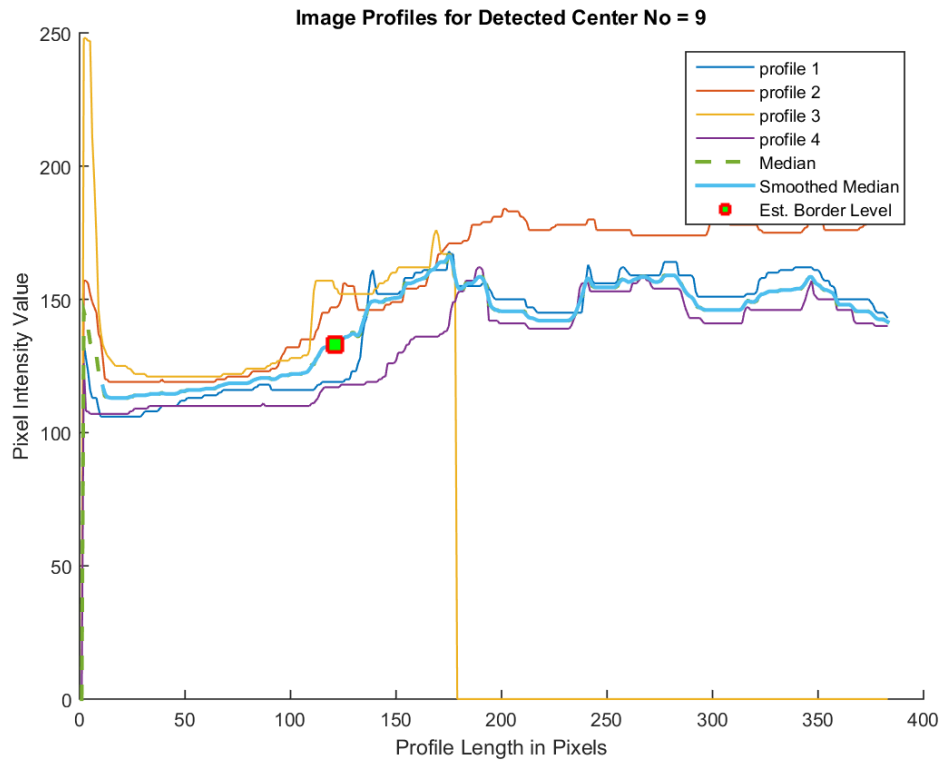


Figure 4. 9 First antibiogram plate image profiles for detected center no.9

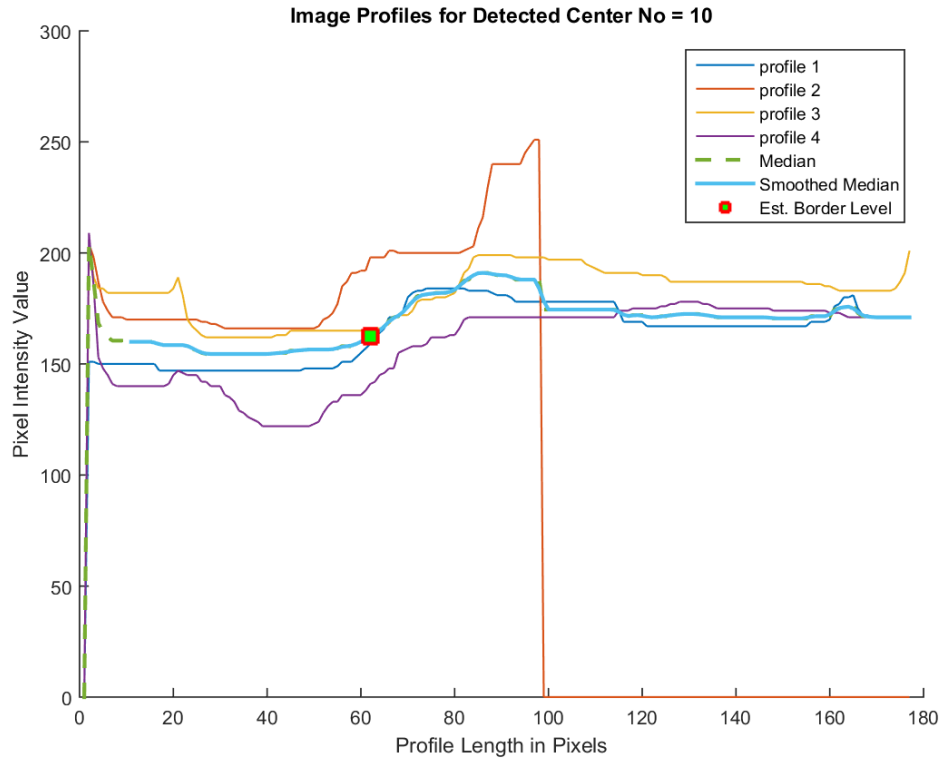


Figure 4. 10 First antibiogram plate image profiles for detected center no.10

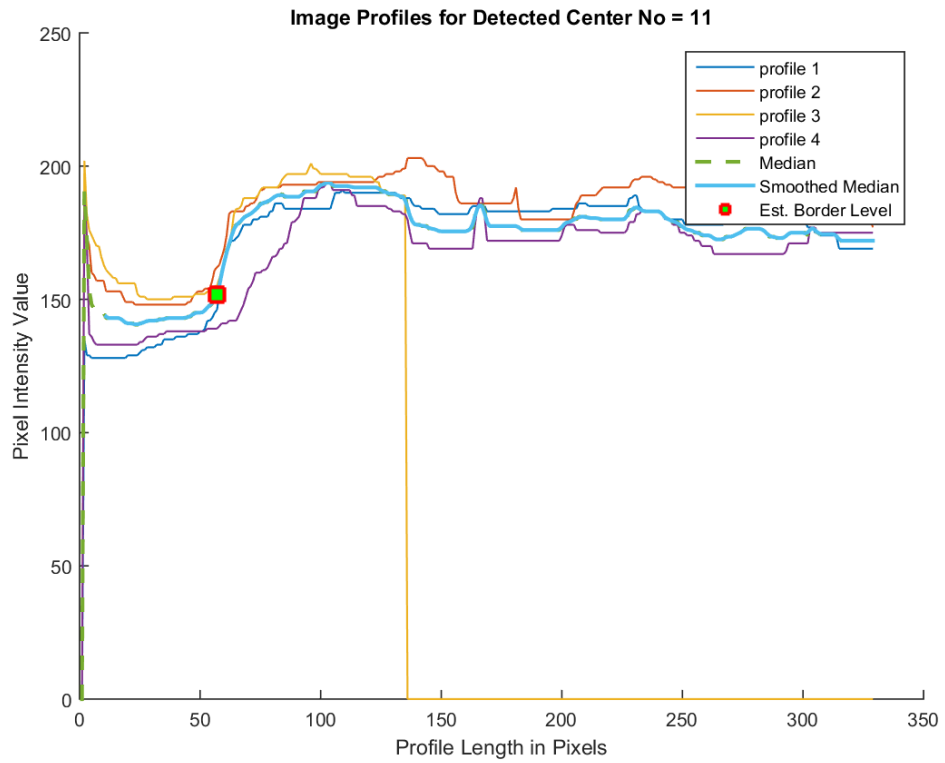


Figure 4. 11 First antibiogram plate image profiles for detected center no.11

On the second antibiogram plate, circles are found showing a total of 11 inhibition zones detected. In each case to achieve good features between the four graphs, it performs averages plots for each group. In the graphs shown in Figure 4.12, Figure 4.15, Figure 4.17, and Figure 4.18, to get the better images profiles center is really difficult. In some profiles, a remarkable decrease in some certain point values and also in some points sharp higher values can be seen. In the first antibiogram plate for each detected inhibition zones, the estimated border level centers are given below:

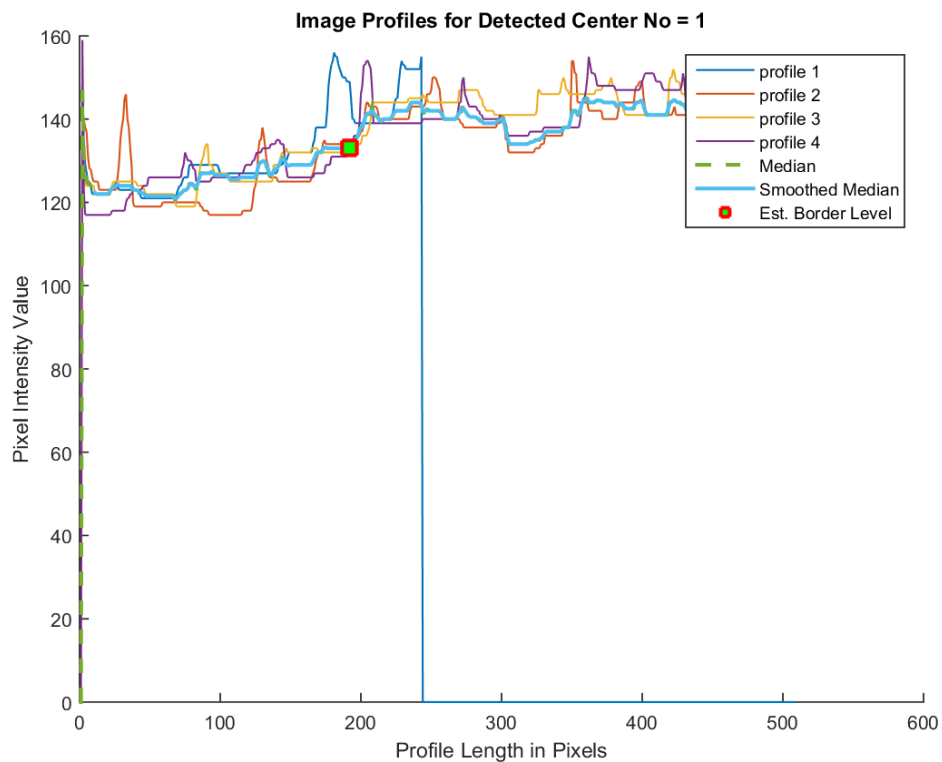


Figure 4. 12 Second antibiogram plate image profiles for detected center no.1

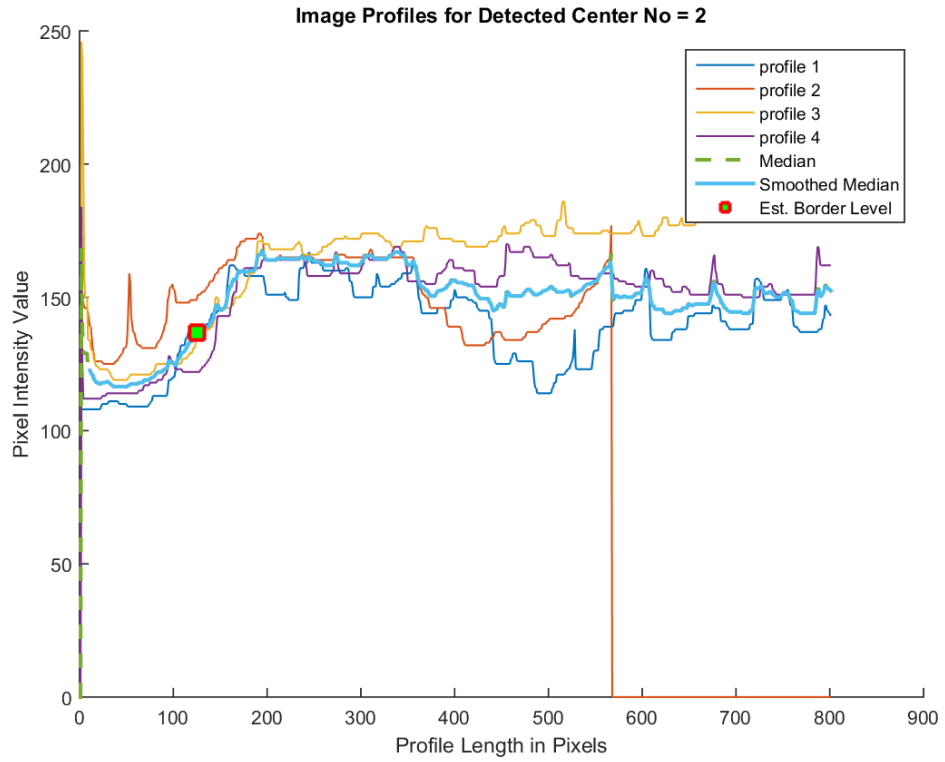


Figure 4. 13 Second antibiogram plate image profiles for detected center no.2

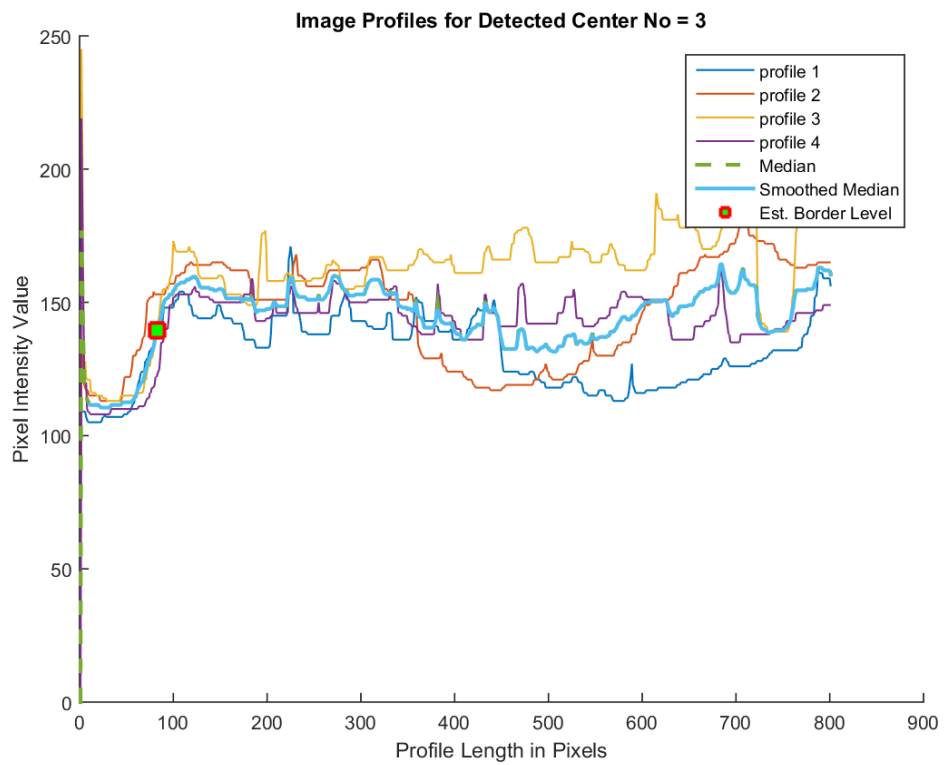


Figure 4. 14 Second antibiogram plate image profiles for detected center no.3

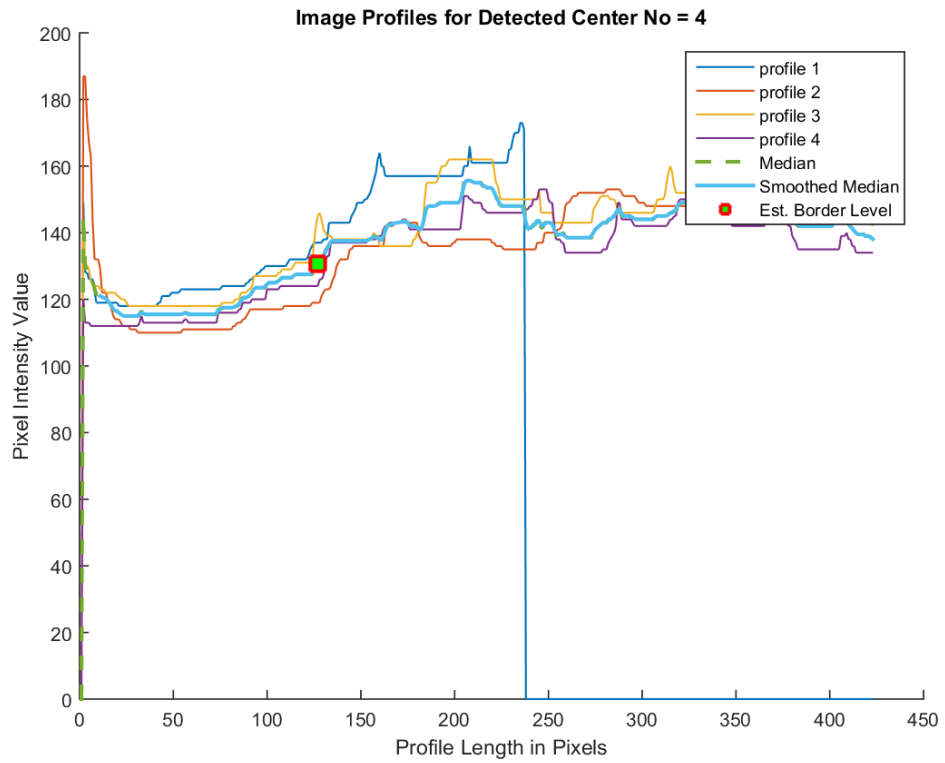


Figure 4. 15 Second antibiogram plate image profiles for detected center no.4

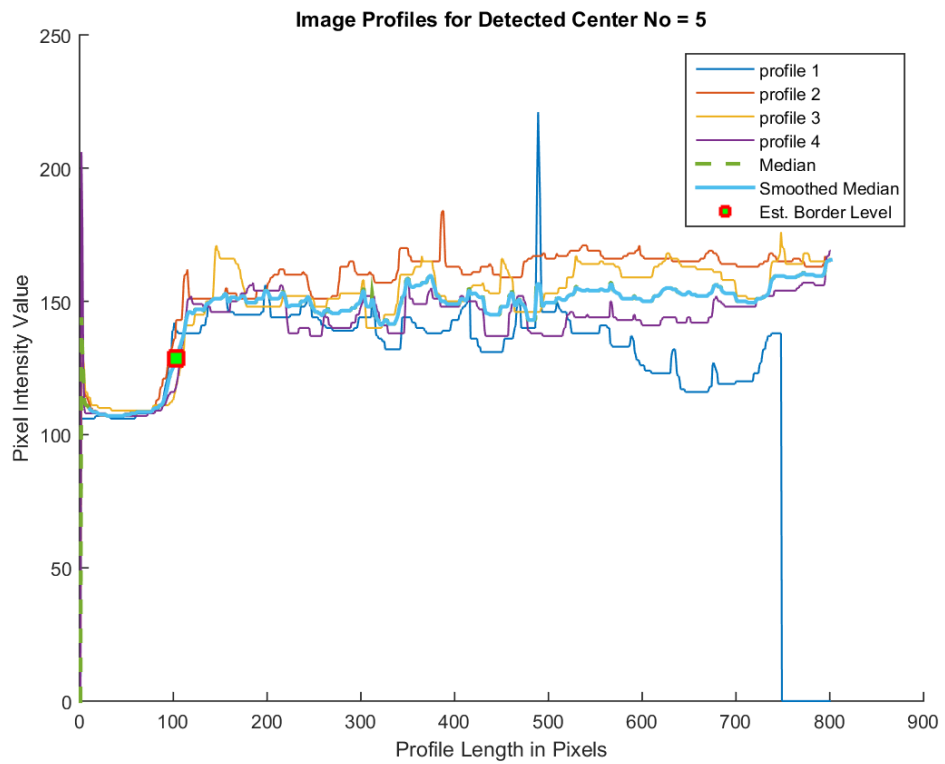


Figure 4. 16 Second antibiogram plate image profiles for detected center no.5

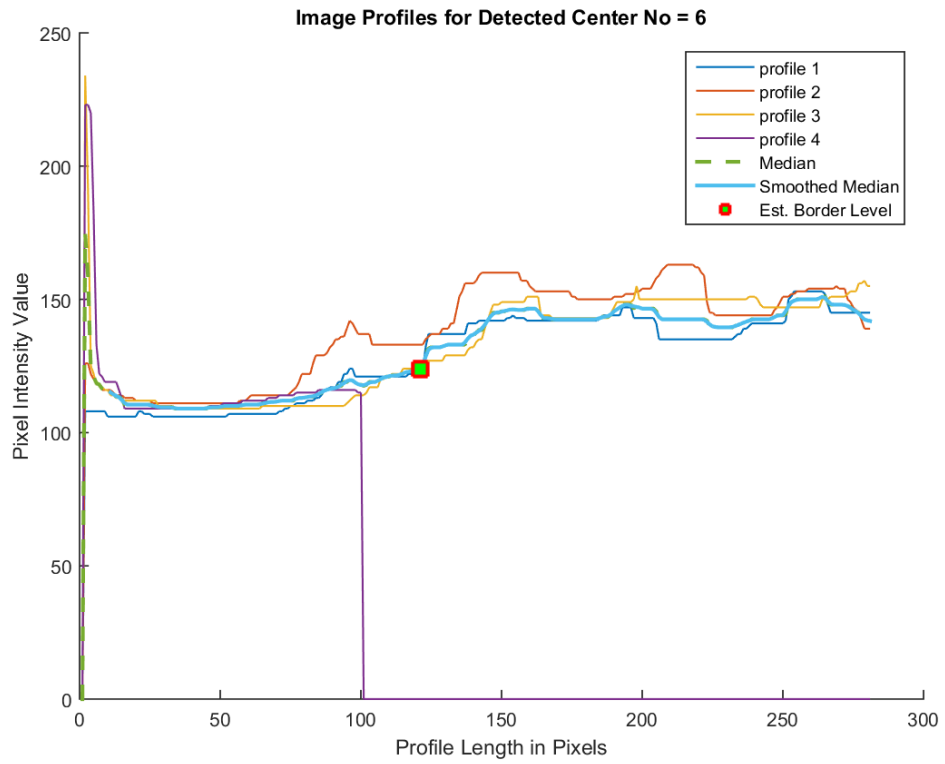


Figure 4. 17 Second antibiogram plate image profiles for detected center no.6

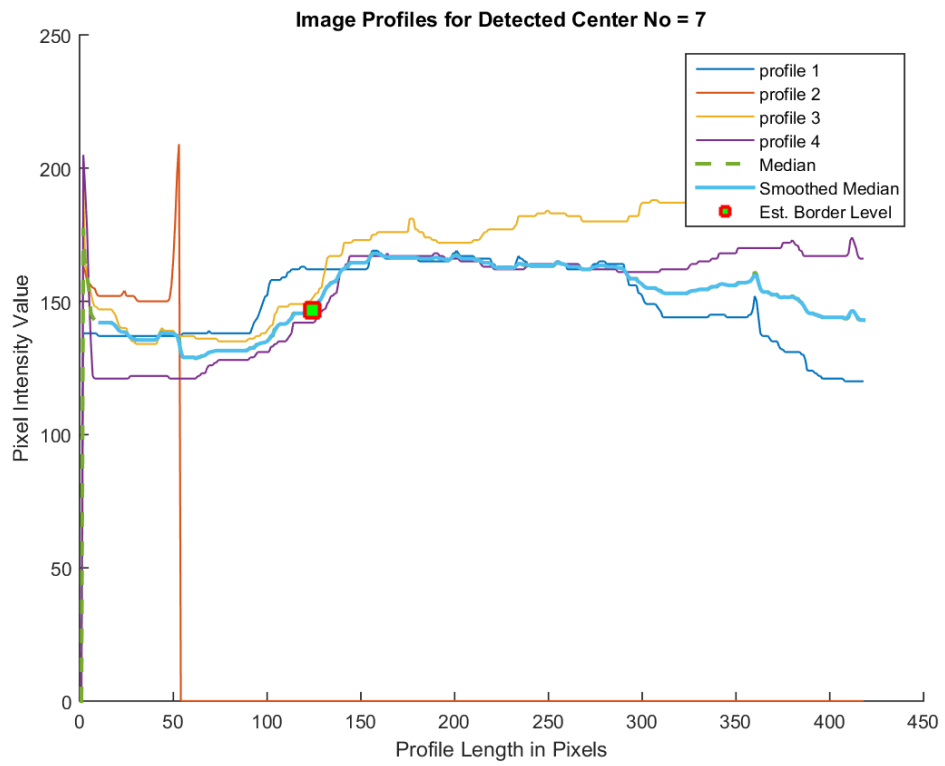


Figure 4. 18 Second antibiogram plate image profiles for detected center no.7

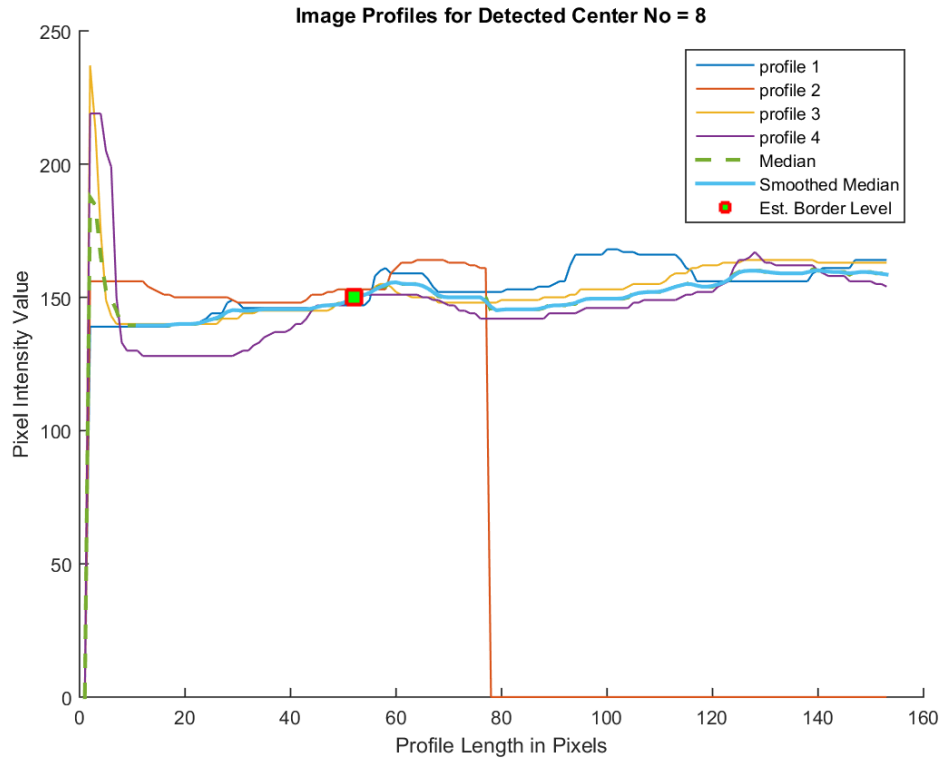


Figure 4. 19 Second antibiogram plate image profiles for detected center no.8

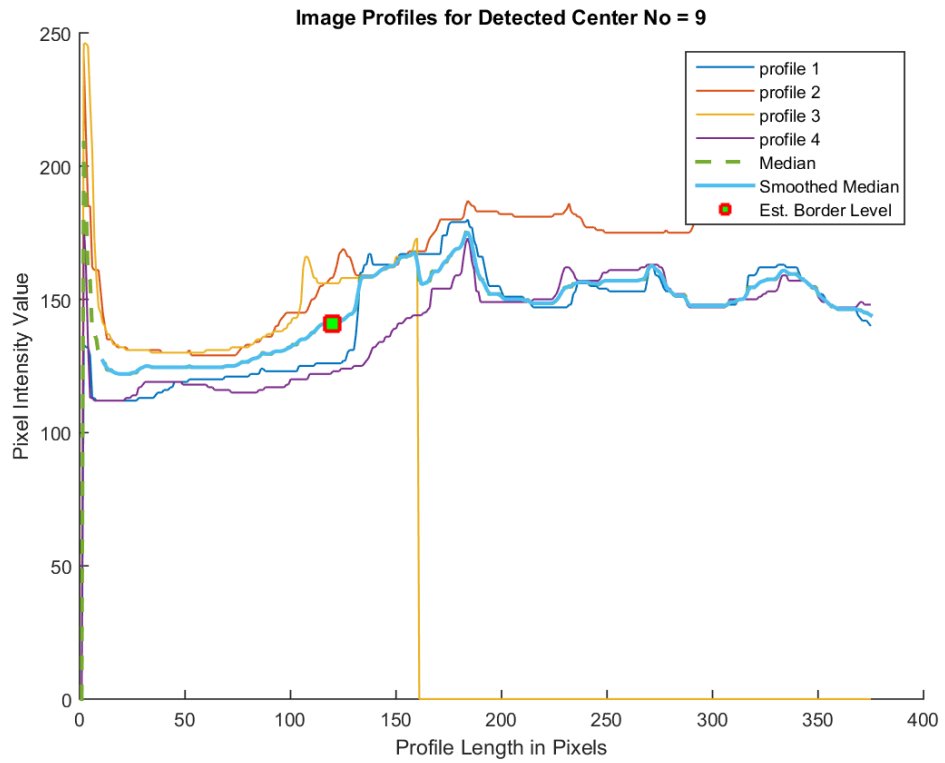


Figure 4. 20 Second antibiogram plate image profiles for detected center no.9

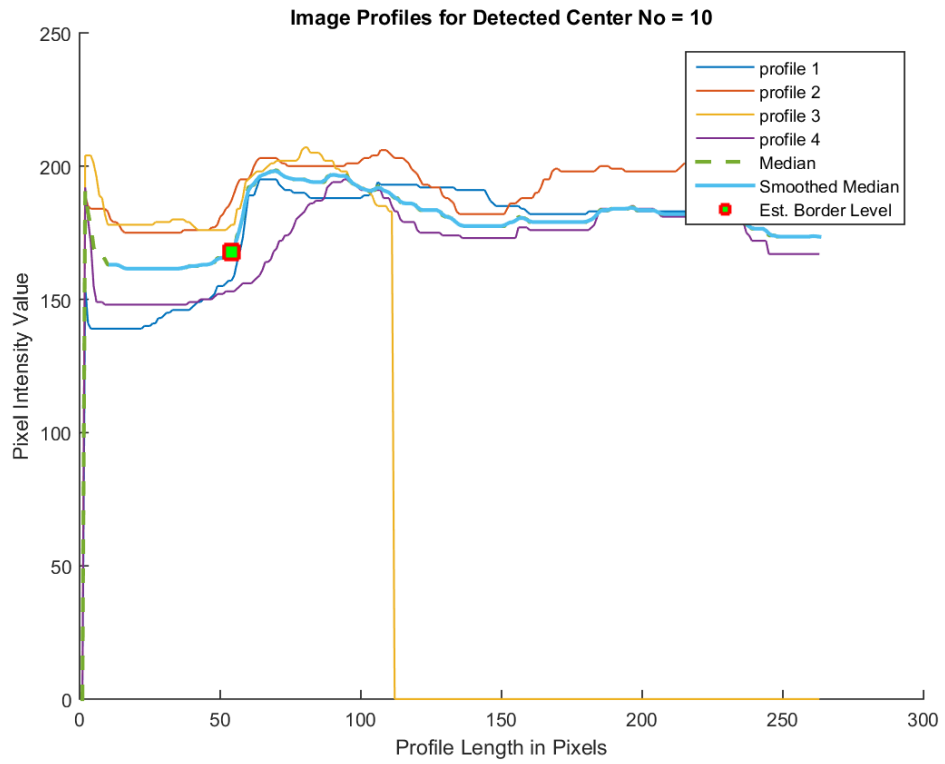


Figure 4. 21 Second antibiogram plate image profiles for detected center no.10

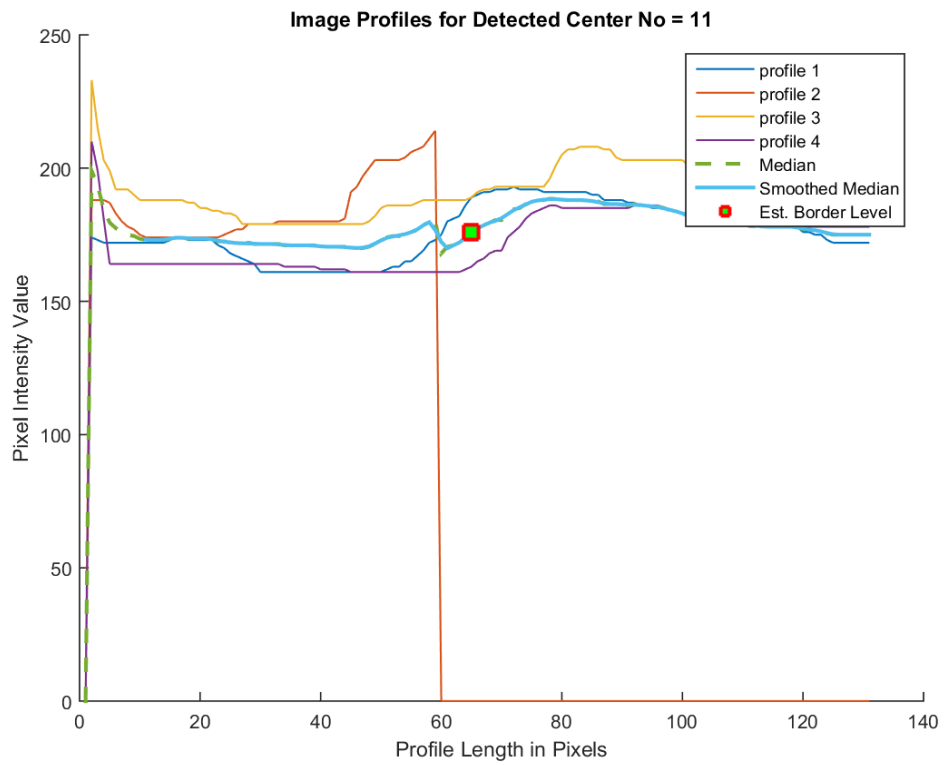


Figure 4. 22 Second antibiogram plate image profiles for detected center no.11

On the third antibiogram plate, circles are found showing a total of 12 inhibition zones detected. In each case to achieve good features between the four graphs, it performs averages plots for each group. In the graphs shown in Figure 4.26, Figure 4.27, Figure 4.30, and Figure 4.32, to get the better images profiles center is really difficult. In some profiles, a remarkable decrease in some certain point values and also in some points sharp higher values can be seen. In the first antibiogram plate for each detected inhibition zones, the estimated border level centers are given below:

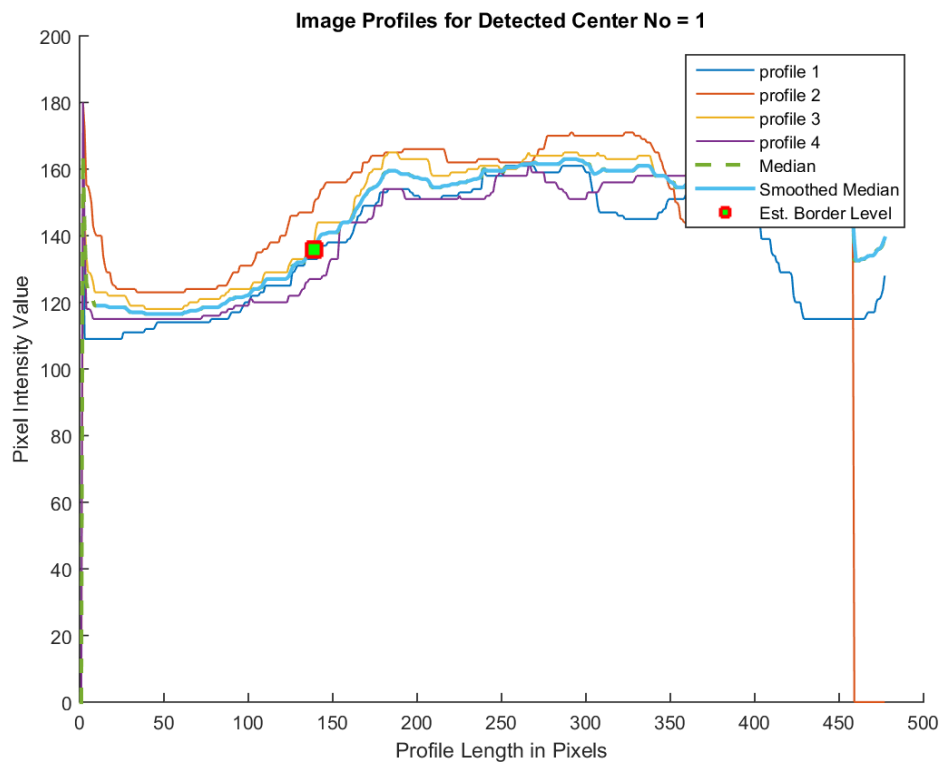


Figure 4. 23 Third antibiogram plate image profiles for detected center no.1

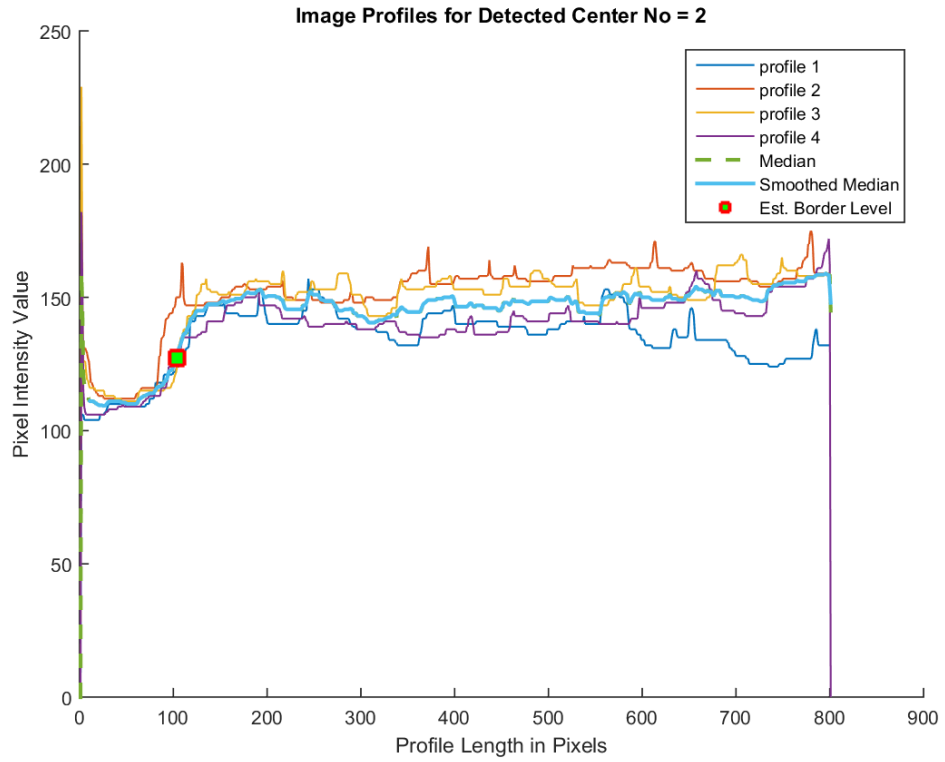


Figure 4. 24 Third antibiogram plate image profiles for detected center no.2

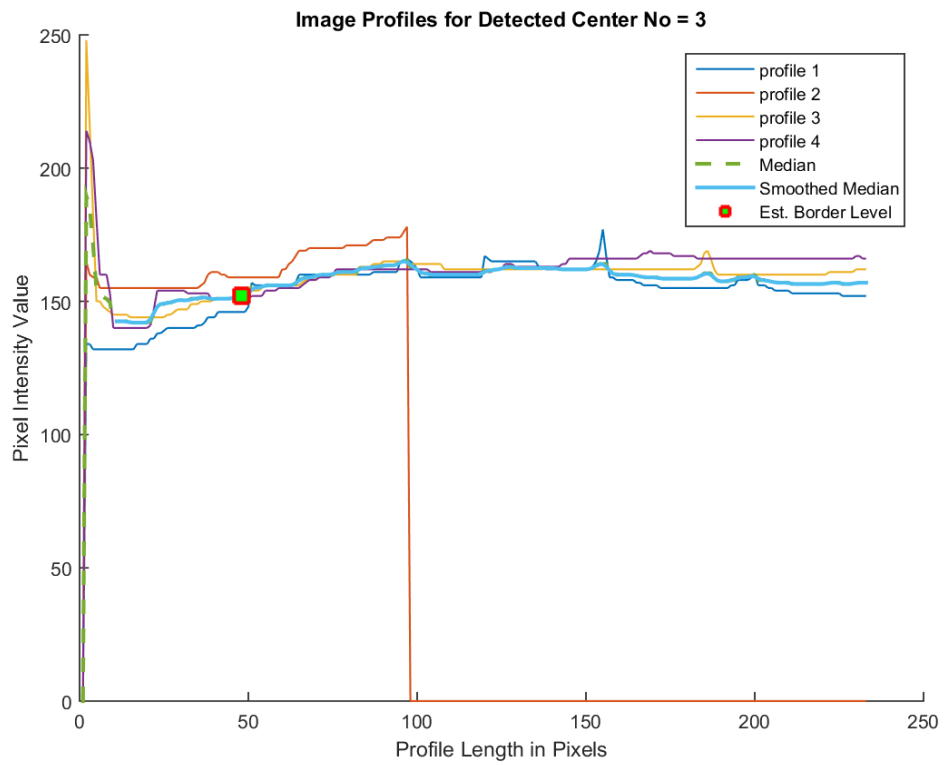


Figure 4. 25 Third antibiogram plate image profiles for detected center no.3

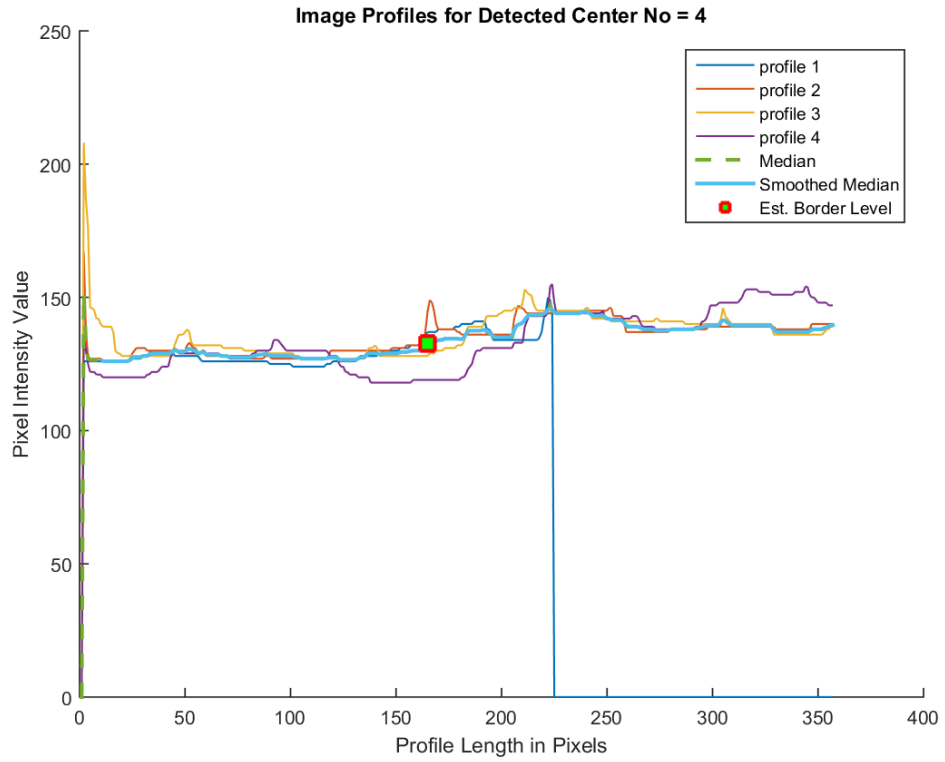


Figure 4. 26 Third antibiogram plate image profiles for detected center no.4

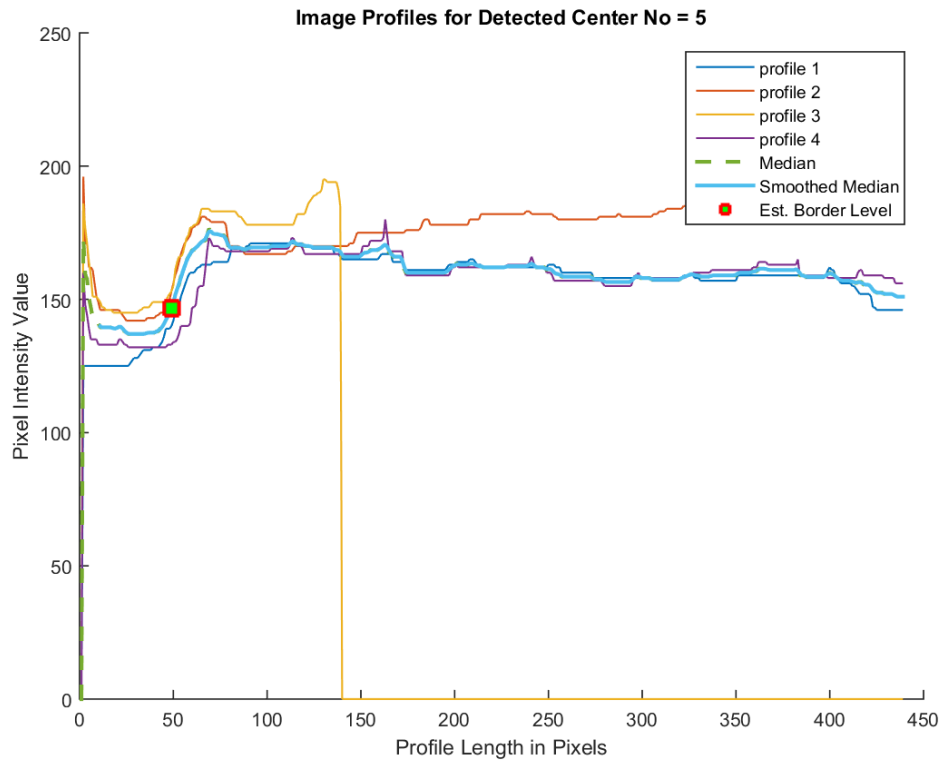


Figure 4. 27 Third antibiogram plate image profiles for detected center no.5

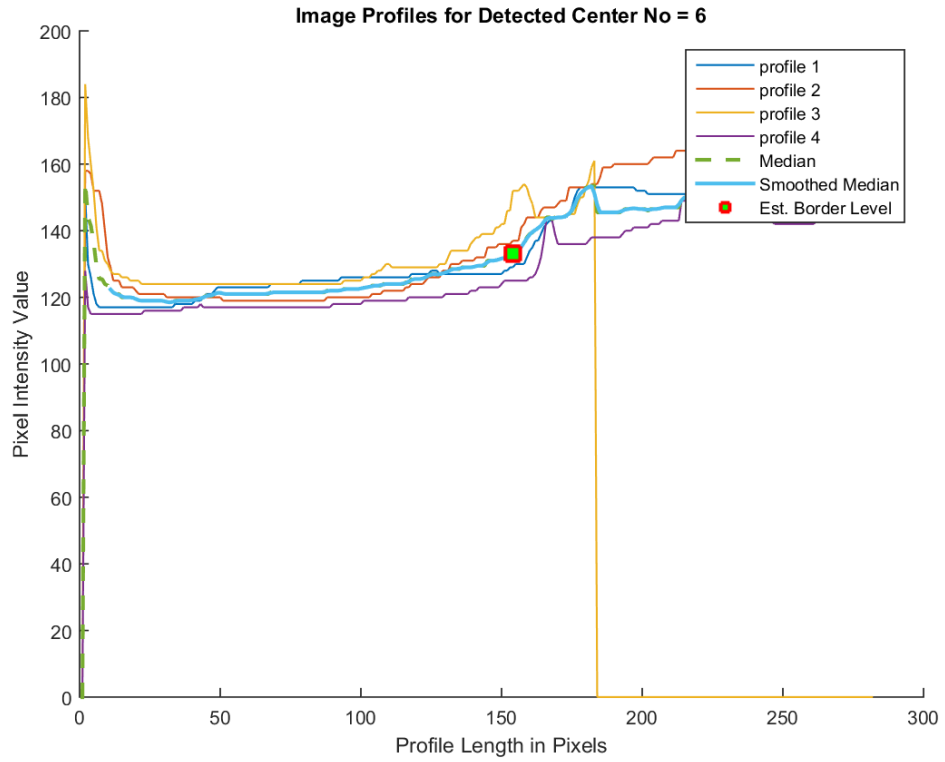


Figure 4. 28 Third antibiogram plate image profiles for detected center no.6

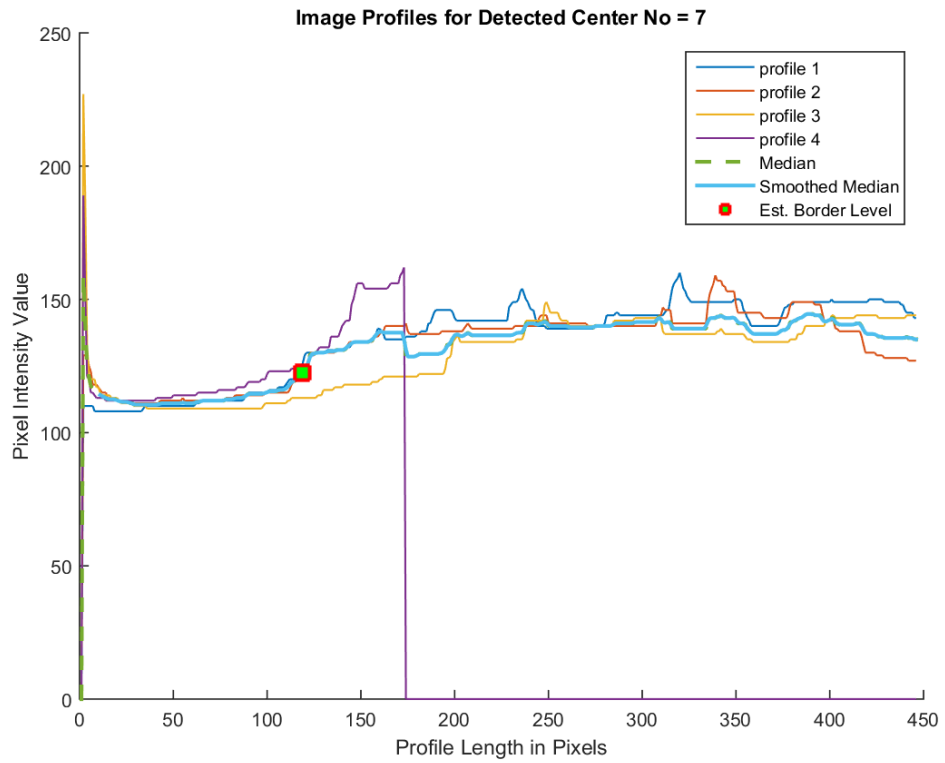


Figure 4. 29 Third antibiogram plate image profiles for detected center no.7

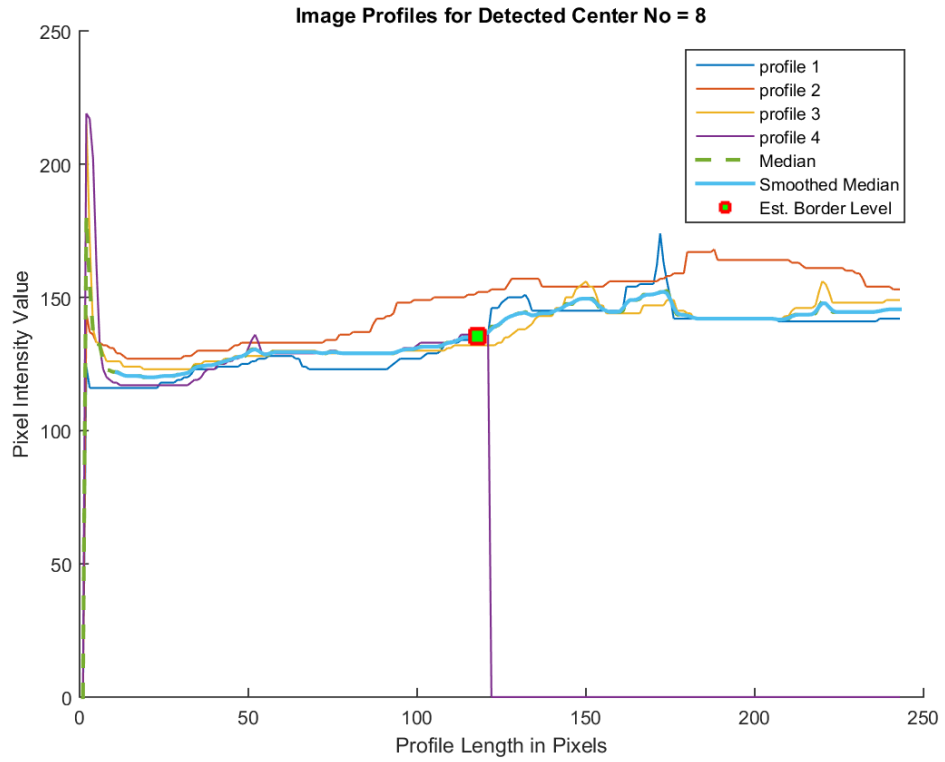


Figure 4. 30 Third antibiogram plate image profiles for detected center no.8

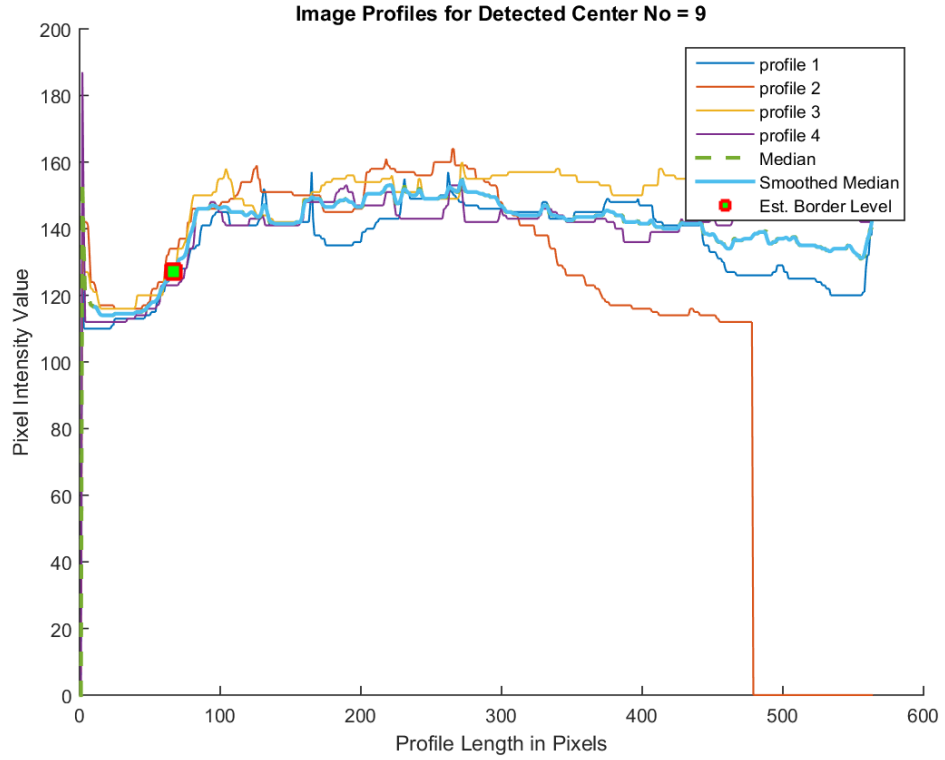


Figure 4. 31 Third antibiogram plate image profiles for detected center no.9

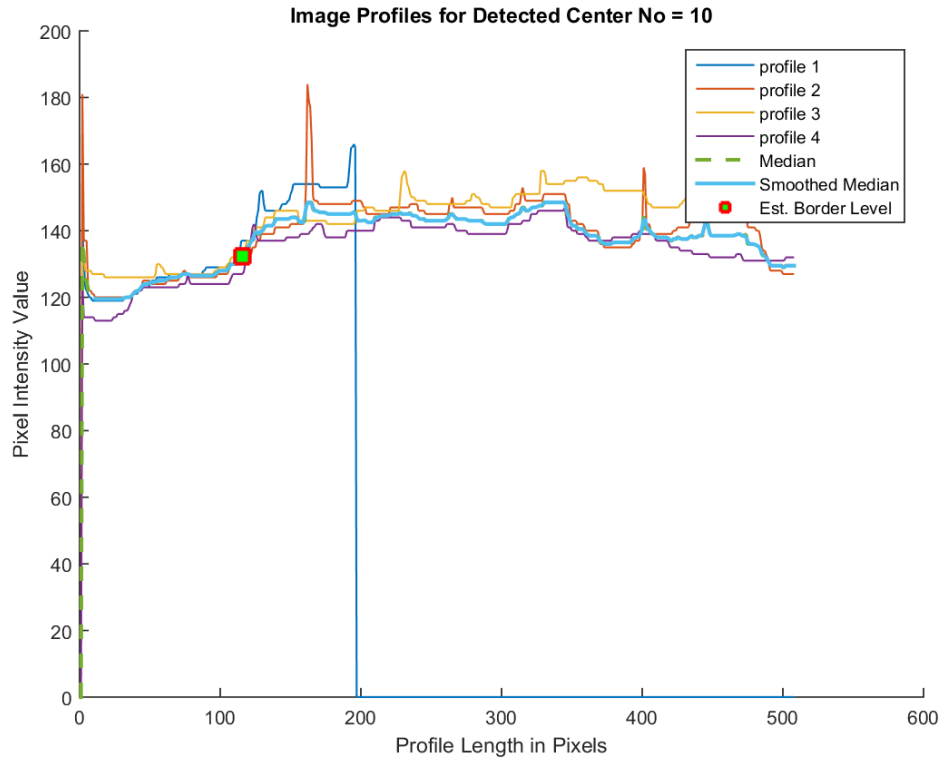


Figure 4. 32 Third antibiogram plate image profiles for detected center no.10

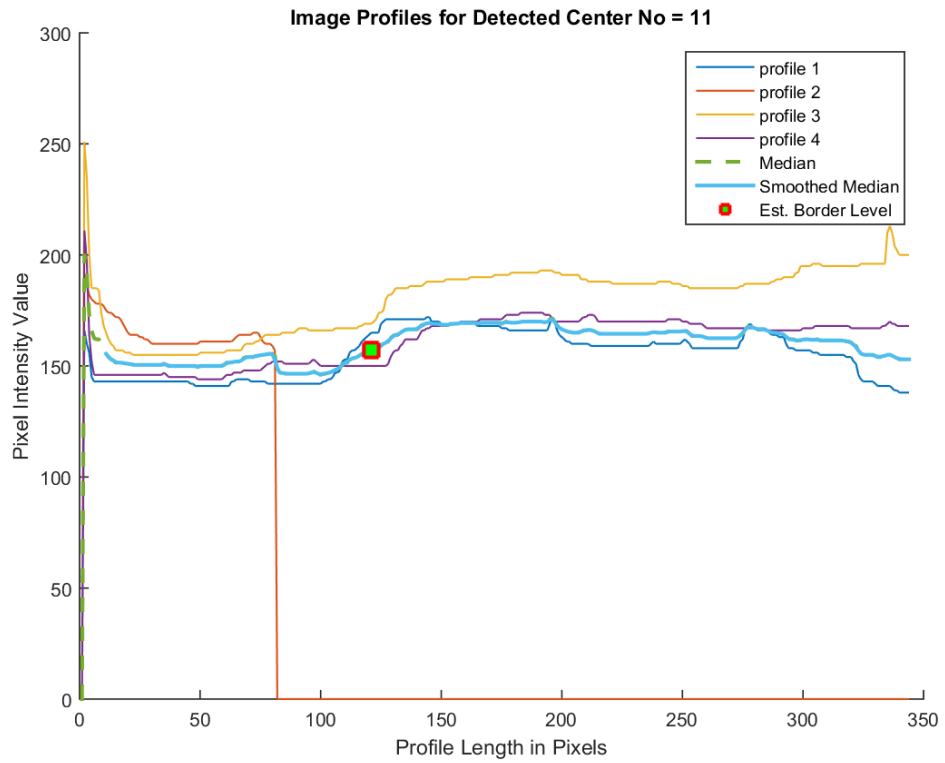


Figure 4. 33 Third antibiogram plate image profiles for detected center no.11

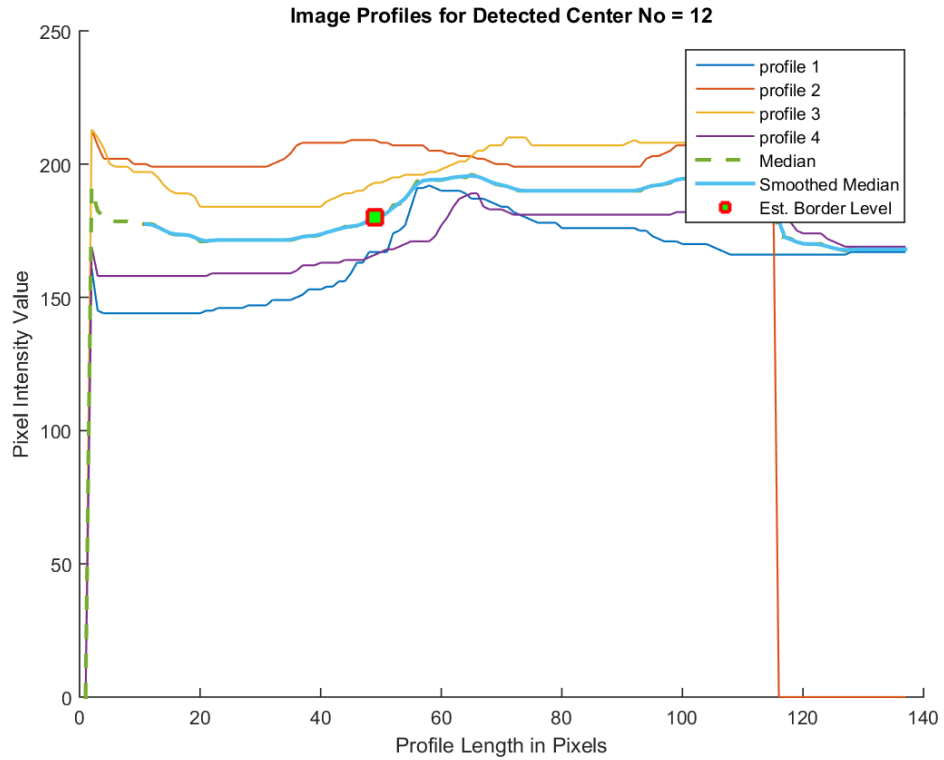


Figure 4. 34 Third antibiogram plate image profiles for detected center no.12

On the fourth antibiogram plate, circles are found showing a total of 12 inhibition zones detected. In each case to achieve good features between the four graphs, it performs averages plots for each group. In the graphs shown in Figure 4.37, Figure 4.38, Figure 4.44, and Figure 4.45, to get the better images profiles center is really difficult. In some profiles, a remarkable decrease in some certain point values and also in some points sharp higher values can be seen. In the first antibiogram plate for each detected inhibition zones, the estimated border level centers are given below:

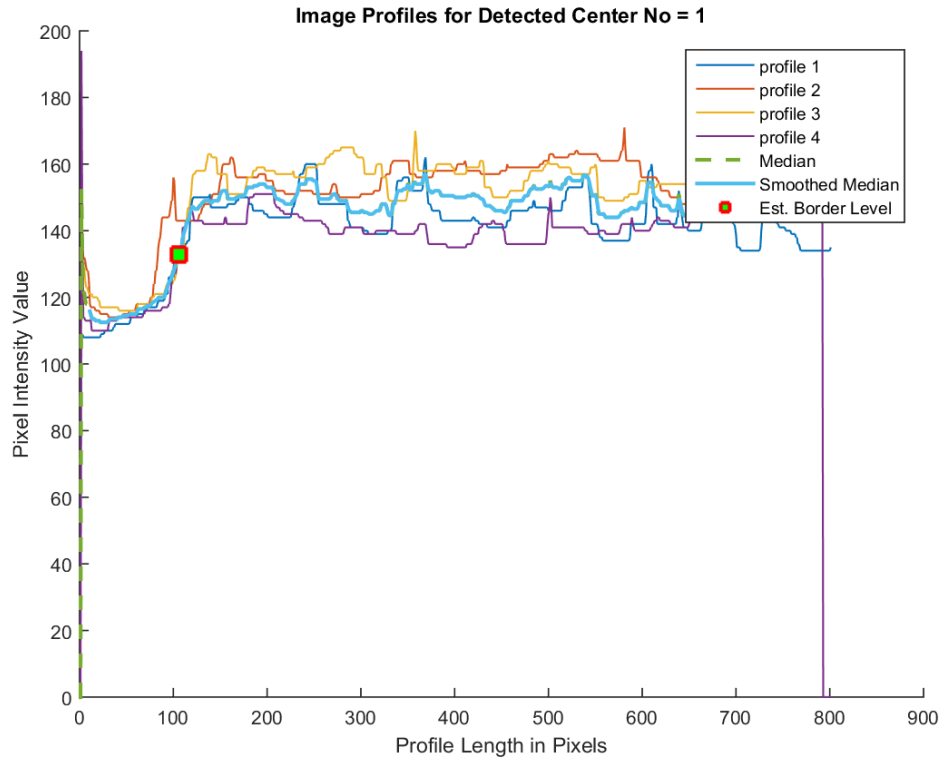


Figure 4. 35 Fourth antibiogram plate image profiles for detected center no.1

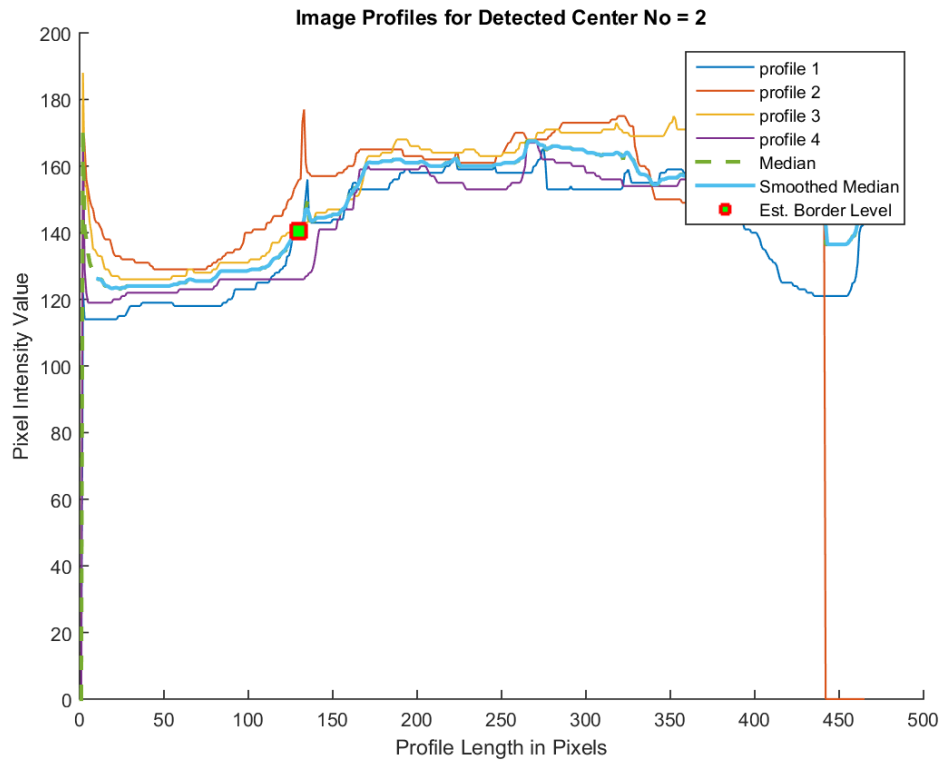


Figure 4. 36 Fourth antibiogram plate image profiles for detected center no.2

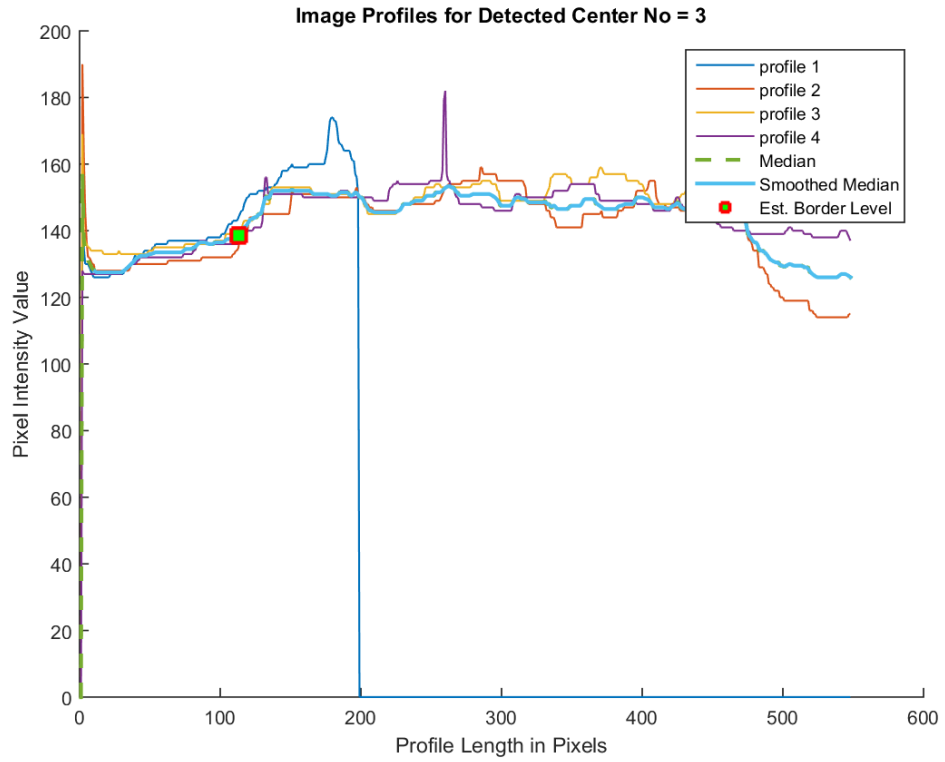


Figure 4. 37 Fourth antibiogram plate image profiles for detected center no.3

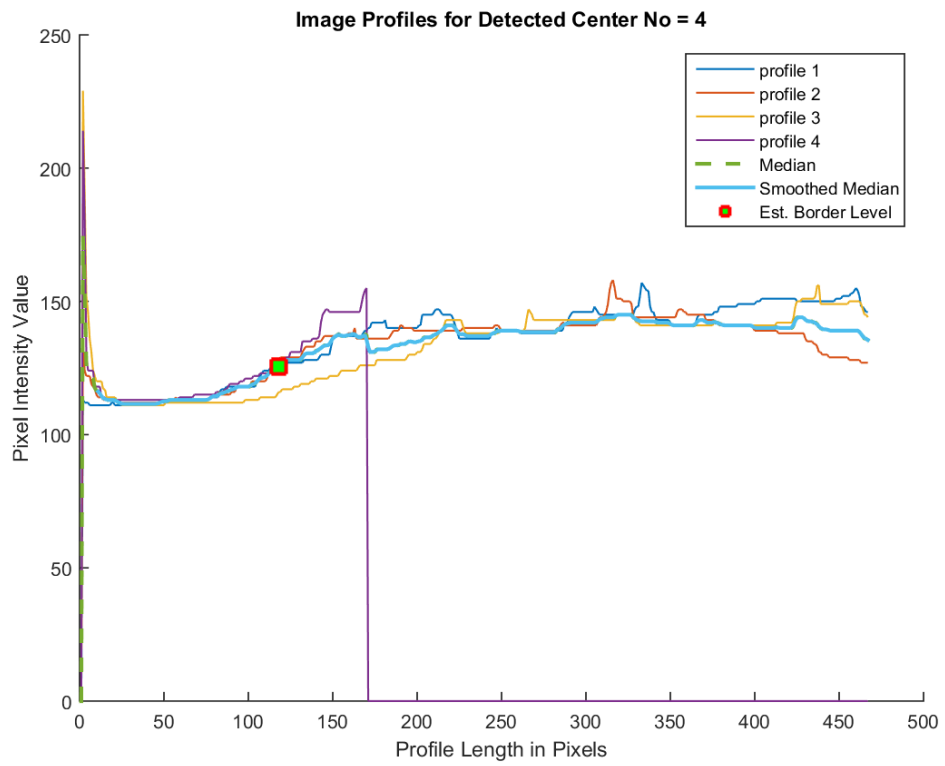


Figure 4. 38 Fourth antibiogram plate image profiles for detected center no.4

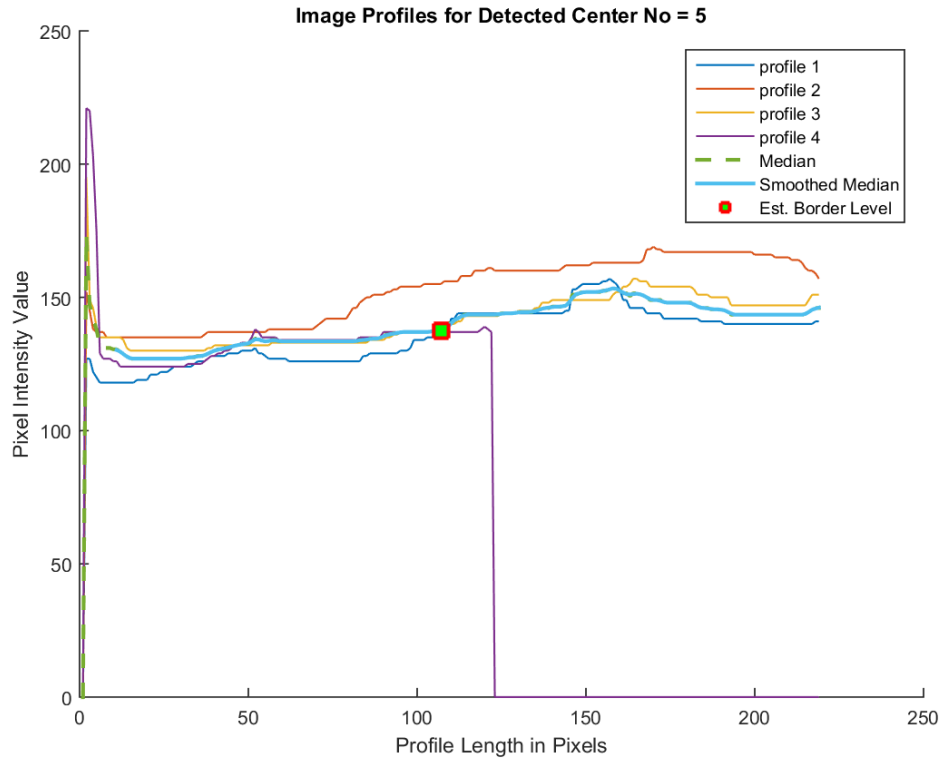


Figure 4. 39 Fourth antibiogram plate image profiles for detected center no.5

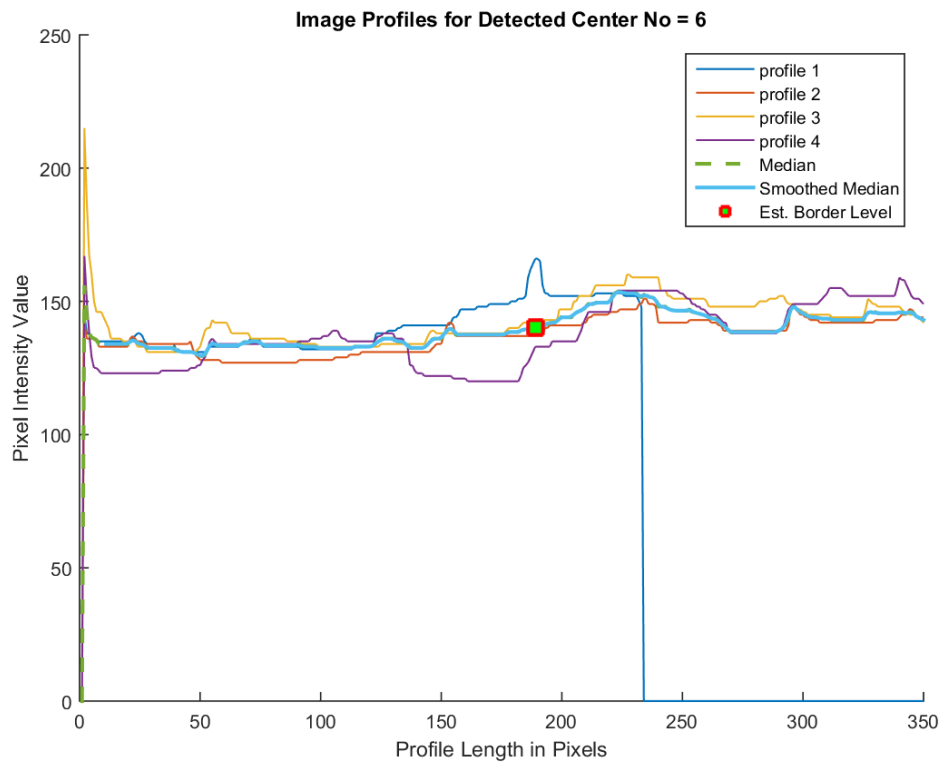


Figure 4. 40 Fourth antibiogram plate image profiles for detected center no.6

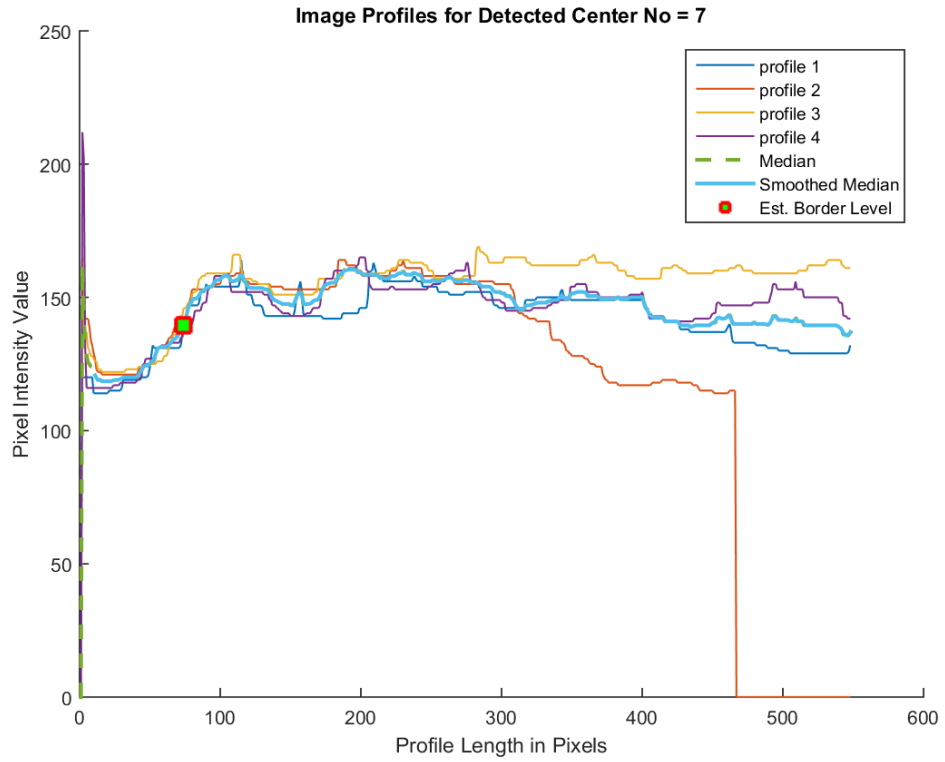


Figure 4. 41 Fourth antibiogram plate image profiles for detected center no.7

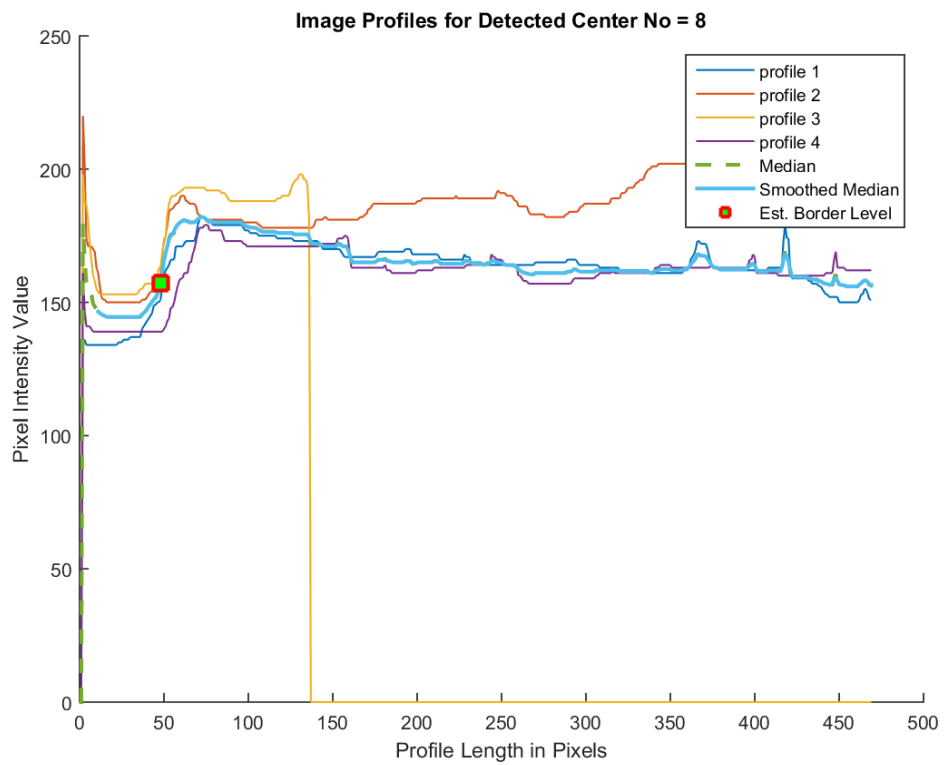


Figure 4. 42 Fourth antibiogram plate image profiles for detected center no.8

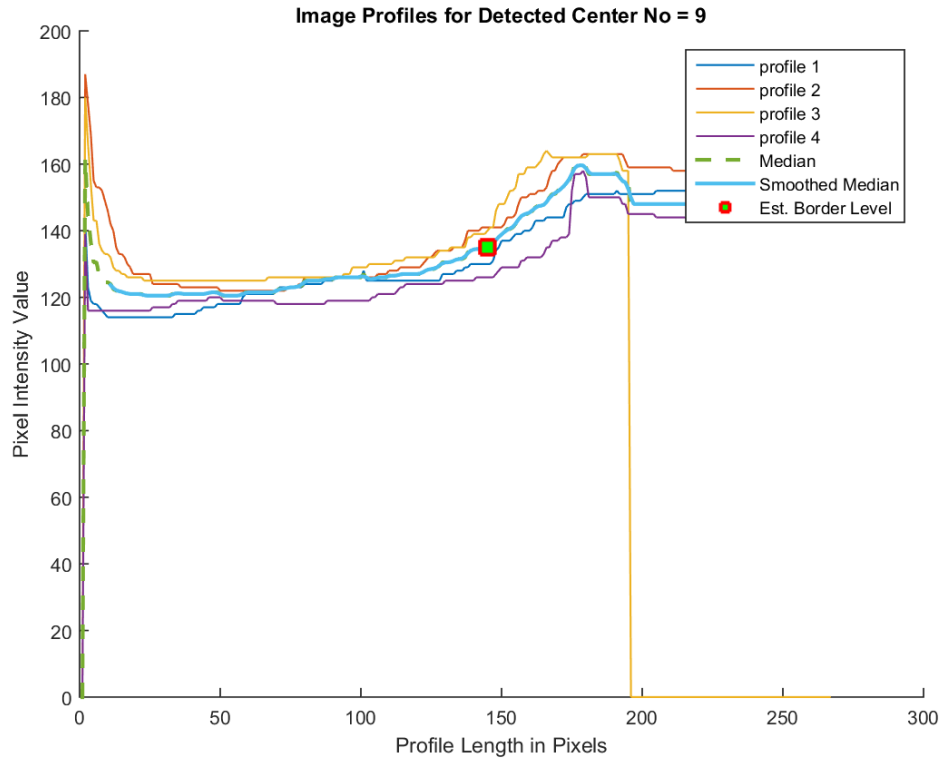


Figure 4. 43 Fourth antibiogram plate image profiles for detected center no.9

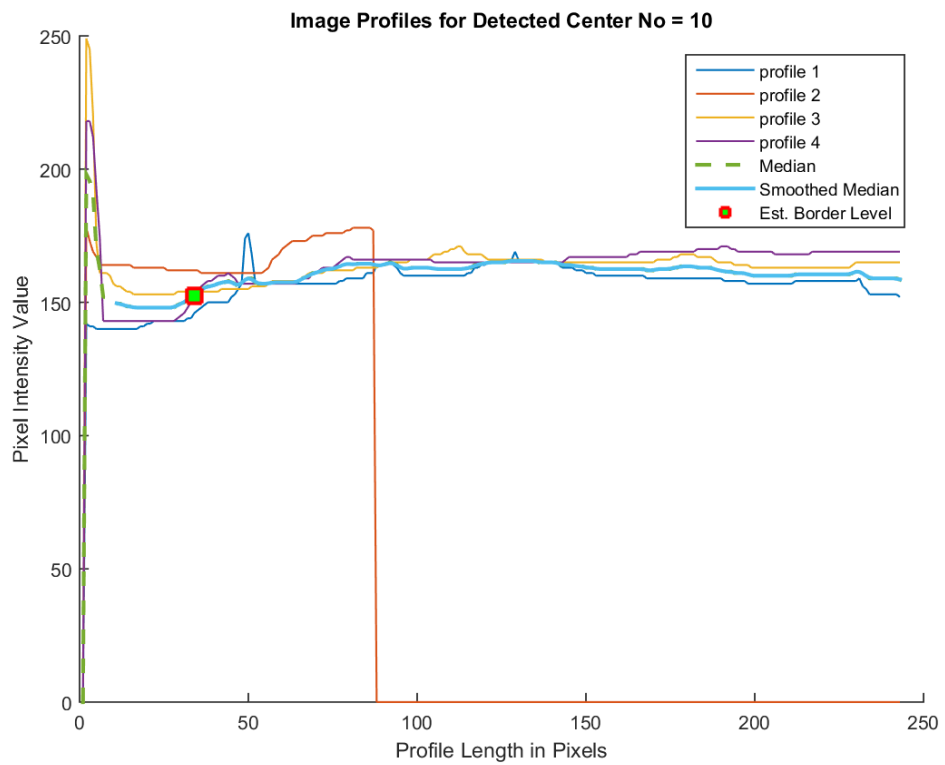


Figure 4. 44 Fourth antibiogram plate image profiles for detected center no.10

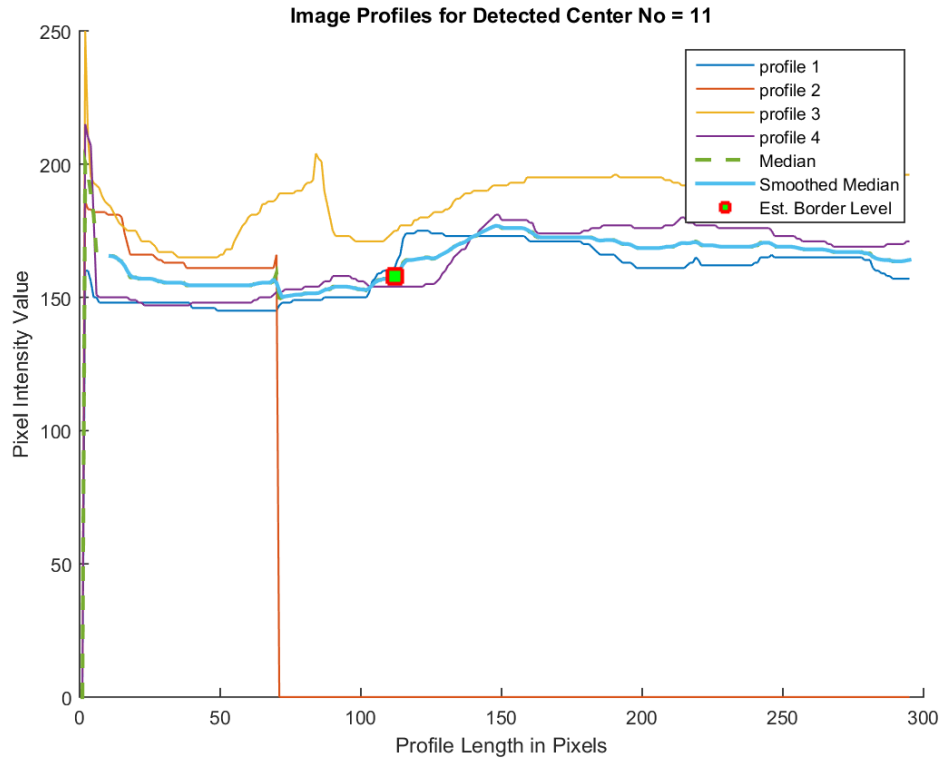


Figure 4. 45 Fourth antibiogram plate image profiles for detected center no.11

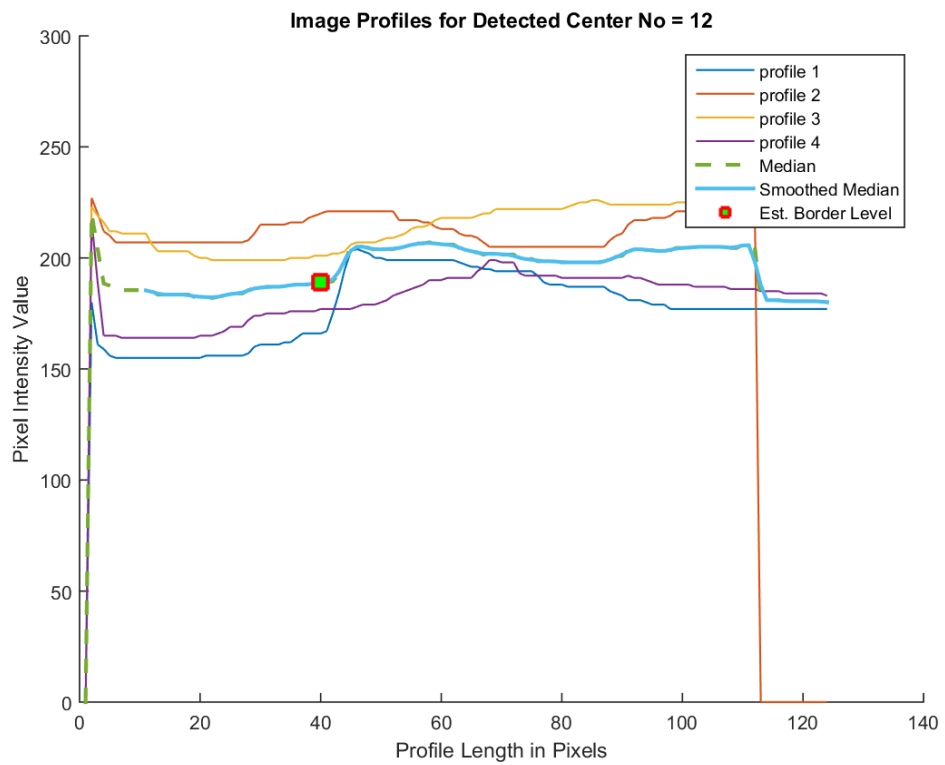


Figure 4. 46 Fourth antibiogram plate image profiles for detected center no.12

On the fifth antibiogram plate, circles are found showing a total of 12 inhibition zones detected. In each case to achieve good features between the four graphs, it performs averages plots for each group. In the graphs shown in Figure 4.50, Figure 4.51, Figure 4.56, and Figure 4.57, to get the better images profiles center is really difficult. In some profiles, a remarkable decrease in some certain point values and also in some points sharp higher values can be seen. In the first antibiogram plate for each detected inhibition zones, the estimated border level centers are given below:

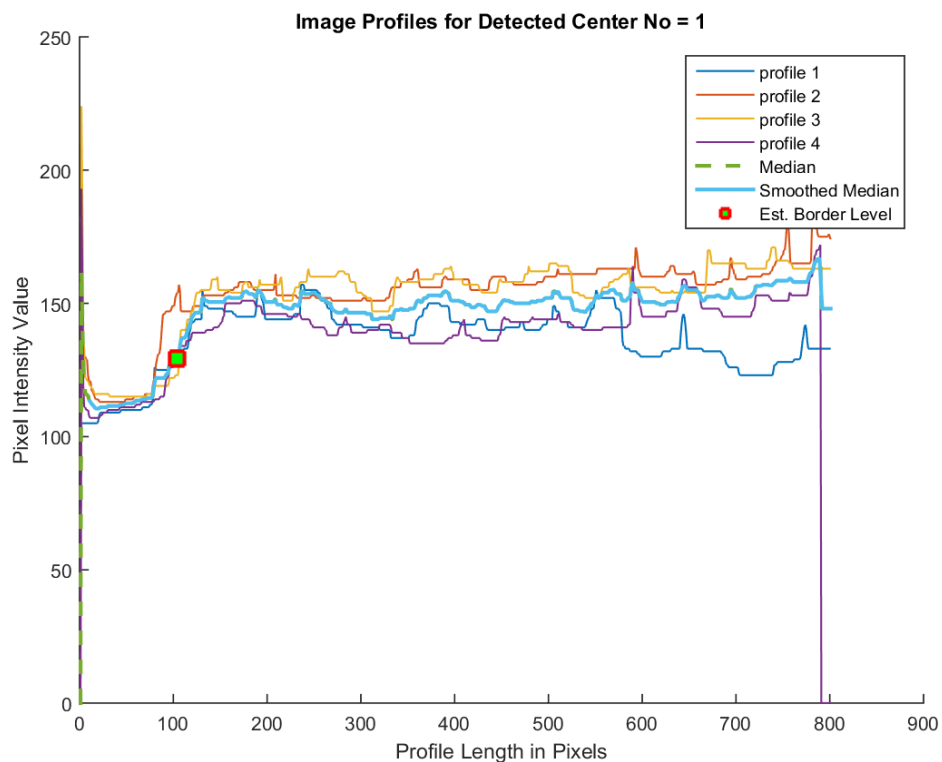


Figure 4. 47 Fifth antibiogram plate image profiles for detected center no.1

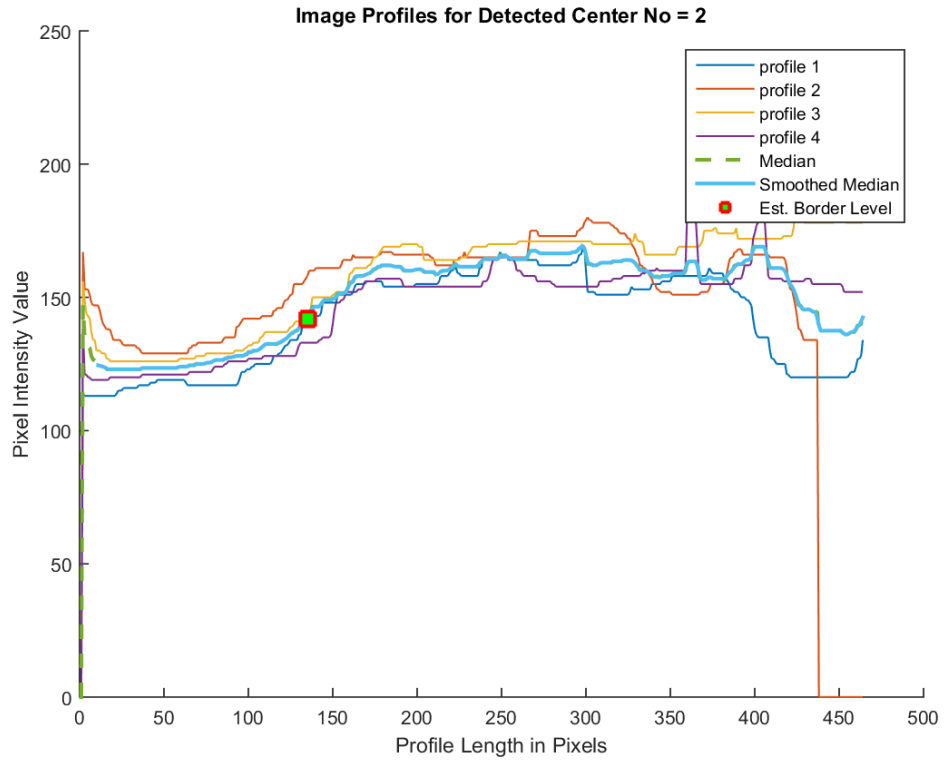


Figure 4. 48 Fifth antibiogram plate image profiles for detected center no.2

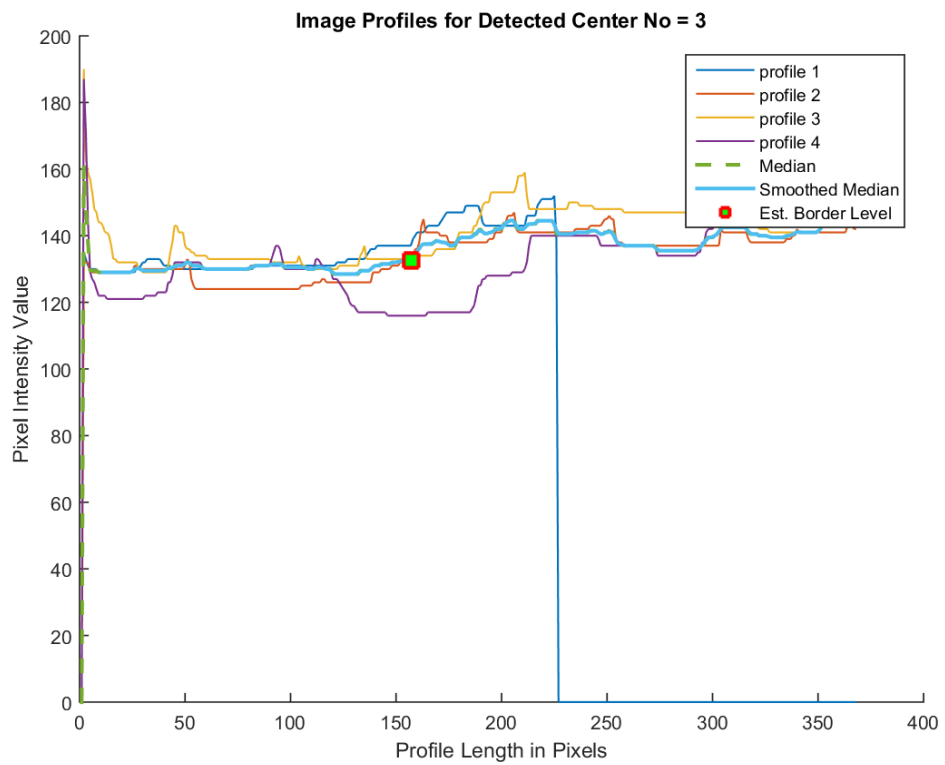


Figure 4. 49 Fifth antibiogram plate image profiles for detected center no.3

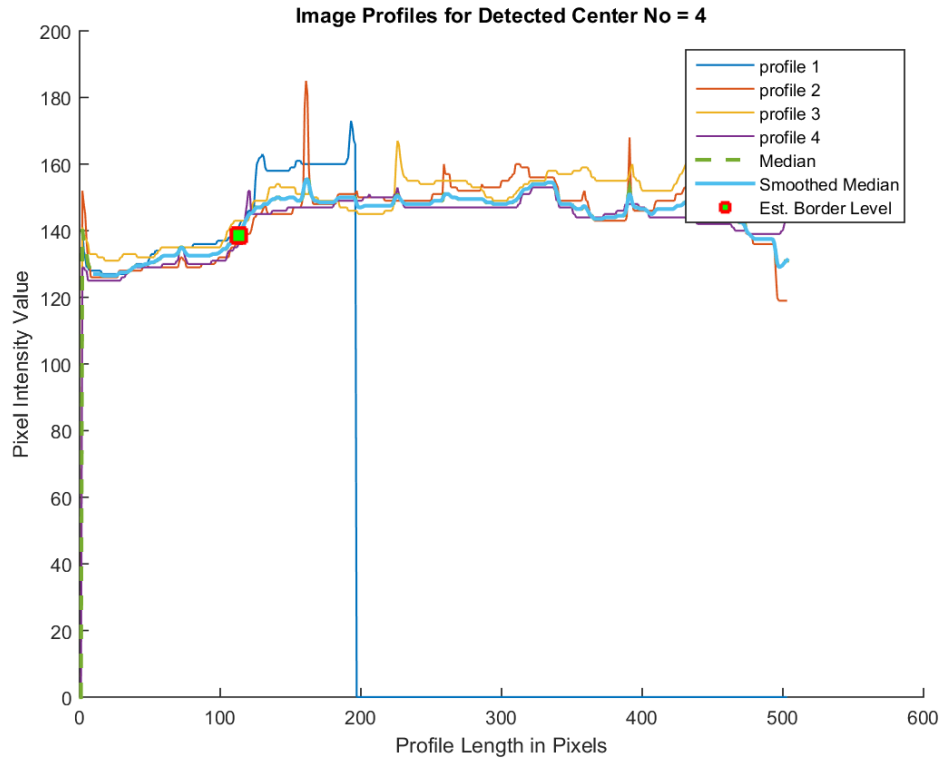


Figure 4. 50 Fifth antibiogram plate image profiles for detected center no.4

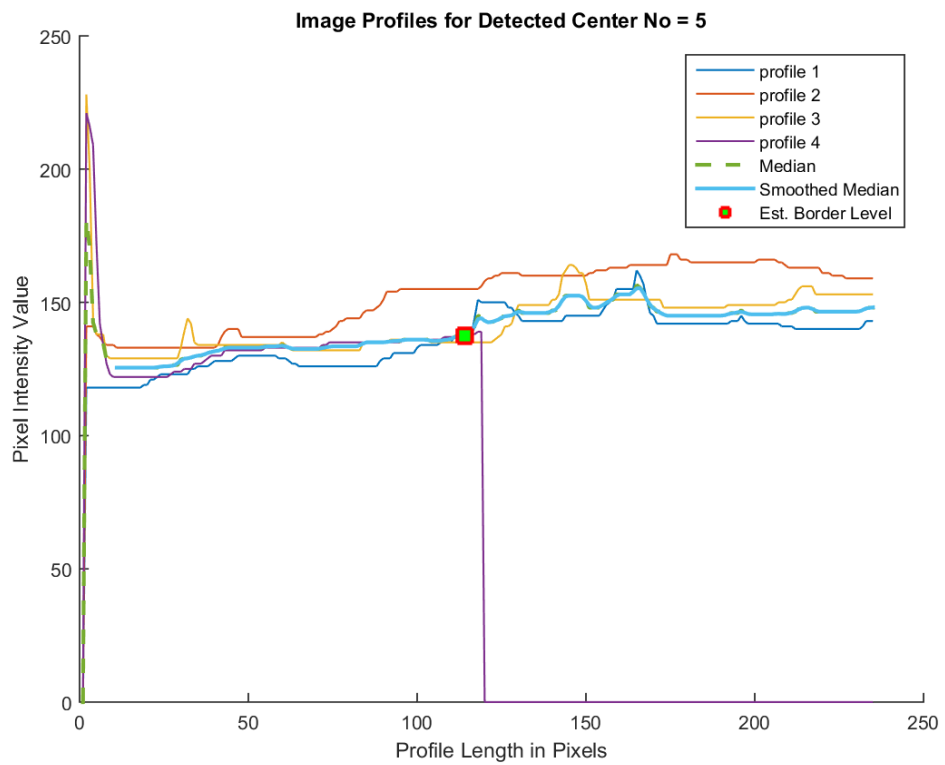


Figure 4. 51 Fifth antibiogram plate image profiles for detected center no.5

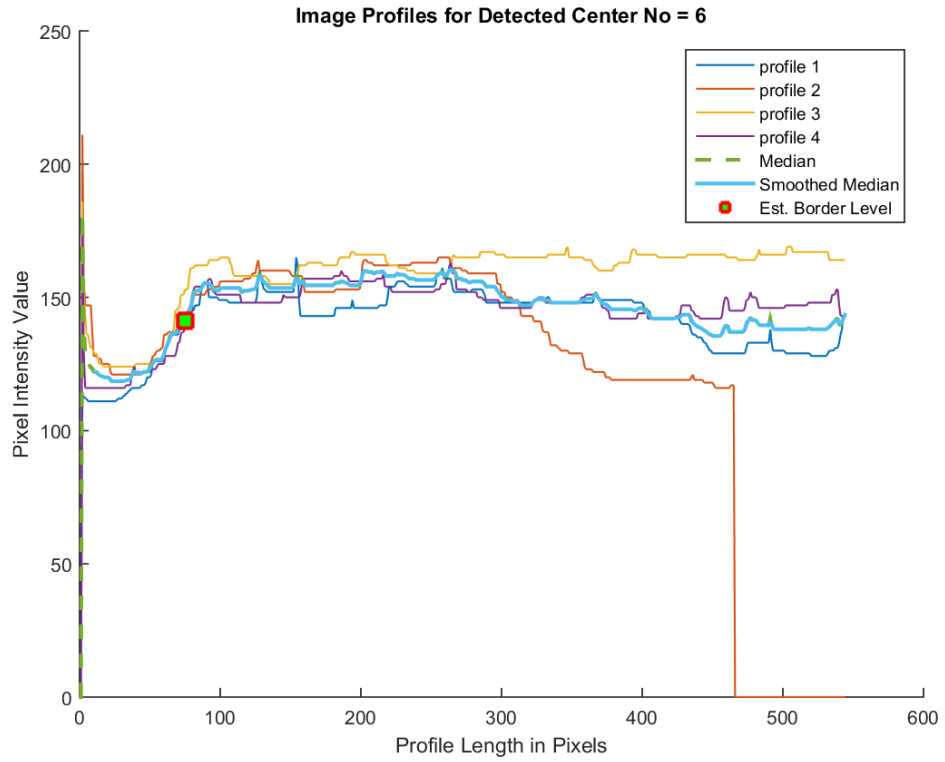


Figure 4. 52 Fifth antibiogram plate image profiles for detected center no.6

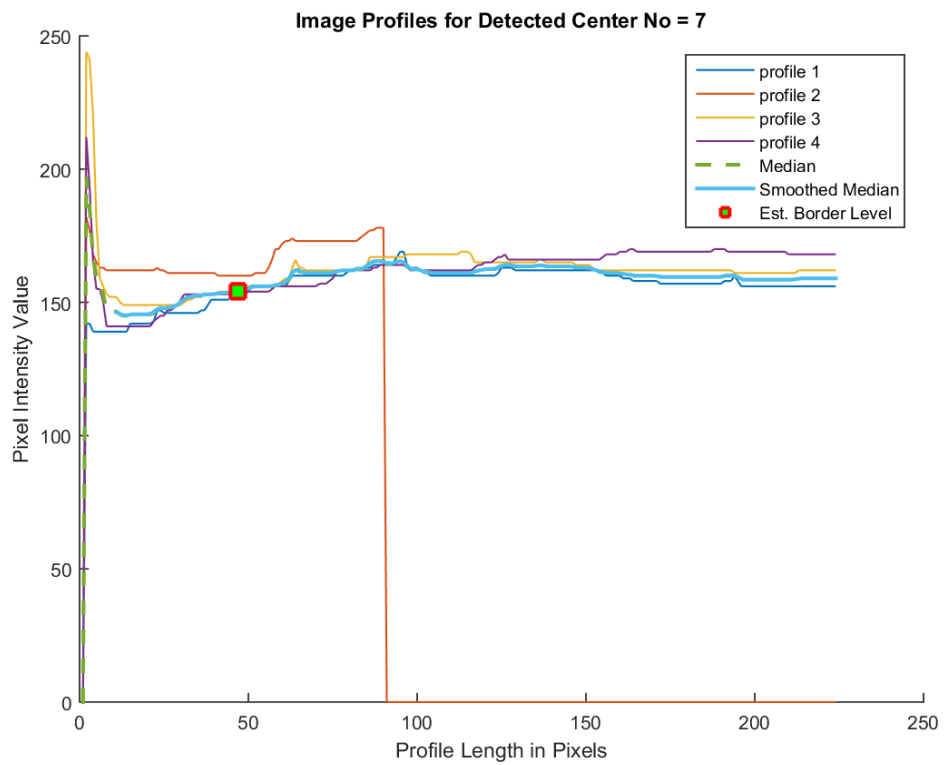


Figure 4. 53 Fifth antibiogram plate image profiles for detected center no.7

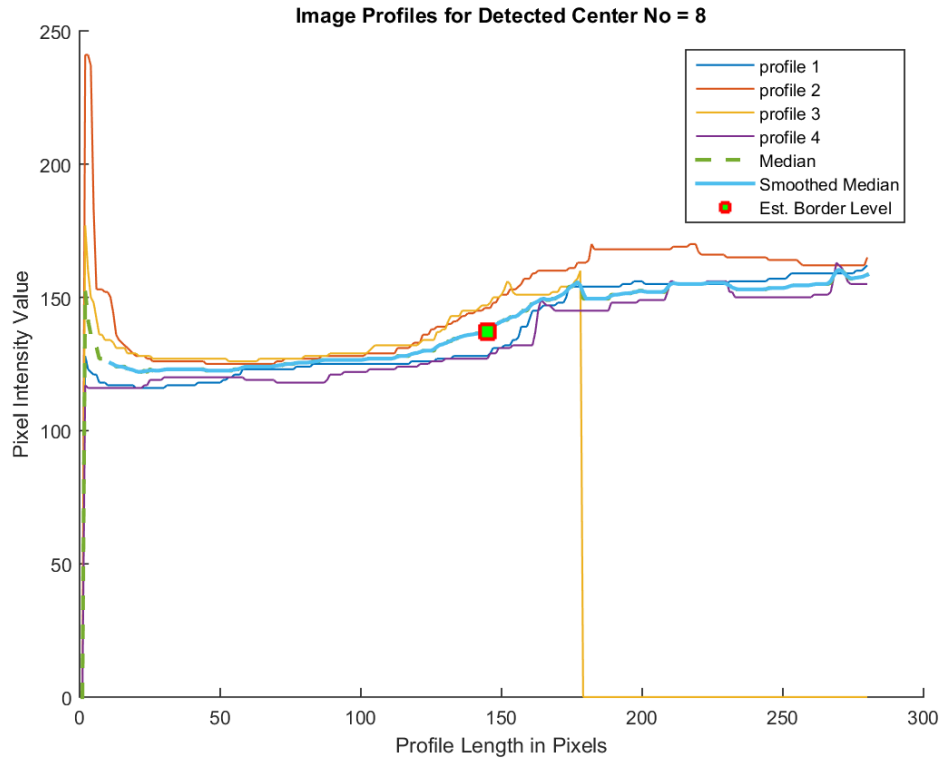


Figure 4. 54 Fifth antibiogram plate image profiles for detected center no.8

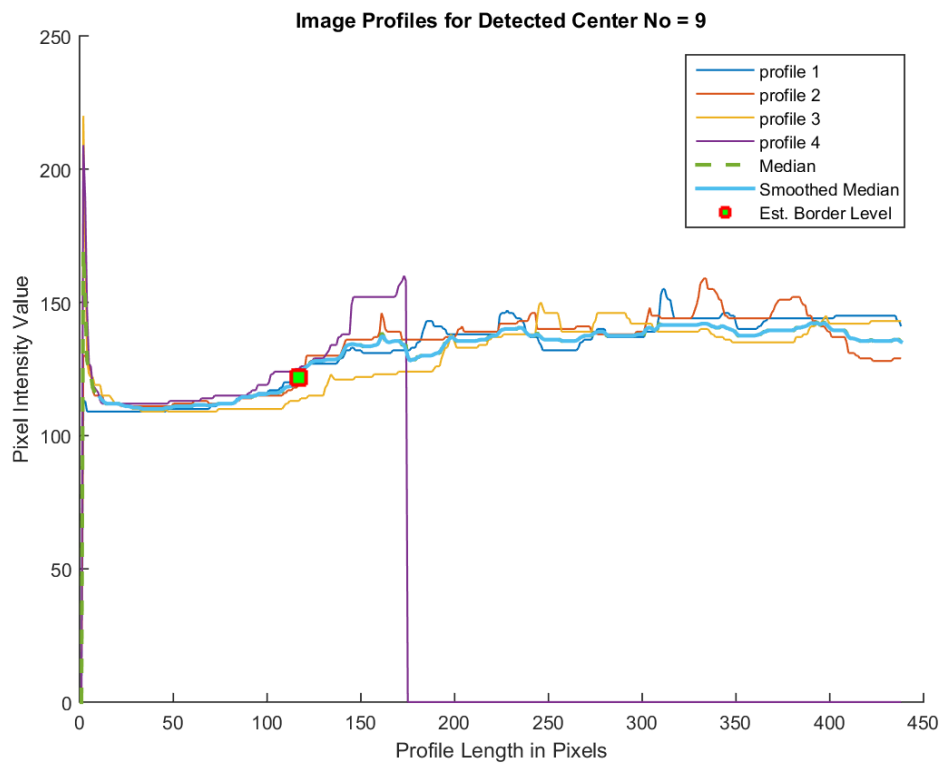


Figure 4. 55 Fifth antibiogram plate image profiles for detected center no.9

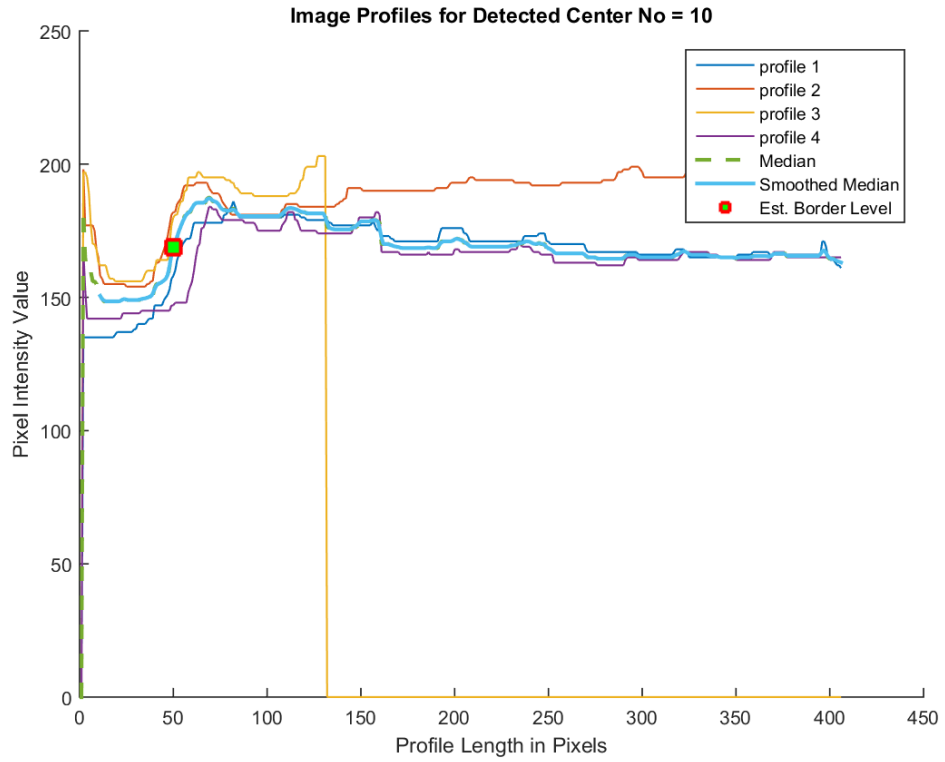


Figure 4. 56 Fifth antibiogram plate image profiles for detected center no.10

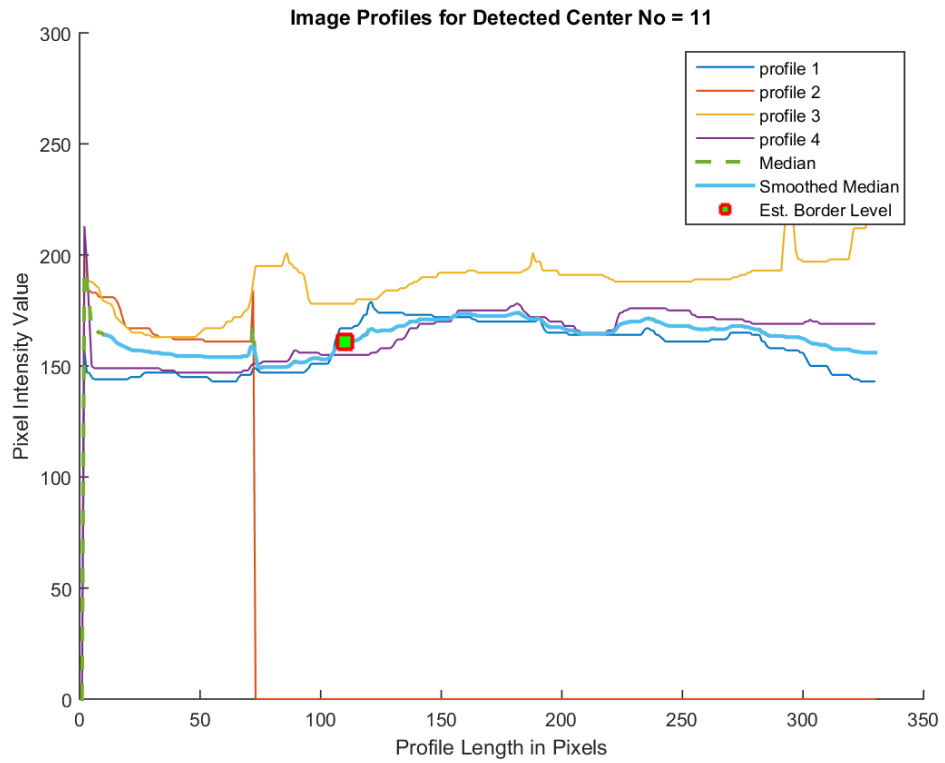


Figure 4. 57 Fifth antibiogram plate image profiles for detected center no.11

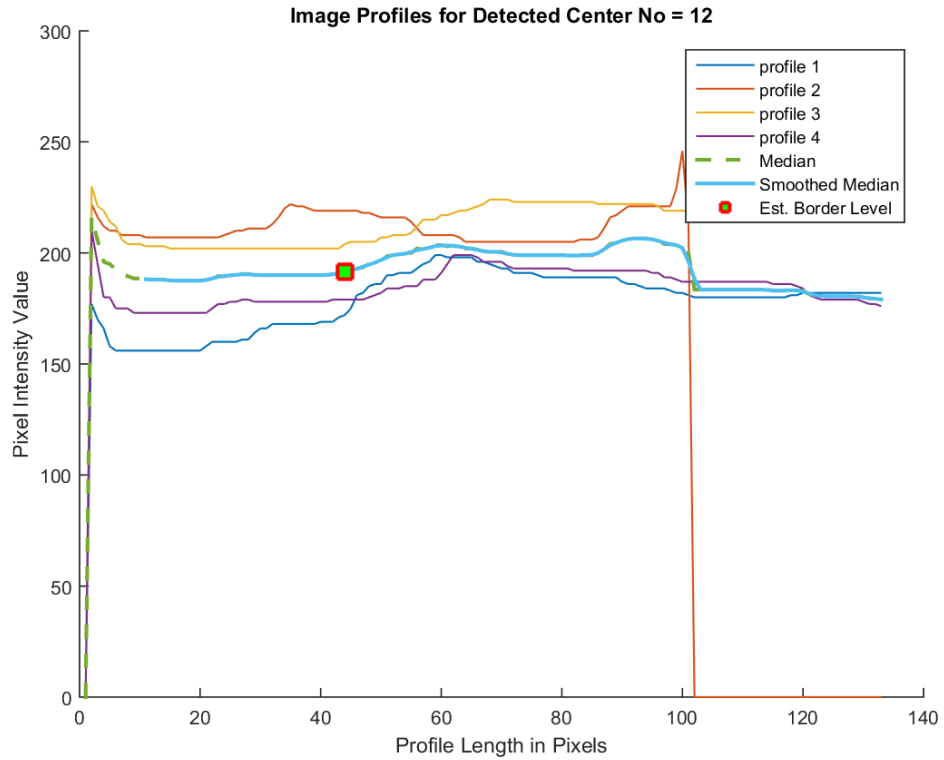


Figure 4. 58 Fifth antibiogram plate image profiles for detected center no.12

4.2 Inhibition Zone Final Reading

As a result of this thesis, manual and numerical features are applied to obtain the inhibition zones extracted from the border regions. Also, there are some tools used to analyze the antibiogram with automated image processing identification methods. The same processes are used for the calculation of inhibition zones for other antibiogram plate images. The application finds antibiotics with their positions and marks the inhibition zones with halos according to two categories. In Figure 4.49, the red circles indicate the detected inhibition zones as rate changed of growth and green circles indicate the boundary of antibiotics. In this study, additional annotations are used to show the diameter of the zones rate changed of growth and category information.

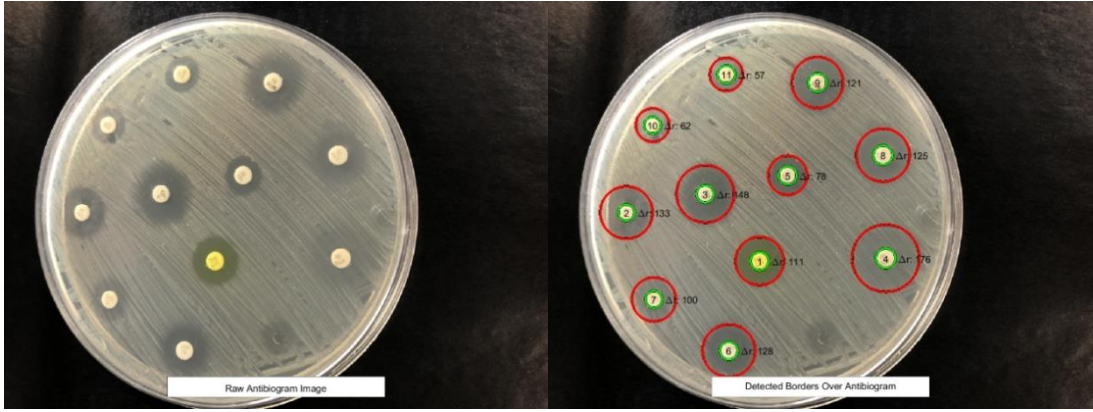


Figure 4. 59 First antibiogram plate images inhibition zones calculation

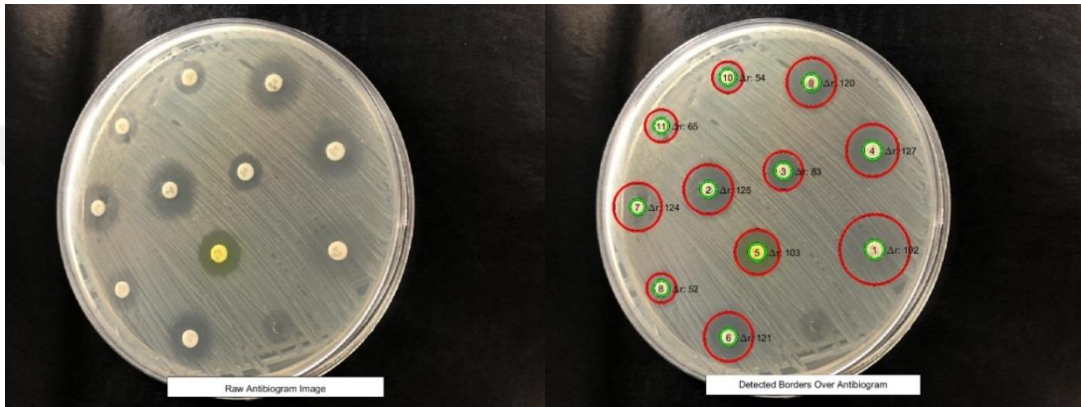


Figure 4. 60 Second antibiogram plate images inhibition zones calculation

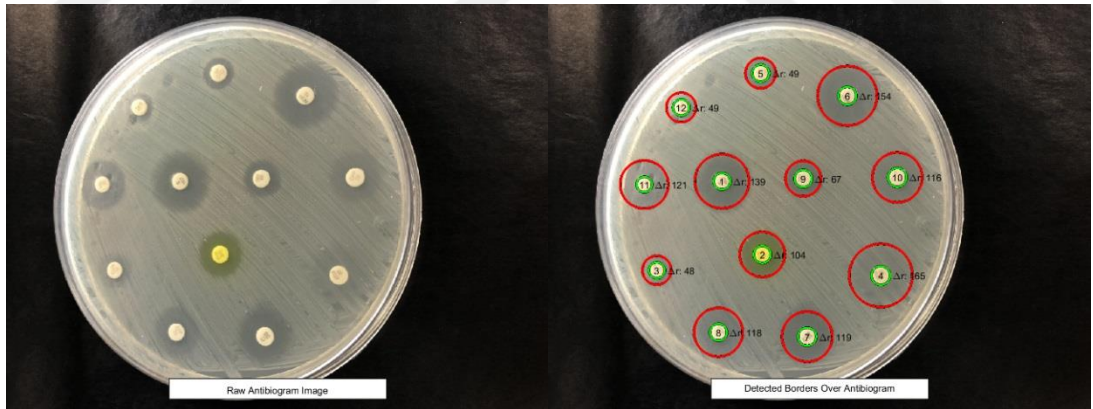


Figure 4. 61 Third antibiogram plate images inhibition zones calculation

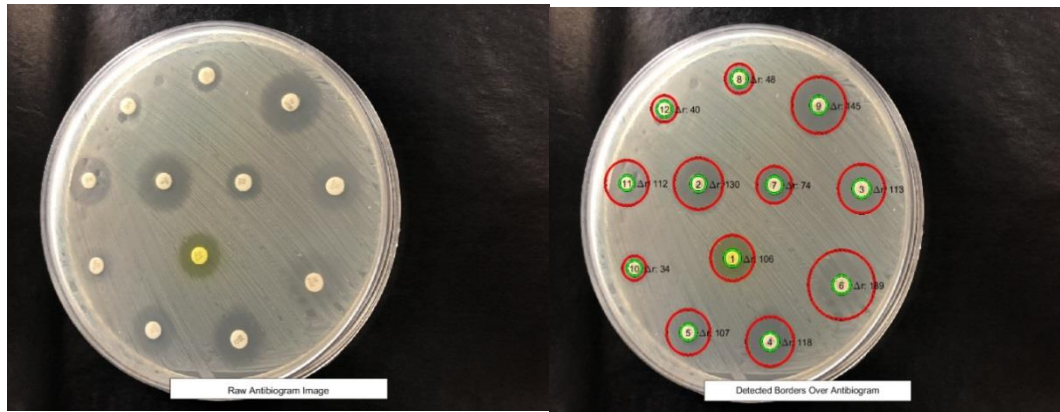


Figure 4. 62 Forth antibiogram plate images inhibition zones calculations

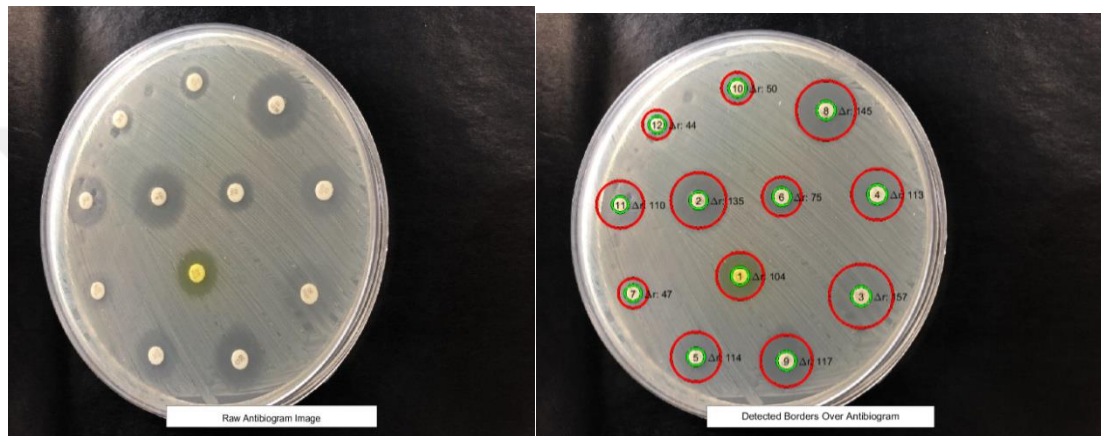


Figure 4. 63 Fifth antibiogram plate images inhibition zones calculations

The results obtained using image processing are evaluated considering those obtained from human measurements using the ruler. Found results are quite proper with the manual results.

4.3 Discussion

In many researches, different types of automatic inhibition zone readers' techniques for determining the antimicrobial susceptibility are introduced. These inhibition zone readers' instruments are combined with hardware and software tools working with image capturing. Currently new robotic handling method with image capture system is still being used for the automatic zone reader. Most of the time, these new tools are combined with the image processing and the laboratory information systems. The most common of these tools are Biomic V3 (Santa Barbara made by USA), VITEK two (Biomérieu made by USA), Adagio (Biorad made by France), Sirscan2000 (i2a,

Montpellier made by France), BD Kiestra (Drachten made by Netherlands), and Maestros (made by France) [12, 21-23]. The advantage of computerization provided by these systems includes advanced standardization result and also greater accuracy and less error [24, 25].

Unfortunately, all new computerized automated systems are too expensive for the clinical laboratory. An additional common problem for integrating these new computerized systems in the clinical laboratory is the change in laboratory design and work plan, as well as training professionals about new technology. Another type of inhibition zone reader measurement problem is a reasonable camera device to capture the images more clearly also the software tools [2, 8]. In addition, most of the advanced integrated system costs are very high and change laboratory design, and also have disadvantages to install software tools. Similarly, image capture positions, environment and user interaction and standards are other factors for image processing analysis [26, 27].

In a study, plate imageJ method is used for plate image analysis [28]. In the process results, diameters of the inhibition zones are internally employed by disc imageR program that determine the degree of drugs susceptibility, factors and changed of growth rate. To analyze the plate image, they used two different features to determine the previously stored antimicrobial disc code in database. In another study, more complete systems implemented in the MATLAB program are used to determine the antimicrobial code and inhibition zone, and using this information, the susceptibility classifications were determined. However, there were some limitations, because the antimicrobial code can only identify 12 limited antimicrobials, that's why all sizes of disks, disk positions also programs are not applicable in this method [29]. As a result, it is clear that not only good quality images, but also good quality antibiograms are important factors to improve algorithm performance. In this study, image quality was standardized and noise factors previously described were avoided.

In another study, an automatic identification method was applied for the antibiogram program and also proposed some new solutions to overcome the problem with the disc diffusion process [30, 31]. In the automatic identification software, the program

was able to scan the direct inhibition zones obtained by the antibiogram. Approximately 60 environmental isolates were analyzed using susceptibility testing for 12 different antibiotics for approximately 756 readings. The results of the automatic identification algorithm and the human manual reading results were compared, approximately 89% of the test result showed no statistically significant differences, additionally showing a correlations index of 0.85 for all images, 0.90 for standards [32].



CHAPTER 5

CONCLUSIONS

In this thesis, automatic identification methods of antibiogram analysis are investigated. In antibiogram inhibition zone of drug measure application, there may be some mistakes in human measurements. This type of mistake, such as misreading or intra-reader deviation, occurred during the investigation procedure, which could be resolved by automatic identification method. Similarly, for the automatic identification method, it is very important to obtain a periodic reading or monitoring system for inhibition zone selection as it changes over time. To overcome the inhibition zone selection reading problem, various methods are established. In this thesis, Antibiogram is presented, an image processing application for identifying, calculating, and classifying growth of inhibition zones from plate images taken with any digital camera or smart tablet. Antibiogram is an open-source tool, self-determining and an accessible platform. Different types of automated antibiogram analysis software packages have been found so far. In addition, in many studies, the rate obtained automatically by the Antibiogram software is very close compared to manual measurement for the automatic measurement inhibition zone reader. In this study, quite good results are also found. Moreover, using this image processing application of antibiogram, experts can easily detect when the automatic analysis has made any error and correct it for accurate clinical results. As further studies, some improvements can be made to the Antibiogram to deal with some issues that currently need to be addressed manually by the researcher. In the future, further improvements in Antibiogram zone reading practice can be introduced to address some of the features that should be checked automatically by the researcher.

REFERENCES

- [1] Critchley IA, Karlowsky JA. Optimal use of antibiotic resistance surveillance systems. *Clin Microbiol Infect.* 2004 Jun; 10(6):502-11.
- [2] C. Llor, A.Moragas, C. Bayona, R.Morros, Efficacy of anti-inflammatory or antibiotic treatment in patients with non- complicated acute bronchitis and discoloured sputum: randomized placebo controlled trial, *BMJ* 5762(2013)1–12.
- [3] E. Matuschek, D.F. Brown , G. Kahlmeter , Development of the EUCAST disk diffusion antimicrobial susceptibility testing method and its implementation in routine microbiology laboratories, *Clin. Microbiol. Infect.* 20 (4) (2014) O255–66.
- [4] A.W. Bauer, W.M. Kirby, J.C. Sherris, M. Turck, Antibiotic susceptibility testing by a standardized single disk method, *Am. J. Clin. Pathol.* 45 (1966) 4 93–4 96.
- [5] L.B. Reller, M. Weinstein, J.H. Jorgensen, M.J. Ferraro, Antimicrobial susceptibility testing: a review of general principles and contemporary practices, *Clin. Infect. Dis.* 49 (11) (2009) 1749–1755.
- [6] Clinical, L.S. Institute, Performance standards for antimicrobial susceptibility testing, CLSI, 26, Clinical and Laboratory Standards Institute, Wayne, PA, 2016. Supplement M100S.
- [7] Bauer, A. W., D. M. Perry, and W. M. M. Kirby. 1959. Single disc antibiotic sensitivity testing of Staphylococci. *A.M.A. Arch. Intern. Med.* 104:208–216.
- [8] Bauer, A. W., W. M. M. Kirby, J. C. Sherris, and M. turck. 1966. Antibiotic susceptibility testing by a standardized single disk method. *Am. J. Clin. Pathol.* 36:493-496.
- [9] Clinical Laboratory Standards Institute. 2006. Performance standards for antimicrobial disk susceptibility tests; Approved standard— 9th ed. CLSI document M2-A9. 26:1. Clinical Laboratory Standards Institute, Wayne, PA.

- [10] Jorgensen, J. H., and J. D. Turnidge. 2007. Susceptibility test methods: dilution and disk diffusion methods, p. 1152–1172. In P. R. Murray, E. J. Baron, J. H. Jorgensen, M. L. Landry, and M. A. Pfaller (ed.), *Manual of clinical microbiology*, 9th ed. ASM Press, Washington, D.C.
- [11] Ira R. Bacteriology, Standard Operative procedure manual for microbiology laboratories, National Institute of Biologicals. 1995, P73-97.
- [12] Sosa, A.J., D.K. Byarugaba, C.F. Ama'bile-Cuevas, P.-R. Hsueh, S. Kariuki, and I.N. Okeke, *Antimicrobial Resistance in Developing Countries*. 2010: Springer New York Dordrecht Heidelberg London.
- [13] Ferraro MJ (2000) Methods for dilution antimicrobial susceptibility tests for bacteria that grow aerobically. *NCCLS* 14: 13-19.
- [14] Wellinghausen N, Pietzcker T, Poppert S, Belak S, Fieser N, et al. (2007) Evaluation of the Merlin MICRONAUT system for rapid direct susceptibility testing of gram-positive cocci and gram-negative bacilli from positive blood cultures. *Journal of clinical microbiology* 45:789-795.
- [15] Haralick RM, Sternberg SR, Zhuang X, *Image Analysis Using Mathematical Morphology*, IEEE Transactions on Pattern Analysis And Machine Intelligence, Vol. Pami-9, No. 4, July 1987.
- [16] Serra J, *Image Analysis and Mathematical Morphology*. Academic Press, 1982.
- [17] R. Boyle and R. Thomas *Computer Vision: A First Course*, Blackwell Scientific Publications, 1988, Chap. 5.
- [18] A. Jain *Fundamentals of Digital Image Processing*, Prentice-Hall, 1989, Chap. 9.
- [19] F. Sun, J. He, || *The Normalized Cuts Based Image Segmentation Techniques*, || 2009 2nd International Convention on Information and Computing Science.
- [20] W. K. Pratt, —*Image Segmentation*, || in *Digital image processing*, 4th ed. Wiley, 2008, pp. 579-622.
- [21] C. Pantofaru, M. Hebert, *The assessment of image segmentation algorithms*, Technical Report CMU-05-40, CMU (2005). 2, 14.
- [22] Puchkov, E.O. (2010) *Computer Image Analysis of Microbial Colonies*. *Mikrobiologiya*, 79,160-165. [*Microbiology*, (Engl. Transl.), 79, 141-146].
- [23] Puchkov, E.O. (2009) *Application of an Automated Colony Counter for Evaluation of the Viability of a Yeast Culture*. *Mikrobiologiya*, 78, 556-

564. [Microbiology (Engl. Transl.), 78, 502-509].

- [24] Colwell, R.R. (2000) Bacterial Death Revisited. Colwell, R.R. and Grimes, D.J., Eds., In: Nonculturable Microorganisms in the environment, ASM, Washington, DC, 325-342.
- [25] Sousa, A.M., Machado, I., Nicolau, A. and Pereira, M.O. (2013) Improvements on Colony Morphology Identification towards Bacterial Profiling. *Journal of Microbiological Methods* , 95, 327-335.
- [26] Puchkov, E.O. (2012) To See More Than It is Visible: Computer Image Analysis in Biology. *Khimiya I Zhizn (Chemistry and Life)*, 11, 13-15. (In Russian)
- [27] E.A. Idelevich , Evaluation of an automated system for reading and interpreting disk diffusion antimicrobial susceptibility testing of fastidious bacteria, *PLoS ONE* 11 (7) (2016).
- [28] E.S. Lestari, et al., Comparison of the accuracy of disk diffusion zone diameters obtained by manual zone measurements to that by automated zone measurements to determine antimicrobial susceptibility, *J. Microbiol. Methods* 75 (2) (2008) 177–181.
- [29] C.A. Alonso , C. Domínguez , J. Heras b , E. Mata b , V. Pascual b , C. Torres a , M. Zarazaga, Antibioqramj: A tool for analysing images from disk diffusion tests. *Computer Methods and Programs in Biomedicine* 143 (2017) 159–169.
- [30] G. Hejblum, V.Jarlier, J.Grosset, A.Aurengo, Automated interpretation of disk diffusion antibiotic susceptibility tests with theradial profile analysis algorithm, *J. Clin. Microbiol.* 31(1993) 2396–2401.
- [31] A.Gavoille, B.Bardy, Measurement of inhibition zone diameter in disk susceptibility tests by computerized image analysis, *Comput.Biol.Med.* 24 (1994)179–188.
- [32] Luan F.R.Costa a, EduardoS.daSilva b, VictorT.Noronha b, IvoneVaz-Moreira b,c, Olga C.Nunes b, Development of an automatic identification algorithm for anti biogram analysis. *Computers in Biologyand Medicine* 67(2015)104–115.
- [33] Himanshu Makkar, Aditya Pundir. Image Analysis Using Improved Otsu’s Thresholding Method. *International Journal on Recent and Innovation Trends in Computing and Communication* ISSN: 2321-8169 Volume: 2 Issue: 8.